UNIVERSITÀ
DEGLI STUDI
DI PADOVA

Università degli Studi di Padova

Dipartimento di Scienze Biomediche

CORSO DI DOTTORATO DI RICERCA IN: Biomedical Sciences
CICLO XXX

TITOLO TESI

STUDY OF MITOCHONDRIA PHYSIOLOGY IN TRANSGENIC MOUSE MODELS OF ALZHEIMER'S DISEASE

Coordinatore: Ch.mo Prof. Paolo Bernardi
Supervisore: Ch.mo Prof. Tullio Pozzan
Co-Supervisore: Dr.ssa Emy Basso

Dottoranda : Giulia Rigotto

INDEX

SUMMARY

Alzheimer's disease (AD) is the most common neurodegenerative disorder and the most frequent form of dementia in developed countries, which leads to severe loss of memory and cognitive dysfunctions.

By far, the majority of AD cases are sporadic (SAD), with unknown etiology, for which the main risk factors are represented by aging and by the presence of the allelic variant APO-ε4 of apolipoprotein E. Only a small but significant percentage of cases, collectively called familial AD (FAD), is inherited and is caused by autosomal dominant mutations in the genes coding for the amyloid precursor protein (APP), presenilin 1 (PS1) and presenilin 2 (PS2) respectively.

APP is a single transmembrane domain protein with a large extracellular domain, expressed at high level in the brain. PSs are homologous membrane proteins specially localized in the endoplasmic reticulum (ER) and Golgi apparatus; they represent the essential components of the γ-secretase complex, which, by cleaving APP in concert with β-secretase, leads to the production of the neurotoxic β-amyloid peptides.

The identification of these genetic factors involved in FAD cases, allowed the development of transgenic mouse models. Given that SAD and FAD cases are morphologically and clinically similar, these models represent an important research tool to investigate potential common molecular mechanisms between the two AD forms, with the aim of devising effective therapies.

In these studies, two transgenic mouse models were used to perform the experiments. The first one is a single transgenic line, homozygous for the FAD-linked PS2-N141I mutation, which is under the prion promoter control and it is ubiquitously expressed. The second model is a double transgenic line homozygous for both the FAD-linked PS2-N141I mutation and APPSwe mutation, which is under Thy.1 promoter control, thus expressed only in neurons.

We investigated the possible, early impairment of mitochondrial functions in the brain of the transgenic animals. Mitochondria are cytoplasmic organelles responsible for most of the energy supplied to the cells through ATP production; furthermore, they are involved in many other roles, such as Ca^{2+} homeostasis, reactive oxygen species production (ROS) and apoptosis.

It is well established that mitochondrial impairment contributes to normal aging and to a wide spectrum of age-related diseases, including neurodegenerative diseases, such as AD, Parkinson's Disease (PD), Amyotrophic Lateral Sclerosis (ALS), and Huntington's Disease (HD).

First of all, we started with mitochondria isolated from the brain of WT, single and double transgenic mice of different ages, from neonatal up to 2 years old animals, to investigate the age-dependent progression in the onset of potential mitochondrial dysfunctions.

We evaluated mitochondrial bioenergetics parameters such as the oxygen consumption rate (OCR), the membrane potential and the calcium retention capacity (CRC). These experiments didn't reveal overt defects in the respiratory complexes activity or in the sensitivity of the permeability transition pore (PTP) to matrix Ca^{2+} overload in transgenic animals compared to WT, suggesting that these FAD-linked mutations do not cause severe primary defects on the organelles.

Isolated mitochondria represent a useful tool in many instances, but being removed from the cellular environment do not allow the study of the complex interaction that mitochondria entertain with other organelles or components of the cell. For this reason, we decided to study mitochondria in primary hippocampal cultures, specifically because the hippocampus is one of the first and main affected brain areas in AD.

In the context of intact cells, the basal respiration and the ATP synthesis coupled respiration measured by the mean of the Extracellular Flux Analyzer (Seahorse) didn't show significant differences among the three genotypes, whereas the maximal respiration was significantly higher in WT neurons compared to PS2APP neurons, suggesting a possible impairment in the supply of substrates to mitochondria.

Measuring the ability of mitochondria to sustain the membrane potential upon the selective inhibition of either the respiratory chain or the ATP synthase suggested the presence of a possible defect in the latter enzyme, in its ability to hydrolyze ATP, or the presence of an unknown metabolic defect/s limiting the supply of ATP to the synthase to sustain its reverse activity. Despite these interesting data obtained in hippocampal neurons, we didn't observe the same strong differences under similar conditions in experiments performed in human fibroblast carrying the same FAD-linked PS2 mutation.

These differences could be due to the fact that fibroblasts are mostly glycolytic cells, which might be less affected than neurons by mitochondrial dysfunctions.

In order to check the ATP synthase reverse activity, we measured NADH oxidation in isolated mouse brain-cortex mitochondria. The preliminary results showed a higher ATP hydrolysis rate in PS2 and PS2APP mitochondria compared with WT, but more experiments are needed to assess the statistical significance of this finding.

Blocking the respiratory chain, or the ATP synthase, in neuronal cells, so likely impairing ATP production, didn't show any major difference in the ability of the cells to handle potentially threatening increased cytosolic calcium concentration, $[Ca^{2+}]_c$. This evidence prompted the conclusion that under these experimental conditions, neurons seem to be equally able to handle a decrease in ATP content, and perhaps prolonged and stronger stimuli would be necessary to disclose possible defects.
Moreover, the basal ROS production in these cells is very low and seems to be similar among the genotypes.

Given the results collected so far, it would be interesting to better clarify the activity of the ATP synthase in the transgenic animals and investigate further the metabolic cross-talk between mitochondria and the rest of the cell.

RIASSUNTO

Il morbo di Alzheimer è la malattia neurodegenerativa più diffusa e una delle principali cause di demenza nei paesi occidentali. Questa patologia determina progressivi danni alla memoria e ad altre importanti funzioni cognitive. La maggior parte dei casi di Alzheimer è sporadica, compare in tarda età e i fattori di rischio più conosciuti sono l'invecchiamento e la variante allelica APO-ε4 del gene che codifica per la lipoproteina E. Esiste tuttavia una piccola ma significativa percentuale di casi ereditari (forma familiare di Alzheimer, FAD) che è causata da mutazioni autosomiche dominanti in tre geni che codificano per la Proteina Precursore dell'Amiloide (APP), per la Presenilina-1 (PS1) e la Presenilina-2 (PS2).

L'APP è una proteina transmembrana espressa principalmente nel cervello. Le preseniline sono proteine omologhe di membrana presenti soprattutto nel reticolo endoplasmatico e nell'apparato di Golgi. Costituiscono ciascuna, indipendentemente, la parte catalitica dell'enzima γ-secretasi che, insieme all'enzima β-secretasi, è responsabile del taglio dell'APP e della conseguente formazione di peptidi Aβ, molto dannosi per il cervello.

L'identificazione di mutazioni genetiche coinvolte nelle forme familiari di Alzheimer, ha permesso lo sviluppo di modelli di topi transgenici. Dato che i casi sporadici e quelli familiari della malattia sono clinicamente molto simili, questi modelli rappresentano uno strumento essenziale per la ricerca, poiché permettono lo studio di possibili meccanismi molecolari condivisi e danno la possibilità di scoprire/migliorare eventuali terapie. In questo progetto, gli esperimenti sono stati effettuati utilizzando due modelli transgenici di topi disponibili in laboratorio.

Il primo è un topo transgenico omozigote per la mutazione PS2-N141 che è stata posta sotto il controllo del promotore prionico e quindi viene espressa in tutti i tessuti. Il secondo modello è omozigote per la stessa mutazione di PS2 e anche per una mutazione dell'APP (APPSwe) che si trova sotto il controllo del promotore Thy.1, ed è quindi espressa solo nel cervello.

L'obiettivo di questo studio è quello di trovare possibili danni precoci nei mitocondri di cervello in questi modelli transgenici di Alzheimer. I mitocondri sono organelli citoplasmatici principalmente coinvolti nel fornire energia alla cellula sotto forma di ATP, ma sono in realtà indispensabili per molte altre funzioni, come ad esempio il controllo dell'omeostasi del calcio, la produzione delle specie radicali di ossigeno (ROS) e l'apoptosi. Al giorno d'oggi, è ampiamente accettato che danni a

questi organelli non sono solo presenti durante il normale invecchiamento ma anche in molte altre malattie legate ad esso, comprese le malattie neurodegenerative come l'Alzheimer, il morbo di Parkinson, la sclerosi laterale amiotrofica e la corea di Huntington.

I primi esperimenti sono stati effettuati in mitocondri isolati dal cervello dei topi WT, PS2 e PS2APP, partendo da quelli di 8 giorni fino a topi di 2 anni, per documentare la possibile presenza e/o progressione di disfunzionalità dei mitocondri. Abbiamo valutato diversi parametri bioenergetici, come la velocità di consumo dell'ossigeno (*oxygen consumption rate*, OCR), il potenziale di membrana mitocondriale e la capacità dei mitocondri di accumulare calcio nella matrice (*calcium retention capacity*, CRC). I risultati di questi esperimenti non hanno tuttavia rivelato particolari differenze tra i topi WT e quelli transgenici, né per quanto riguarda l'attività dei complessi della catena respiratoria, né per la sensibilità del poro di transizione della permeabilità mitocondriale (*permeability transition pore*, PTP) ad un elevato aumento di Ca^{2+} nella matrice. Tali dati suggeriscono che probabilmente, queste mutazioni FAD non inducono direttamente danni ai mitocondri.

I mitocondri isolati sono uno strumento molto utile per studiare le caratteristiche e la funzionalità di questi organelli, ma presentano tuttavia alcuni svantaggi: per esempio, in queste condizioni il mitocondrio è separato dal suo ambiente fisiologico e non è così possibile studiare le sue interazioni con le altre componenti del citoplasma. Per questo motivo, abbiamo deciso di spostare la nostra attenzione sulle colture primarie neuronali di ippocampo, perché quest'area del cervello è una delle regioni maggiormente e precocemente colpite dall'Alzheimer.

Per prima cosa, abbiamo comparato la respirazione basale e la respirazione accoppiata alla sintesi di ATP misurate con *l'Extracellular Flux Analyzer* (Seahorse) senza però trovare differenze significative tra le colture dei tre genotipi. La misura della respirazione massima è invece più alta nei WT rispetto a PS2 e PS2APP, e la differenza è significativa tra WT e PS2APP, suggerendo una possibile alterazione nel rifornimento di substrati ossidabili ai mitocondri.

In seguito, le misure effettuate per valutare la capacità dei mitocondri di mantenere il potenziale di membrana dopo l'inibizione selettiva dei complessi della catena respiratoria o dell'ATP sintasi, hanno rivelato un possibile difetto in quest'ultima, che potrebbe limitare la capacità di idrolizzare l'ATP, oppure alla presenza di difetti metabolici sconosciuti che limitano il rifornimento di ATP del citoplasma per sostenere l'attività idrolitica. Visti questi risultati, abbiamo provato a ripetere gli

esperimenti in fibroblasti provenienti da pazienti caratterizzati dalla stessa mutazione di PS2 presente nei modelli transgenici di topo. In questo caso però, la differenza tra fibroblasti provenienti da controlli sani e quelli provenienti dai pazienti non è così marcata come quelli emersi dagli studi nelle colture neuronali primarie. Questo può essere spiegato dal fatto che i fibroblasti sono cellule molto diverse dai neuroni, potrebbero ad esempio utilizzare di più la glicolisi, o semplicemente potrebbero risentire meno dell'effetto della mutazione in PS2.

Per verificare se effettivamente potesse esserci un difetto a livello dell'attività idrolitica dell'ATP sintasi, abbiamo provato a misurare indirettamente la velocità di idrolisi dell'ATP in mitocondri isolati da cervello di topi dei tre genotipi tramite l'ossidazione del NADH. Al momento, sembra che la velocità di idrolisi sia più veloce nei transgenici, anche se il numero di esperimenti non è ancora sufficiente per stabilire se tale differenza sia significativa o meno.

Abbiamo inoltre verificato che bloccando la catena respiratoria o l'ATP sintasi, di fatto diminuendo la quota di ATP prodotto dai mitocondri, i neuroni WT, PS2 e PS2APP sono ugualmente in grado di regolare il calcio citosolico. Questo suggerisce che in queste condizioni sperimentali i neuroni sono in grado di sopperire alla riduzione dell'ATP e che probabilmente per evidenziare delle differenze tra i genotipi bisognerebbe utilizzare uno stimolo più forte o prolungato.

Un altro parametro verificato è la produzione di ROS, che in condizioni basali è molto basso e che sembra essere simile tra i genotipi.

Dati i risultati ottenuti fino ad adesso, sarebbe interessante studiare nel dettaglio l'attività dell'ATP sintasi che potrebbe essere alterata nei modelli transgenici e soprattutto potrebbe essere interessante studiare le interazioni metaboliche tra i mitocondri e il resto della cellula.

INTRODUCTION

1. Alzheimer's disease

As described by Alois Alzheimer in 1906 and named by Emil Kraepelin in 1910, Alzheimer's disease (AD) is a primary and progressive neurodegenerative disorder, marked by severe impairments in memory and cognitive functions.

AD is the main cause of dementia in developed countries, accounting for 50-70% of cases (Winblad et al., 2016), and according to the World Alzheimer Report 2015, it was estimated that 46.8 million people worldwide were living with dementia in 2015 and the number is expected to double every 20 years, representing a severe economic burden on societies (Sasaguri et al., 2017).

The time course of AD averages 7-10 years, and inevitably ends up with death. Impaired recent memory is usually the first symptom during the early stage of mild AD dementia but other cognitive dysfunctions could be present, such as changes in attention and decreased problem solving abilities. The mild AD stage, the longest one, is marked by stronger memory dysfunction and usually the person loses the capacity to operate independently in the community and in the routine tasks at home. During the late-stage of the disease, which appears 5-10 years after the first symptoms, memory and cognitive skills keep worsening and individuals are completely non self-sufficient (Holtzman et al., 2011; Förstl and Kurz, 1999).

The neuropathology is initially present in the trans entorhinal cortex before encroaching on the entorhinal cortex and hippocampus. In the end, also the temporal, frontal and parietal lobes exhibit neuronal loss (Lazarov and Hollands, 2016). Clinically, the pathology of AD begins before the cognitive symptoms (figure 1) and comprises increased levels of extracellular amyloid plaques, intracellular neurofibrillary tangles (NFTs) and chronic neuroinflammation which are followed by loss of neuronal cells, particularly in the cortex and hippocampus (Dubois et al., 2016; Crous-Bou et al., 2017; Sasaguri et al., 2017).

The major component of plaques is the amyloid-β (Aβ) peptide, a 38-43 aminoacid (aa) peptide derived from the amyloid precursor protein (APP) (figure 2, black arrow). The brain areas surrounded by the senile plaques are characterized by "gliosis", which consists in hypertrophy and alterations of the morphology, as well as proliferation of astrocytes and microglia (Holtzman et al.,

2011; Hardy and Selkoe, 2002). As mentioned before, in addition to Aβ plaques deposition, neuronal soma and its processes develop NFTs, which are intracellular structures composed of hyperphosphorylated and aggregated forms of microtubule binding protein tau (figure 2, red arrowhead) (Goedert et al., 1988). In normal conditions, tau is produced by neurons and it binds tubulin, stabilizing microtubules. Instead, during AD tau becomes hyperphosphorilated, thus disassociating from microtubules with self-aggregating forms in cell bodies (Holtzman et al., 2011).

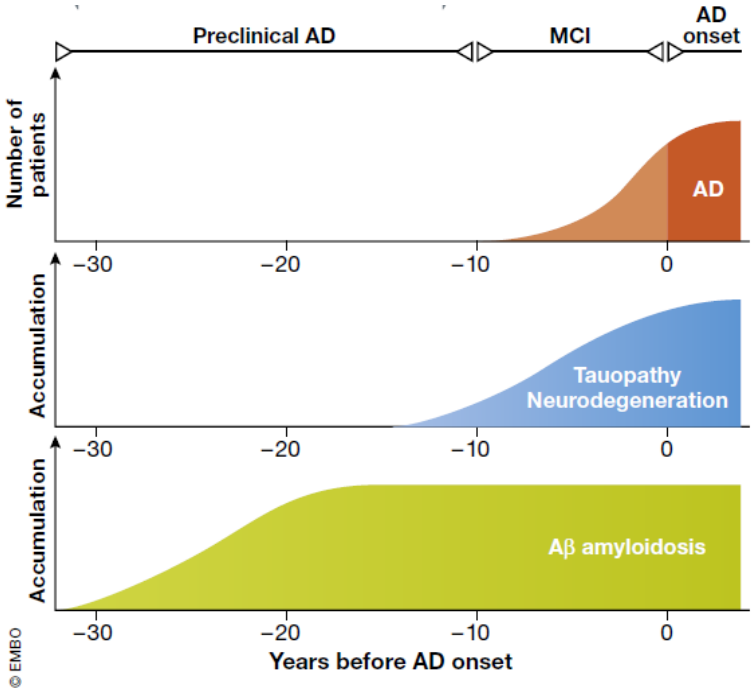

Figure 1: clinical phases of AD and development of amyloidosis and tauopathy neurodegeneration (modified from Sasaguri et al., 2017).

The loss of neurons is associated with a coordinated breakdown in vascular, astroglial and oligodendrocytic response, suggesting that AD is a system disorder and both the role and interactions of different cell types in the impairment of brain homeostasis and the resultant dementia must be considered (De Strooper & Karran, 2016).

The majority of AD cases (more than 95%) is sporadic with unknown etiology where the presence of the allelic variant APO-ε4 (the main cholesterol carrier that sustains lipid transport and injury repair in the brain), and aging represent the main risk factors. Indeed, the pathology usually starts after 65 years of age and it is called “sporadic” or “late-onset” AD (LOAD). The remaining 5% of cases includes the so-called “early-onset” AD (EOAD) cases which can manifest at 35 years of age;

and among them, a small but significant percentage (less than 1% of total AD cases) defined as Familial Alzheimer's disease (FAD), is due to autosomal dominant mutations in genes coding either for presenilin 1 (PS1), presenilin 2 (PS2) or amyloid precursor protein (APP).

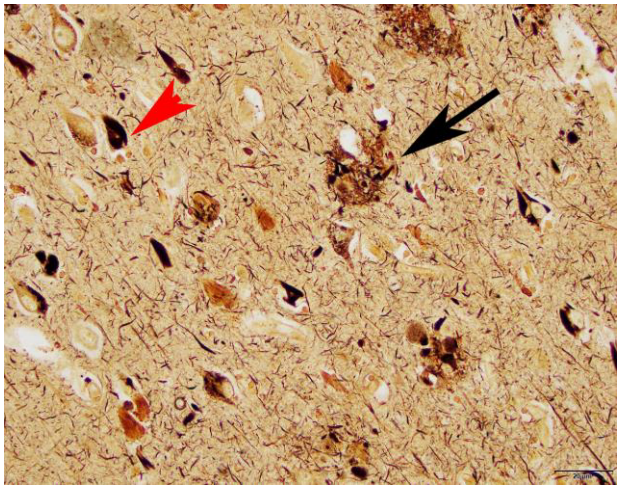

Figure 2: representative image with amyloid plaque (black arrow) and neurofibrillary tangle (red arrowhead) (modified from columbia.edu.html).

1.1 Neurofibrillary tangles and beta amyloid plaques

The beginning of AD is marked by the appearance of abnormally phosphorylated tau (p-tau). It is thought that the process begins in young adulthood or even before puberty, when soluble phosphorylated tau (pre-tangles) can be immunologically identified in the proximal axons of some brain areas (Braak and Del Tredici, 2011, 2012, 2015). The soluble p-tau of this pre-tangle state gradually aggregates into non-soluble fibrillary inclusions within dendrites, forming neuropil threads (NTs), and within nerve cell bodies, leading to NFTs formation. These insoluble aggregates are present in the early middle age and they are resistant to autophagy removal or to other cellular clearing mechanisms (Knopman, 2014). Neurons seem to be able to tolerate the presence of pre-tangles, NTs and NFTs and to survive for many decades, even if their activity may be already impaired.

The progress of tau pathology is not clear yet and it is different among individuals. Despite this, it is known that after developing in brainstem and subcortical neurons, the pre-tangles appear in the trans-entorhinal cortical region and diffuse to specific regions of the brain among neurons, according to their anatomical relationship and independently from the cell type. For this reason,

only defined neuronal circuits are targeted in AD. It has been also proposed that abnormal tau molecules may propagate from region to region in a prion-like manner through synaptic contacts, even if other manners cannot be excluded (Liu et al., 2012; McKee et al., 2015; Wu et al., 2013). Signs of cognitive impairment become evident once lesions involve the hippocampus, the temporal and insular cortex and the anterior cingulate gyrus (Mamelak, 2017).

Of note, only few among the different types of neurons present in the brain develop abnormal tau aggregates, whereas other adjacent cells maintain their morphology. Indeed, it has been found that the most vulnerable cells have two main features: they are all projection neurons with high concentrations of neurofilaments and, among them, only cells with very long and thin axons are more prone to develop lesions (Mamelak, 2017).

Furthermore, these long and thin axons usually present also a thin myelin sheath, or remain unmyelinated. Since myelin is very important because it reduces the metabolic demand for the transmission of impulses (Morrison et al., 2013), rapid-firing projection neurons that are poorly myelinated or unmyelinated have higher energy requirements, thus becoming more vulnerable to energy insufficiency and oxidative stress. (Braak et al., 2006; Morrisonet al., 2013). Additionally, it has been found in these neurons a decrease in the number of microtubules, suggesting an early breakdown of axodendritic transport and synaptic loss (Braaket al., 1994; Terry, 1998).

The anatomical distribution and temporal development of Aβ plaques are different from that of tau lesions, suggesting the independent development of these two AD hallmarks (Braak et al., 2013; Braak and Braak, 1997; Nelson et al., 2012; Price and Morris, 1999). The first diffuse deposits of aggregated Aβ first appear between the ages of 30 and 40 in the poorly myelinated regions of basal temporal cortex and then they extend into the hippocampus, entorhinal cortex, cingulate cortex and amygdala and then into all areas of the cortex (Mamelak, 2017). Aβ plaques accumulate very slowly over a 15-year period, and reach a plateau level which doesn't increase while dementia progresses further (Jack et al., 2013; Knopman, 2014).

1.2 γ-secretase

In 1993, the name "γ-secretase" was used for the first time to describe the proteolytic activity that cleaves APP in its transmembrane domain (Haas and Selkoe, 1993). Ten years later, all the different components of the molecular machinery responsible for this cleavage were finally identified (De Strooper, 2003).

It is now clear that γ-secretase is a multi-subunit aspartyl protease that cleaves not only APP, but also many other type-1 transmembrane proteins such as Notch, Delta1, E- and N- cadherins, CD44, Nectin-1α, ErbB4 and the β2 subunit of the voltage dependent Na^+ channel (McCarthy J.V. et al., 2009). The γ -secretase is able to mediate intra-membrane protein cleavage, capacity shared with only few other enzymes, called intramembrane-cleaving proteases (I-CLiPs).

The four γ-secretase components that are necessary for the enzymatic activity are Presenilin (either PS1 or PS2), Nicastrin (NCT), Anterior Pharynx-defective 1 (Aph-1) and Presenilin Enhancer-2 (Pen-2). They seem to have a stoichiometry of 1:1:1:1 (figure 3) and it is also reported that additional proteins may be involved in the regulation of the activity, or of the subcellular localization of the complex (De Strooper et al., 2012).

The Presenilins (PS) provide the catalytic core of the protease (see below for more details about the two proteins), whereas the other three proteins probably have a more structural function (Tolia and De Strooper, 2009).

Nicastrin (NCT) is an evolutionarily conserved, 130-kDa type I integral membrane protein that is highly glycosylated and tightly folded on maturation (Shirotani et al., 2003). The transmembrane (TM) domain of NCT is the principal site for the interaction with Aph-1 and PS. The large extra-cellular domain undergoes significant post-translational modifications during the incorporation into the γ-secretase complex and contains a DYIGIS and peptidase domain (DAP) that may be critical for the initial binding of the enzyme to the substrates.

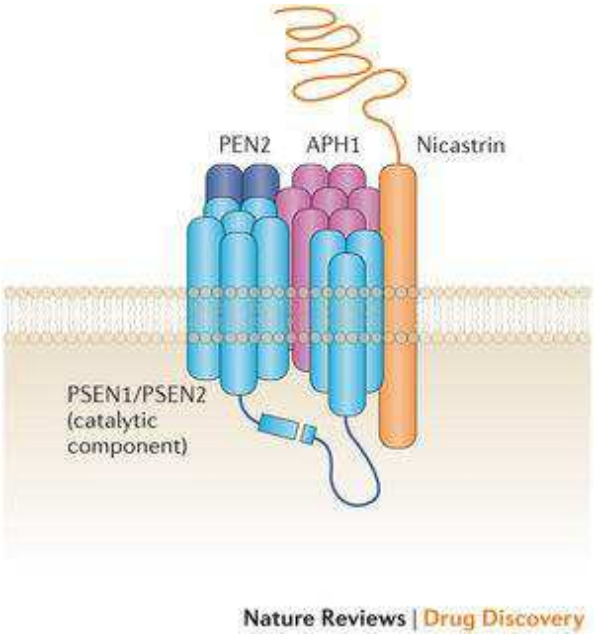

Figure 3: schematic representation of γ-secretase complex (modified from Emma et al., 2014).

Aph-1 is a 7-TM domains, 30 kDa protein with the N- and C-terminus located on the luminal and cytoplasmic side, respectively (Fortna et al., 2004). In humans there are two genes encoding for Aph-1 (*Aph-1a* and *Aph-1b*). In the TM4 domain there is a GxxxG motif necessary for the interaction with Pen-2 and PS, but not with NCT. Its role is not completely understood, but it seems to work like an initial scaffold for the proper assembly of the complex.

Pen-2 is a small protein of 101 aminoacids, and it spans the membrane twice, with both the N- and C-termini on the luminal side (Crystal et al., 2003). The N-term is crucial for the interaction with PS, whereas the C-term and the TM1 domain are necessary for the endo-proteolysis and the subsequent activation of PS, though the mechanism is not known yet.

It has been reported that NCT and multiple TMDs of Aph-1 form the initial γ-secretase subcomplex in the endoplasmic reticulum (ER) (LaVoie et al., 2003; Chiang et al., 2010). Afterwards, NCT/Aph-1 subcomplex interacts with the PS to form an intermediate trimeric complex; the incorporation of Pen-2 in the hetero-tetramer results in the endoproteolysis of PS that reaches its mature and active structure. The tetrameric state has been reported to assemble immediately before or within COPII vescicles, the ER exit carriers (Kim et al. 2007). It seems that less than 10% of the total γ-secretase complexes are active and they are located in the plasma membrane or in endosomes, while the majority of complexes is present in endomembranes but in an inactive state (Kaether C. et al., 2006a and b; Chyung G.H. et al., 2005).

As mentioned before, among its numerous targets, γ-secretase has a crucial role in cleaving APP thus producing Aβ peptides. Because of this, many efforts have been made to discover and develop small-molecule inhibitors as potential drugs against AD. Unfortunately, extended periods of treatments with available inhibitors can cause gastrointestinal toxicity, immunosuppression and also skin cancer, in some patients, due to the interference with Notch signaling (Wong et al., 2014; Demerhi et al., 2009).

1.3 Presenilins

Presenilin-1 (PS1) and Presenilin-2 (PS2) are homologous membrane proteins of 467 and 448 aa, respectively, with a molecular weight around 50 kDa. The sequence identity between them is around 65% and they are considered the catalytic core of the γ-secretase (De Strooper et al., 1998, 1999). Presenilins are expressed in several tissues including the brain, where they are present mainly in neurons (Kovacs et al., 1996). With antibodies against the individual γ-secretase complex components, it has been demonstrated that presenilin 1 and presenilin 2 or Aph-1a and Aph-1b are never in the same complex (Hèbert et al., 2004; Shirotani et al., 2004), hence allowing the coexistence of several different γ-secretase complexes next to each other, even in the same cell line.

These proteins are mainly localized in the ER, and Golgi apparatus (GA) whereas it has been proposed that only a small amount is present in the plasma membrane, endosomes, lysosomes, phagosomes and mitochondria (Chyung et al., 2005; Vetrivel et al., 2004).

In humans, the PS1 gene is located on the chromosome 14 and it is composed of 12 exons. The protein has eight TM domains and a hydrophilic domain between domains 6 and 7. To date, more than 185 PS1 mutations have been found in 405 families with familial form of AD (Campion et al., 1996; Meraz-Rìos et al., 2014; Wisniewski et al., 1998) (figure 4 A). In 1997, Shen and colleagues demonstrated that PS1-knockout mice were not able to survive because this protein is necessary for the proper formation of the axial skeleton and for the neurogenesis in mice. Moreover, they also showed that PS1 has a crucial role for neuronal viability in specific brain subregions (Shen et al., 1997).

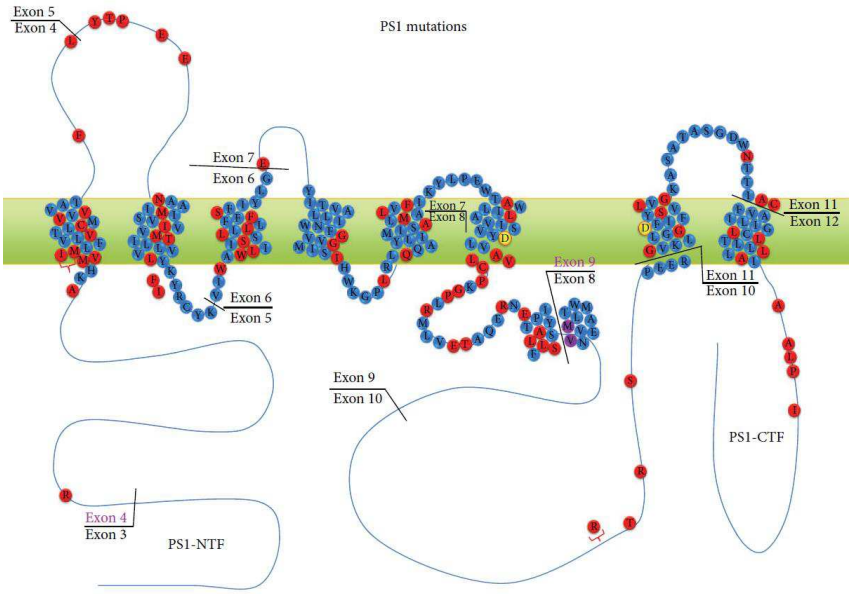

Figure 4 A: schematic representation of Presenilin 1 and the mutations related to familial forms of AD. Most of them are in the transmembrane region (modified from Meraz-Rìos et al., 2014).

The human PS2 gene, instead, is localized on the chromosome 1 and it is composed of 12 exons as well.

This protein has 9 TM domains and it is characterized by tissue-specific alternative splicing (Prihar et al., 1996). Differently from PS1, PS2 mutations are very rare and 13 of them were reported in the literature (figure 4 B). Unlike PS1, PS2 knock-out mice are viable and show at most a mild pulmonary phenotype (Herreman et al., 1999).

Under physiological conditions, presenilins undergo endoproteolytic processes, producing stable N- and C-terminal fragments (NTF and CTF, respectively). As mentioned above, these fragments can interact with other proteins, thus forming the macromolecular complex γ-secretase, which is responsible for the intermembrane proteolysis of APP and other proteins (Li et al., 2003; Nunan and Small, 2000; Vassan and Citron, 2000). These homologue proteins share the conserved aspartate residues required for the γ-secretase activity (Wakabayashi and De Strooper, 2008; Wolfe et al., 1999).

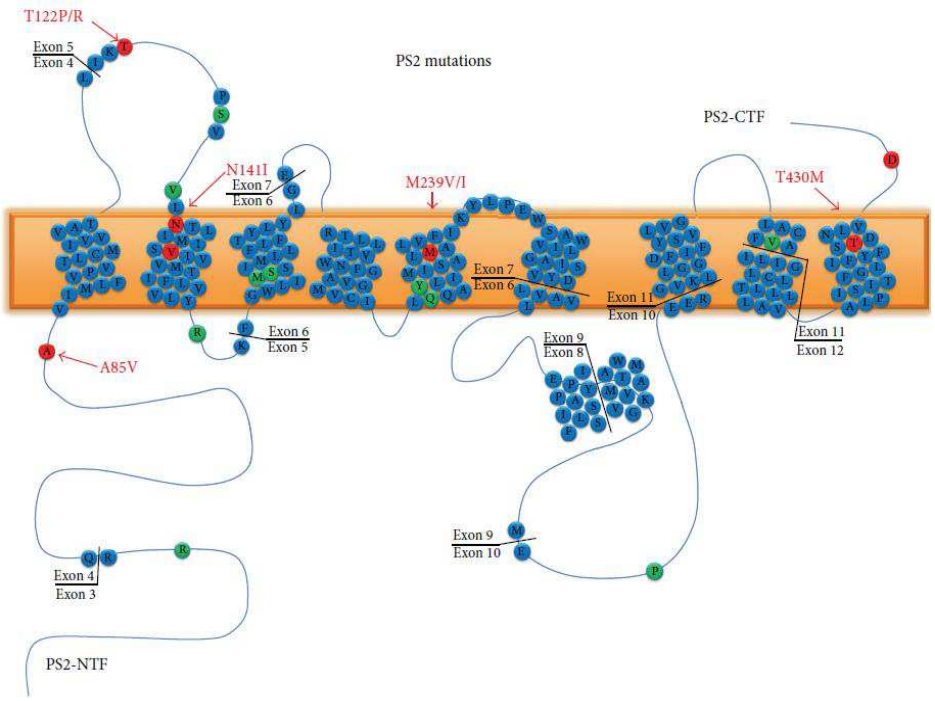

Figure 4 B: schematic representation of Presenilin 2. FAD-linked mutations found in the protein are reported (modified from Meraz-Rìos et al., 2014).

Several studies demonstrated that presenilins are also involved in non-protease, γ-secretase-independent functions. For example, many studies suggest that presenilins are involved in the β-catenin signaling. On the one hand, there are a series of evidences suggesting that presenilin 1 acts as a scaffold in order to present β-catenin for phosphorylation by PKA and GSK-3, with a consequent fast proteasomal degradation (Kang et al., 2002). On the other hand, it has been hypothesized that presenilin forms complexes with cadherins at the cell surface, and the interaction with β-catenin occurs through E-cadherin (Wakabayashi and De Strooper, 2008). Of note, this interaction seems to be γ-secretase activity dependent, because proteolysis of E-cadherin disassembles the complex and redistributes β-catenin in the cell (Marambaud et al., 2002; Serban et al., 2005; Wakabayashi and De Strooper, 2008).

The involvement of presenilins in Ca^{2+} homeostasis is also widely accepted, and both γ-secretase-dependent and -independent mechanisms have been hypothesized. Presenilin clinical mutations alter the inositol 1, 4, 5-triphosphate (InsP3)-mediated intracellular Ca^{2+} release (Leissring et al., 1999a; Leissring et al., 1999b), ryanodine-sensitive Ca^{2+} pools (Chan et al., 2000) and the

capacitative calcium entry (CCE) (Lessring et al., 2000; Yoo et al., 2000) in different cell models (Cheung et al., 2008) and in neurons from AD mice models (Smith et al., 2005).

As mentioned before, PS1 and PS2 are highly homologous and their roles in cell activity are often considered overlapping. However, in our lab it has been found that, regarding Ca^{2+} homeostasis, presenilins have both similar and different roles.

For example, both PS1 and PS2 overexpression in WT and FAD-linked mutants decrease the ER Ca^{2+} content (Brunello et al., 2009) and favor Ca^{2+} leak from this organelle, but only PS2 strongly reduces the sarco-endoplasmic reticulum Ca^{2+} ATPase (SERCA) activity and increases ER-mitochondria tethering (Brunello et al., 2009; Zampese et al., 2011). Along with these results, another group published that cells from PS2 (but not PS1) knockout animals show a significant decrease in mitochondria activity; the energetic deficit may be due to the reduction of ER-mitochondria Ca^{2+}transfer (Càrdenas et al., 2010).

Moreover, these findings were also confirmed in acute brain slices from transgenic mice carrying a PS2 FAD-linked mutation (Kipanyula et al., 2012).

Concerning the γ-secretase activity, APP can be cleaved at different positions, which results in the production of different Aβ peptides that vary at the carboxyl terminus. Mutations in presenilin could have several effects on Aβ peptide release, but consistently a larger amount of long (≥ Aβ42) and a smaller amount of short (Aβ40) peptides are generated.

This change in the spectrum of Aβ peptides increases the proportion of Aβ42 with respect to Aβ40 peptide, which is one of the most reproduced findings in patients with presenilin mutations (Scheuner et al., 1996; Wakabayashi and De Strooper, 2008).

1.4 Amyloid precursor protein (APP)

The amyloid precursor protein (APP) is a single transmembrane domain protein that belongs to the type I family. In mammals, there are other members of this family, such as APP like protein 1 and 2 (APLP1/2), which have several well conserved domains, especially in the extracellular portion. It has been recently reported that APLP1 is a molecule involved in synaptic cell adhesion (Schilling et al., 2017), whereas APLP2 seems to be important for glucose and insulin homeostasis, and growth (Needham et al., 2008).

The human APP gene is located on chromosome 21, it consists of 18 exons and it can generate several isoforms through alternative splicing. The isoforms found in the central nervous system are APP695, 751, 770 and 563, the first one is mainly expressed in neurons. To date, about 36 different missense mutations in the APP gene have been found in 85 families (Meraz-Rìos, 2014). The majority of them is localized in exons 16-17, in the TMD, in which the recognition sites for α-, β- and γ- secretases cleavage are present.

APP has been extensively studied for its role as precursor of the β-amyloid peptides in AD, however its physiological function remains largely unknown. It has been reported that APP is able to influence cell proliferation, differentiation, neurite outgrowth, cell adhesion and synaptogenesis (Dawkins and Small, 2014). Several studies reported that the extracellular domain can stimulate cellular growth and for instance, it has been demonstrated that sAPPα (soluble N-terminal fragment which is produced after α-secretase-mediated APP cleavage) is able to alter the growth of fibroblasts, keratinocytes, B109 cells, FRTL-5 cells, PC12 cells and neurons *in vitro* (Araki et al.1991; Hoffmann et al. 2000; Jin et al. 1994; Milward et al 1992; Ninomiya et al. 1994; Pietrzik et al. 1998; Saitoh et al.1989; Young-Pearse et al.2008).

Moreover, it has been suggested that APP may be involved in the regulation of stem-cell proliferation or differentiation. Indeed, APP is processed in a manner that is very similar to the protein Notch, which regulates neural stem cell differentiation (Ables et al.2011; Kimberly et al. 2001).

It has been already demonstrated that APP can promote neurite outgrowth in cell cultures (Small et al., 1994), maybe by regulating cell-substrate adhesion. Indeed, it has been reported that APP can bind laminin, collagen type I and heparan sulphate (Beher et al. 1996; Clarris et al. 1997; Kibbey et al 1993) and all these proteins can regulate neurite outgrowth.

Other studies suggested that APP might be involved in cell-cell adhesion (Soba et al., 2005), regulation of synaptogenesis, synaptic plasticity and also blood coagulation (Dawkins and Small, 2015).

APP can undergo two distinct and competitive maturation pathways (figure 5). The first is called non-amyloidogenic pathway and it is the predominant one, where APP is cleaved by the α-secretase within the sequence that contains the amyloidogenic peptides (Aβ peptides), thus preventing their formation.

This first APP cleavage produces a soluble N-terminal fragment that is released in the extracellular space (APPsα) and a C-terminal fragment (C83) that remains bound to the membrane.

In the amyloidogenic pathway, the protein is first cleaved by the β-secretase, keeping the entire Aβ fragment and thus originating a shorter soluble portion (sAPPβ) and a longer C-terminal peptide, called C99, that also stays membrane-bound. C83 and C99 can be further processed by γ-secretase inside the TM domain of APP: C83 cleavage produces the release of the extracellular, non-pathogenic peptide p3 and the intracellular AICD (that may migrate to the nucleus to regulate transcription), whereas C99 cleavage produces AICD and the amyloidogenic Aβ peptide (released in the extracellular space).

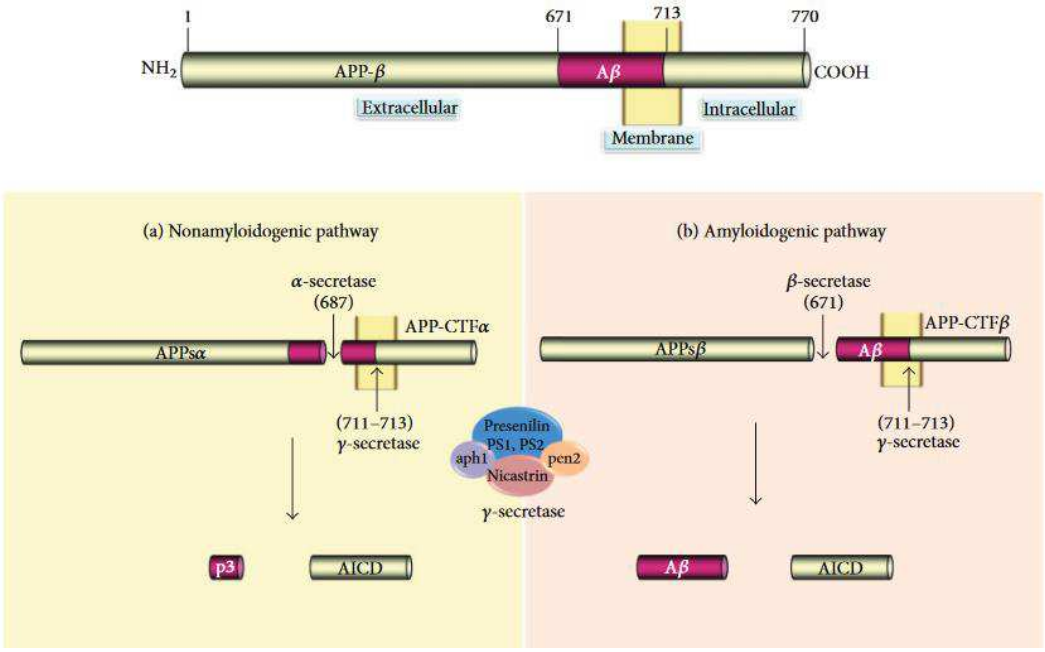

Figure 5: the two alternative pathways for APP processing (modified from Meraz-Rìos et al., 2014).

However, γ-secretase does not have a single site of cleavage and can produce in sequence Aβ peptides of different length, ranging from 49 to 38 aa. The most abundant is Aβ40, whereas about 10% is constituted of Aβ42, which is more hydrophobic and more prone to aggregation.

APP mutations linked to FAD are mainly localized close to the cleavage sites of α/β/γ -secretase, and this favors the amyloidogenic pathway, promoting the APP processing mediated by β- and γ-secretases. These findings, together with the APP overexpression and the fact that mutations

within the Aβ peptide induce its aggregation, are associated to an early onset of symptoms compatible with the disorder, providing strong genetic support to the amyloid cascade hypothesis for AD pathogenesis.

Even if the udertsanding of AD has increased dramatically and continues to grow, the exact etiology of the disorder is still unknown. Many hypotheses have been proposed over time and we will focus our attention on three of them: the amyloid cascade hypothesis, the calcium hypothesis and the mitochondria cascade hypothesis.

1.5 The amyloid cascade hypothesis

More than 25 years ago, it was proposed for the first time that the neurodegeneration observed in AD may be caused by deposition of Aβ plaques in brain tissue (Hardy and Selkoe, 2002).

According to this hypothesis, the Aβ plaques accumulation acts as a pathological trigger for a cascade that is characterized by neuronal injury, neurofibrillary tangles formation that lead to neuronal dysfunction and cell death (Barage and Sonawane, 2015; Hardy and Higgins, 1992; Selkoe, 1999;) (figure 6).

Aβ plaques are mainly composed of Aβ peptides (Masters et al., 1985) that are 39-43 amino acid long peptides derived from the sequential enzymatic cleavage of APP. Within the plaques, these peptides are characterized by a β-sheet conformation and they can polymerize into structurally distinct forms including protofibers, fibrillary and polymorphic oligomers (Selkoe, 1994).

It is known that the increase of Aβ42 favors oligomers formation that can lead to severe and permanent changes in synaptic function. Additionally, Aβ42 forms microscopic deposits in the brain, first as non-fibrillar plaques. The appearance of Aβ fibrils in those plaques is followed by inflammatory response, synaptic spine loss and neuritic dystrophy. Over time, these conditions lead to oxidative stress and altered ionic homeostasis. Neurofibrillary tangles appear after the alteration of kinase and phosphatase activities, contributing to additional impairments. The cascade culminates in widespread synaptic/neuronal dysfunction and cell death, inducing progressive dementia with substantial Aβ and tau pathology (Haas and Selkoe, 2007).

It is reported in literature that some neuropeptides could play a role in the amyloid cascade hypothesis. These molecules are important for cognitive and behavioral functions and furthermore, they can influence APP processing, Aβ-degradation and accumulation.

Among them, there is the corticotrophin-releasing hormone (CRH), a peptide that regulates the stress response by acting on the hypothalamic-pituitary-adrenal axis. It has been hypothesized that CRH may increase the expression or the activity of α-secretase and, at the same time, reduce β-secretase expression or activity (Walter et al., 2001).

In vivo studies demonstrated that another hormone, Angiotensin II has a central role in amyloidogenesis through the regulation of different components of the APP processing pathway (Kehoe et al., 2009).

Additionally, in AD patients it has been found a decrease in somatostatin, which is important for learning and memory processing, and neuropeptide Y, which is known to play a crucial role in pathological conditions such as anxiety, chronic pain and neurodegenerative diseases (Barage and Sonawane, 2015; Foster et al., 1986).

The main weak point of the theory is that even if Aβ amyloid pathology is found in all AD patients, a relationship with cognitive dysfunctions is not clear. The problem is that Aβ peptides accumulation is not always related to neuronal loss and cognitive dysfunction. Indeed, 20-40% of cognitively normal individuals between the ages of 60 and 90 show high levels of Aβ in their brains, arguing against the hypothesis that Aβ is a neurotoxin that directly impairs cognition, but it has been demonstrated that individuals with high Aβ levels in the brain show a significantly greater extent of grey matter atrophy and memory decline than those with low levels (Chetelat et al., 2013; Knopman, 2014).

Nevertheless, the major support for this hypothesis derives from the combination of pathophysiology and human genetics (Karran and De Strooper, 2016). Indeed, many studies associate FAD to autosomal dominant mutations in three genes coding for APP, PS1 and PS2, involved in the production of Aβ peptide. These mutations have the effect of increasing the amount of C-terminally extended Aβ peptides, or the ratio of aggregatory, longer forms of Aβ over shorter, more soluble forms, or to directly increase the Aβ peptide propensity to aggregation (Karran and De Strooper, 2016).

Recently, a variant of the amyloid cascade hypothesis has been proposed, the Aβ oligomer one. The Aβ oligomer hypothesis states that small molecular weight Aβ oligomers are neurotoxic agents that cause synaptic damage in AD.

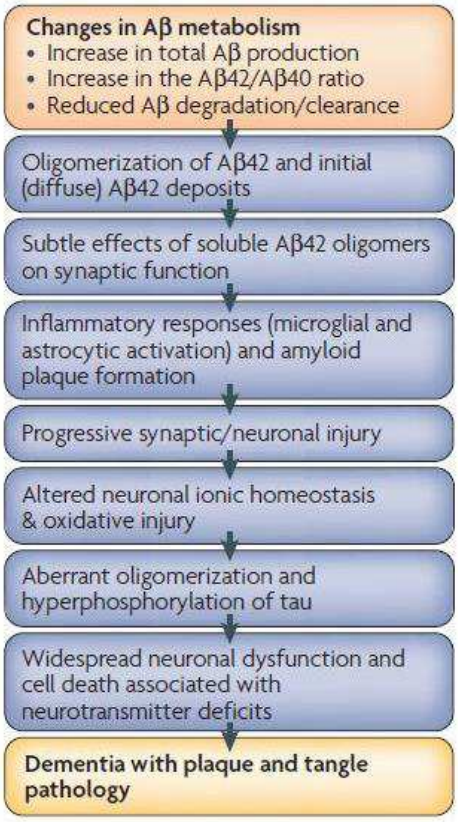

Figure 6: the amyloid cascade hypothesis (modified from Haas and Selkoe, 2007).

Indeed, it is difficult to figure out how very insoluble and relatively inert protein deposits can damage the brain. On the other hand, soluble Aβ species are very stable, long lived and prion-like (Ye et al., 2015; Karran and De Strooper., 2016).

On this line, it has been reported that soluble oligomers are able to inhibit the maintenance of the long term potentiation (LTP) reponse in the hippocampus, a phenomenon related to learning and memory (Haas and Selkoe, 2007). The biochemical mechanism by which soluble oligomers bind to synaptic plasma membrane and interfere with the system of receptor and/or channel proteins and signaling pathways that are necessary for synaptic plasticity is still matter of intensive studies (Hass and Selkoe, 2007).

It has been suggested that oligomeric Aβ interferes with signaling pathways downstream of NMDA (N-metyl-D-aspartate) or AMPA (α-hydroxy-5-metyl-4-isoxazole) receptors at synaptic plasma membrane level, allowing an initial but not persistent LTP response (Haas and Selkoe, 2007). Moreover, it has been demonstrated that soluble oligomers can indirectly block LTP by inhibiting the ubiquitin C-terminal hydrolase (UCH) (Gong et al., 2006).

These mechanisms of oligomer-induced neuronal and also glial membrane alteration can probably lead to many downstream biochemical changes, including impairment in cellular Ca^{2+} handling (Arispe et al., 2007), triggering of inflammatory cascades, and mitochondrial dysfunctions. (LaFerla 2010; LaFerla et al., 2007).

All these effects produced by soluble oligomers may lead to synaptic dysfunction/neuronal loss, responsible for the dementia that is present in AD patients.

1.6 The calcium hypothesis

Calcium (Ca^{2+}) is a ubiquitous second messenger that regulates diverse functions in eukaryotic cells, generating concentration gradients and binding to several proteins, receptors and ion channels. The regulation of intracellular calcium homeostasis is a very complex mechanism that is crucial for several functions and it is also involved in cell survival and death (Sanabria-Castro et al., 2017).

In particular, calcium plays an important role in regulating several neuronal processes. For example, it is well established that a transient increase in cytosolic Ca^{2+} levels $[Ca^{2+}]_c$ enhances neurogenesis and neurite growth; in contrast, a sustained increase in $[Ca^{2+}]_c$ is a basic molecular mechanism which increases sensitivity of cells to toxicity that can possibly lead to cell death (Wang and Sun, 2010).

The calcium hypothesis speculates that the main driving force for neurodegeneration in AD is the dysregulation of cellular calcium homeostasis. It has been already reported that in AD, the ability of neurons to regulate the influx, efflux and subcellular compartmentalization of calcium is impaired (Wang and Sun, 2010; Sanabria-Castro 2017).

These disruptions include several mechanisms, such as alterations in calcium buffering capacity, deregulation of calcium channels activities, excitotoxicity or disruption of mitochondrial functions

(Sanabria-Castro et al., 2017). Moreover, many evidences show that mutated presenilins directly cause Ca^{2+} dysregulation in AD (Pchitskaya et al., 2017).

1.7 The mitochondria cascade hypothesis

A growing amount of evidences suggests that mitochondria dysfunction is an early event during the development of AD. Many studies have already reported on the association between mitochondria impairment and Aβ/tau toxicity. Moreover, both genetic and environmental factors can directly or indirectly cause mitochondria impairment, including the increase of fragmented organelles, mtDNA damages, decrease of ATP, mitochondrial membrane potential and mitochondrial transport. The oxidative stress may form a vicious circle, which ends up with synaptic failure or cell death (Hu et al., 2017) (figure 7).

The mitochondria cascade hypothesis was proposed for the first time by Swerdlow and colleagues more than 10 years ago.

This hypothesis posits that age-related mitochondrial dysfunction eventually leads to the pathology and symptomatology of sporadic, late-onset AD (Karran and De Strooper, 2016; Swerdolw and Kahan, 2004; Swerdolw et al., 2014;).

The hypothesis consists of three aspects:

1) the genetic inheritance defines an individual's baseline mitochondria activity.
2) inherited and environmental factors can influence the rate at which age-associated mitochondrial changes develop and manifest. This means that greater mitochondrial performance should associate with slower brain aging and lesser mitochondrial durability should be related to faster brain aging (Swerdlow et al., 2014).
3) AD chronology depends on individual's baseline mitochondrial function and functional change rate. Those with low baseline function and fast rates of mitochondrial decline will develop symptoms at younger ages than those with high baseline function and slow rates of mitochondrial decline (Swerdlow et al., 2014).

There are many evidences that support this hypothesis, showing that mitochondria dysfunction may play a critical role on the onset and on the progress of late-onset AD cases. Some of these supporting data derive from basic epidemiologic studies of aging. Indeed, longevity analysis

reveals that although the best predictor of an individual's longevity is biparental longevity, the maternal one has a greater impact (Swerdlow and Khan, 2004). Moreover, data about both AD and Parkinson's disease (PD) suggest that among the affected parents there is a maternal overrepresentation. Taken together, all these findings suggest that a maternally inherited genetic factor (mtDNA) may determine not only how long one lives, but also may contribute to AD risk (Duara et al., 1993; Edland et al., 1996; Swerdlow et al., 2000).

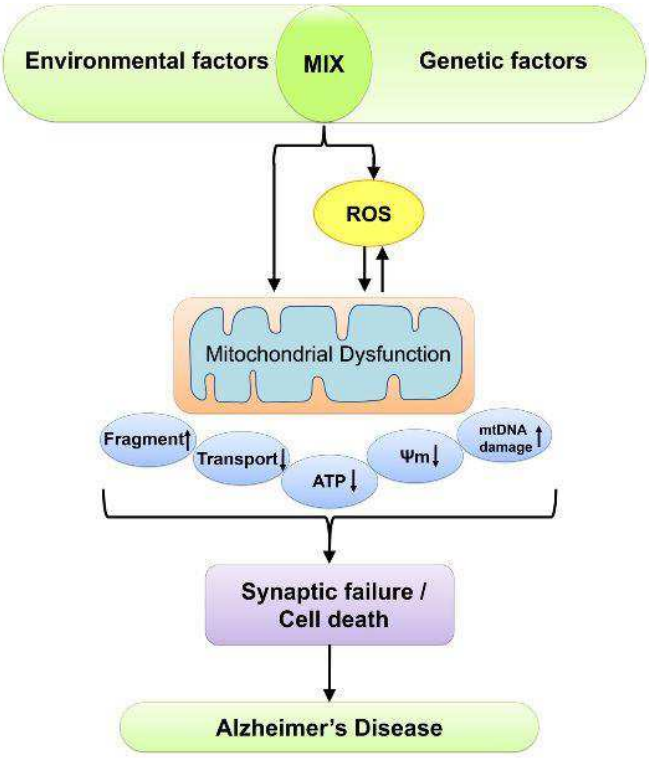

Figure 7: this figure explains how both environmental and genetic factors can directly or indirectly cause mitochondrial dysfunctions in AD (modified from Hu et al., 2017).

1.8 Transgenic mouse models of AD

The use of animal models of AD that display some features of the human clinical pathology is fundamental to better understand the molecular mechanisms of the disease and improve preclinical studies.

Nowadays, the genetically modified APP mouse models are the most widely used approach for *in vivo* screening and validation of preventive medications (Zash and Ashe, 2010), since without gene

manipulations, no small animal model is available to mimic the pathology for experimental and clinical studies of AD.

The AD research community has historically used the first-generation transgenic (Tg) mouse models overexpressing protein linked to FAD, such as mutated APP, or APP and presenilins. The use of these mouse models with genetically engineered FAD mutations to understand SAD is validated by the fact that, in general, Aβ amyloidosis and tauopathy symptoms are morphologically similar in both sporadic and familial cases of AD.

These mice exhibit key features of amyloid pathology such as extracellular Aβ plaques deposition in the brain followed by neuroinflammation and cognitive dysfunctions, even if specific details such as plaque age of onset, size and regional distribution, and Aβ species content depend on the specific transgenic line.

Since, these models don't display neurofibrillary tangles (NFT) formation or neuronal loss., in the effort to reproduce also NFT pathology, crossbreeding of mutant Tau-Tg mice with APP-Tg mice has been carried out, and an increase in tau pathology in some brain areas has been observed without affecting Aβ pathology (Bolmont et al., 2007; Lewis et al., 2001).

There are some limitations related to the first-generation mouse models: for instance, APP overexpression may induce *per se* behavioral abnormalities before AD pathology (Mucke et al., 2000). Moreover, it results in the overproduction of different APP fragments in addition to Aβ, making difficult to discriminate between the functional effects of additional Aβ and the excessive production of other pathological fragments. However, the main criticism to this generation of transgenic mouse models is mainly focused on the inconsistent drug effects occurred in some cases (Ohno, 2016).

Nevertheless, the first generation of mouse models has been essential to understand many aspects of AD pathology and still remains important for the research field.

In order to overcome the drawbacks due to APP overexpression, the second-generation mouse models were created by using the knock-in strategy. For example, an *App* knock-in mouse model has been developed allowing the overproduction of pathogenic Aβ peptides such as Aβ42 without overexpressing APP levels.

In the single *App* knock-in mouse models the murine Aβ sequence is humanized by changing three amino acids that are different between mouse and human (G678R, F681Y, H684R) and introducing

two FAD mutations into the endogenous mouse *App* gene (KM670/671NL: Swedish and I716F: Beyreuther/Iberian mutations) (Saito et al., 2014).

Mice carrying NL-F mutations, named App^{NL-F} are marked by higher Aβ42 production and increased Aβ42/ Aβ40 ratio without alterations in the expressions levels of APP or other fragments (Sasaguri et al., 2017). The high Aβ42 levels present in this model, lead to pathological Aβ deposition in cerebral cortex and hippocampus, which is followed by increased neuroinflammation around plaques from 6 months of age. Additionally, these mice develop cognitive dysfunctions at 18 months of age, that include deficits in spatial memory and flexible learning, enhanced compulsive behavior and reduced attention performance (Masuda et al., 2016).

As already observed in APP overexpression mice, also the knock-in mice don't exhibit tau pathology and the presence of multiple mutations in the *App* gene (which are not present in human patients) may interact with each other in some cases and could not exactly represent clinical AD (Sasaguri et al., 2017). Despite some disadvantages, *App* knock-in mice could be useful as preclinical AD models, for instance to find biomarkers for preclinical cases, identify molecules that cause tauopathy in an Aβ pathology-dependent manner, studies for preventive drugs, create a platform for the generation of improved AD models and to study cellular phase of AD (Sasaguri et al., 2017; De Strooper and Karran, 2016).

The second-generation mouse lines solved some limitations of previous models, thus allowing the first steps for the future third generation models. Even if many studies about this disorder have been carried out with the best available mouse lines at time, we always have to consider the species differences between human beings and rodents in terms of neuroanatomy, genetics and behaviors (Nithianantharajah and Grant, 2013).

In order to overcome part of these problems, Espuny-Camacho and colleagues have recently developed a new chimeric AD mouse model by transplanting human pluripotent stem cells (PSCs) into AD mouse brain (Espuny-Camacho et al., 2017). Furthermore, Okano's group is going to generate non-human primate models of AD which may limit species barriers, thus reducing time and cost of drug development (Okano et al., 2016; Sasaguri et al., 2017).

1.9 PS2.30H transgenic line

This mouse model, also known as single transgenic mouse (Tg), is a homozygous single transgenic line expressing the human FAD-linked mutation PS2-N141I which is driven by prion promoter and ubiquitously expressed (Ozmen et al., 2009). They were obtained by embryo revitalization from Charles Rivers Laboratories (CRL, Lecco, Italy).

Even if this line has not been completely characterized, our lab published that in brain homogenates from 2-week-old PS2 mice and in primary neuronal culture at 10-12 days DIV, the total amount of PS2 was 1.8-2.2 higher compared to WT mice. Moreover, in brain slices, upon GABA-A antagonist picrotoxin (PTX) addition, PS2 neurons display increased Ca^{2+} excitability (Kypanyula et al., 2012).

The immunohistochemistry studies performed in hippocampal slices didn't show any significant differences neither in extracellular amyloid deposition, in 6 or 12-month-old mice, nor in astrogliosis, in 6-month-old mice. Additionally, the accumulation of Aβ42 in PS2 and WT mice is comparable at any age (Fontana et al., 2016). These mice have been used in our study to evaluated possible effects due to the mutated PS2 protein.

1.10 B6.152H transgenic line

The B6.152H mice are a homozygous double transgenic line, also called PS2APP or 2Tg. These mice carry the same human FAD-linked PS2 mutation already described in the PS2 mice, plus the human APP Swedish mutation (K670N, M671L) under the control of the Thy.1 promoter, which is expressed only in neurons.

It has been found that the co-expression of PS2 and APPSwe alters the metabolism of APP, increasing Aβ42 production. In particular, 5-month-old PS2APP mice show Aβ peptides (both Aβ40 and Aβ42 peptides) in cortex and hippocampus (Richards et al., 2003; Ozmen et al., 2009). More precisely, there is an age-related accumulation of these peptides, which is accompanied by inflammation (astrogliosis and microgliosis) and cognitive deficits, such as the alteration in the acquisition of spatial learning (Ozmen et al. 2009; Fontana et al., 2016) (figure 8). Behavioral studies have been performed from 4 months up to 16 months of age. In 4-month old mice, the general appearance and all reflexes of the PS2APP mice were similar to controls, except the body

weight that was 10% lower. Neurological tests showed subtle differences, such as a higher locomotor activity, reduced grip strength and slower swim speed in PS2APP mice compared to controls and similar results were found in the other age groups. PS2APP mice demonstrated an age related cognitive impairment after 8 months (Richards et al., 2003).

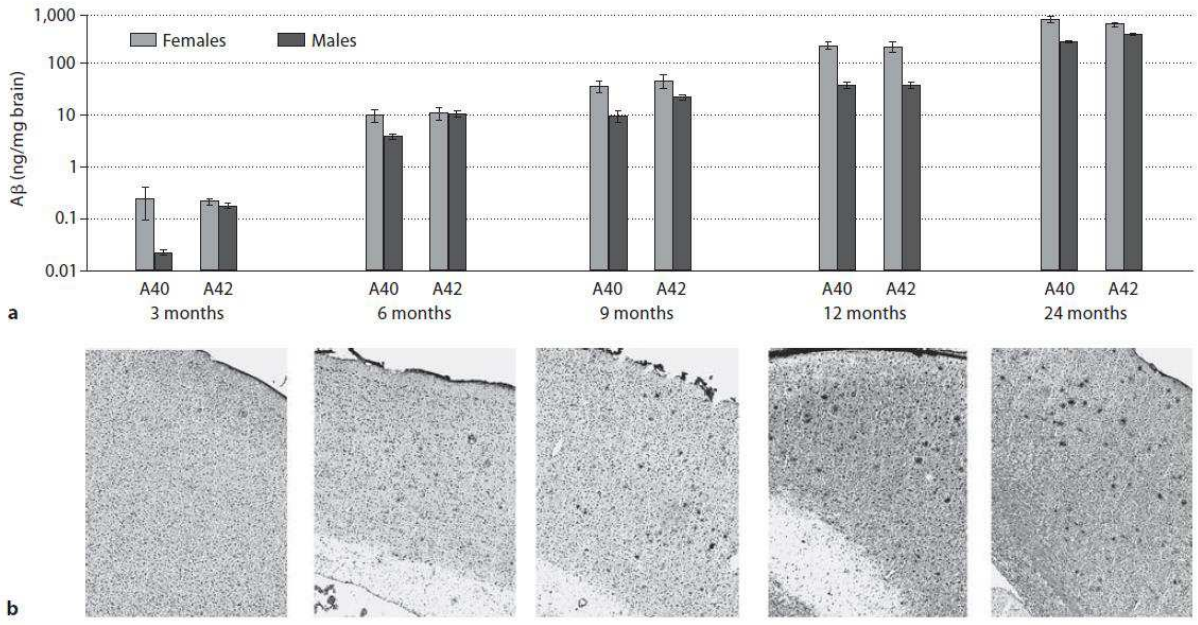

Figure 8: analysis of cerebral amyloidosis in PS2APP mice. In this case, the levels of Aβ40 and Aβ42 were measured in urea extracts of brain homogenates of PS2APP mice, ranging from 3 to 24 month of age (upper part); congophilic deposits are detectable from the age of 6 months (lower part). (modified from Ozmen et al., 2009).

1.11 Hippocampus and AD

The hippocampus is a small region in the brain located in the medial temporal lobe, under the cerebral cortex. It belongs to the limbic system and it plays a key role in episodic memory and spatial navigation (Lazarov and Hollands, 2016). The so-called hippocampus proper consists of the CA3, CA2 and CA1 regions (CA comes from *cornus ammonis*), and together with the dentate gyrus (DG) and the subiculum, forms a functional brain system called the hippocampal formation (HF) (figure 9).

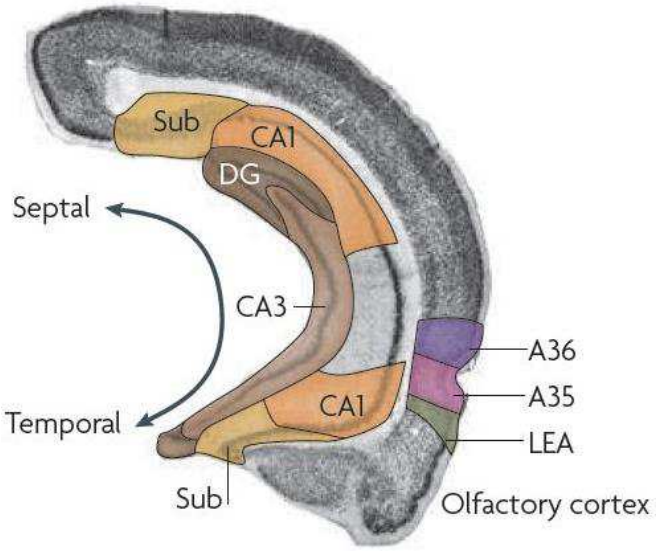

Figure 9: coronal section showing the anatomical structure of the hippocampal formation (HF), consisting of the dentate gyrus (DG; dark brown), CA3 (medium brown), CA2 (not indicated), CA1 (orange) and the subiculum (Sub; yellow), (modified from Van Strien et al., 2009).

The main imput to the hippocampus is the perforant pathway emanating from the enthorinal cortex (EC), which forms excitatory synapses with the granule cells present in the DG. It is divided into two sets of fibers: the medial and the lateral perforant pathways (MPP and LPP, respectively).

The first one is generated at the medial portion of the EC, it makes connection onto the proximal dendritic area of the granule cells and it is involved in spatial information; the other one is generated at the lateral portion of the EC and synapses onto the distal dendrites of these same cells, mediating visual object information (for example odors or objects) (Marchetti and Marie, 2011).

In contrast to normal aging where the DG is primarily impacted, AD postmortem studies show that the CA1 subregion and the subiculum are the most affected hippocampal regions (Lazarov and Hollands, 2016).

Indeed, it has become clear that the neuronal cell loss in the entorhinal cortex and hippocampus which occurs in AD, is preceded by a long period of deficits in the connectivity of the HF that contributes to the vulnerability of these circuits (Lazarov and Hollands, 2016).

Several evidences suggest that the neurogenesis is impaired in mouse models of FAD, but it is still not clear how hippocampal neurogenesis and its gradual impairment with age may contribute to

the cognitive dysfunction in the disease (Lazarov and Marr, 2010,). Additionally, it has been found that neuronal hyperactivity precedes amyloid plaques formation, suggesting that it may represent one of the earliest dysfunction in the pathophysiological cascade of AD initiated by Aβ oligomers (Busche and Konnerth, 2016).

2. Mitochondria

Mitochondria are double membrane-bound organelles that are present in eukaryotic cells. There are two main hypothesis regarding their origin:

1-The autogenous hypothesis states that mitochondria were born by splitting of a DNA portion from the nucleus of the eukaryotic cell at the time of divergence with the prokaryotes, which portion would have been enclosed by membranes (Martin et al., 2015).

2-The endosymbiotic hypothesis posits that mitochondria were originally prokaryotic cells, able to implementing oxidative mechanisms that were not possible for eukaryotic cells. Over time, they became endosymbionts living inside the eukaryote cells (Martin et al., 2015).

The latter one is the most widely accepted hypothesis, since these organelles share many feature with bacteria: they have their own DNA and their replication is not coupled to cell division.

As already mentioned, mitochondria are surrounded by a double-membrane system consisting of an inner (IMM) and an outer (OMM) mitochondrial membrane separated by an intermembrane space. The IMM forms numerous folds called cristae, which extend into the matrix of the organelle. The matrix is the mitochondria internal space enclosed by the IMM. Each of these components plays distinct functional roles, with the matrix and IMM representing the major working compartments of mitochondria.

The volume of mitochondrial matrix is tightly regulated by osmotic balance between mitochondria and the cytosol and this regulation is crucial for maintaining the structural integrity of the organelle (Kaasik et al., 2007). The matrix contains the mitochondrial DNA and the enzymes involved in the oxidative metabolism. The oxidative breakdown of glucose and fatty acids is the principal source of metabolic energy in animal cells.

The first part of glucose metabolism, the glycolysis, occurs in the cytosol, where glucose is converted to pyruvate and the resultant free energy is used to form ATP and NADH. Pyruvate is

then transported into the mitochondria, where it is completely oxidized to CO_2 and H_2O. This process involves the initial oxidation of pyruvate to acetyl CoA, which is broken down to CO_2 via the tricarboxylic acid cycle (TCA). The oxidation of fatty acids also provides acyl-CoA which is similarly metabolized first by the beta-oxidation and then by the TCA cycle in mitochondria.

2.1 The electron transport chain

The electron transport chain (ETC) in mitochondria consists of a series of protein complexes that transfer electrons from electron donors to electron acceptors via redox reactions, coupling this transfer with the pumping of protons from the matrix to the intermembrane space (figure 10).

To start, two electrons are initially carried to the first complex (Complex I) through NADH. Complex I (also called NADH-dehydrogenase or NADH-Q oxydoreductase) is a very large enzyme composed of 46 subunits. Complex I contains flavin mononucleotide (FMN) that is the entry point for electrons from NADH, and at least 6 different iron-sulfur (Fe-S) clusters (Lenaz et al., 2006). FMN, which is derived from vitamin B_2 (also called riboflavin), is one of several prosthetic groups or co-factors that are present in the electron transport chain. Electrons in the iron-sulfur clusters of complex I are shuttled to coenzyme Q, allowing also the flux of four hydrogen ions out of the matrix of the mitochondrion. At the level of complex II (the succinate dehydrogenase or succinate-coQ reductase) other electrons originating from succinate are delivered to coenzyme Q by flavin adenosine dinucleotide (FAD). The complex II is a parallel electron transport pathway to complex I, but differently from it, it doesn't transport protons into the intermembrane space.

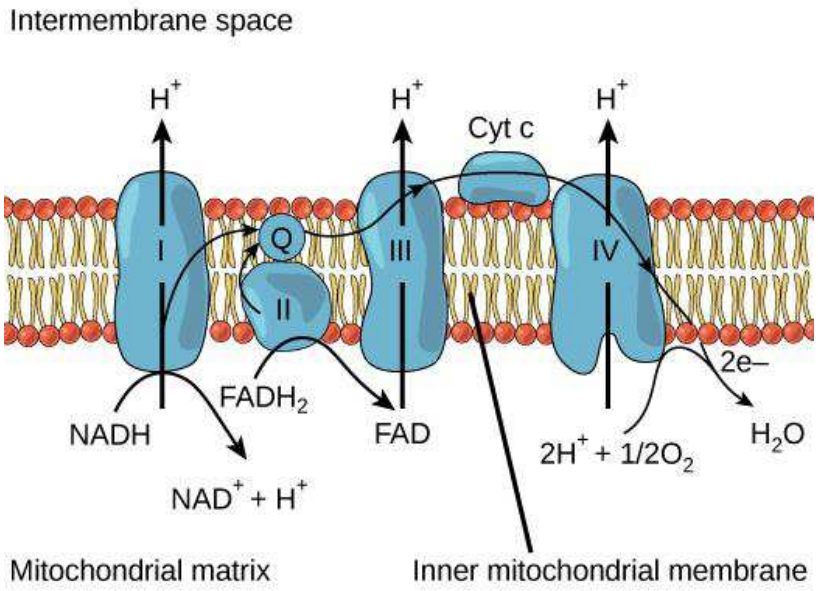

Figure 10: the electron transport chain is composed by a series of electron transporters placed in the IMM that shuttles electrons from NADH and $FADH_2$ to molecular oxygen. In this pathway, protons are pumped from the mitochondrial matrix to the intermembrane space, and oxygen is reduced to form water (modified from Lumen Learning).

Afterwards, the electrons delivered by coenzyme Q are accepted by complex III (also known as cytochrome bc_1 complex, or $CoQH_2$-cytochrome *c* reductase).

The third complex is composed of cytochrome b, another Fe-S protein, Rieske center (2Fe-2S center), and cytochrome c proteins provided of a prosthetic heme group. In this way, the iron ion at its core is first reduced and then oxidized, as it transfers the electrons, fluctuating between different oxidation states: Fe^{2+} (reduced) and Fe^{3+} (oxidized). Complex III pumps protons through the membrane and moves its electrons to cytochrome c for transport to the fourth complex of proteins and enzymes.

The complex IV (cytochrome c oxydase) is composed of cytochrome proteins c, a, and a_3. This complex contains two heme groups (one for each of the cytochromes a and a_3) and three copper ions (a pair of Cu_A and one Cu_B in cytochrome a_3). The cytochromes hold an oxygen molecule very tightly between the iron and copper ions until the oxygen is completely reduced. Indeed, the complex IV receives four electrons from four molecules of cytochrome c that are transferred to molecular oxygen (O_2) which picks up two hydrogen ions from the surrounding medium producing water (H_2O). The removal of the hydrogen ions from the system also contributes to the ion

gradient used in the process of chemiosmosis. Coupled to the electron flow through the respiratory chain, eight protons are removed from the mitochondrial matrix (although only four are pumped across the membrane), contributing to the proton gradient.

According to the chemiosmotic theory proposed by the Nobel Prize winner Peter Mitchell, the proton gradient originating from the ETC activity generates the proton motive force used to drive ATP production (see below for more details).

2.2 The ATP synthase

The ATP synthases are multisubunit enzyme complexes that are integral components of the energy-transducing membranes of bacteria, chloroplasts and mitochondria (Walker, 1998).

The mitochondrial F-ATP synthase is a well conserved multi-subunit complex located in the IMM (Boyer 1997; Futai et al., 2012). The complex consists of a hydrophilic catalytic F_1 subcomplex protruding in the mitochondrial matrix, and by a membrane-embedded F_o subcomplex, linked by central and peripheral stalks. Several atomic structures reveal that the F_1 subcomplex is composed of three copies of each of the nucleotide-binding subunits α and β, which alternate around the γ subunit (Bernardi et al., 2015). The γ-subunit, together with the F_1 subunits δ and ε forms the central stalk that is associated to the F_o c-ring, a structure composed by 8 copies of subunit c, whereas the remaining part of F_o comprises subunits a, b, d, e, f, g A6L, OSCP (the oligomycin sensitive conferring protein) and F6 (figure 11).

Electron microscopy of mitochondria from different sources (Davies et al., 2011) clearly show that F-ATP synthase is organized in dimers, which are crucial to maintain a high local curvature of the IMM and normal cristae morphology, and it forms long rows of oligomers at the cristae edges of mitochondria (Bernardi et al., 2015; Davies et al 2012; Habersetzer et al., 2013).

The detailed structure of most of the bovine mitochondrial ATP synthase has been resolved by X-ray crystallography by John Walker and his group in 1994.

In his chemiosmotic theory, Mitchell described how the redox energy coming from oxidative metabolism is used to create a proton electrochemical gradient across the IMM. He coined the name “protonmotive force” (*pmf* or Δp) to describe this gradient and he also proposed that this gradient is used to drive ATP synthesis.

Indeed, to synthesize ATP, the F_o "motor" translocates H^+ ions across the membrane taking advantage of this Δp to drive rotation of a ring of c-subunits relative to subunit a. Protons flow into the cytoplasm concurrent with clockwise rotation, thus forcing conformational changes in the catalytic sites of F_1 and leading to ATP synthesis.

Few years ago, it has been proposed that the ATP synthase is involved in the mitochondrial permeability transition (PT) (Giorgio et al., 2013).

The PT defines an increased permeability of the IMM to ions and solutes triggered by matrix Ca^{2+} alone or together with specific inducers; among them, the most classical are Ca^{2+}, P_i and thiol oxidants (Bernardi et al., 2006), whereas the opening probability can be reduced by several compounds, including Mg^{2+} ions, adenine nucleotides and the immunosuppressant cyclosporin A (CsA) (Crompton et al., 1988).

The high-conductance channel responsible of the PT was first identified by patch-clamping of the IMM and called mitochondrial megachannel (MMC) (Kinally et al., 1989; Petronilli et al., 1989; Szabò and Zoratti, 1991; Szabò et al., 1992)

The PTP is regulated by matrix cyclophilin D (CyPD) (Basso et al., 2008), which also regulates the F-ATP synthase (Giorgio et al., 2009). These observations, together with the fact that purified ATP dimers have a similar PTP channel activity, suggest that the PTP may be composed by dimers of F-ATP synthase (Giorgio et al., 2013).

Interestingly, in a recent paper it has been reported the physical interaction between OSCP and Aβ peptides and the selective loss of OSCP in brains from AD mouse models and AD patients. (Beck et al., 2016).

It has been suggested that as the pathology progresses, brain mitochondria gradually undergo OSCP loss and OSCP /Aβ interaction. The latter event alters the OSCP capability to keep the ATP synthase complex integrity, causing severe mitochondrial dysfunction, including decreased ATP production, increased ROS production as well as the PTP opening.

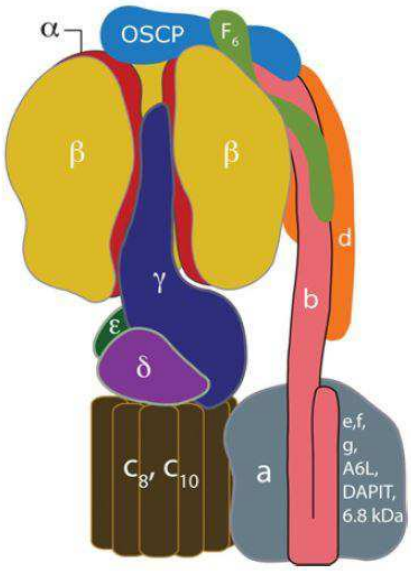

Figure 11: structure of mitochondrial ATP synthase. The human form consists of two functional domains, F_1 and F_o. F_1 comprises 5 different subunits (three α, three β, and one γ, δ and ε) and is located in the mitochondrial matrix. F_o contains subunits c, a, b, d, F_6, OSCP and the accessory subunits e, f, g and A6L. F_1 subunits γ, δ and ε constitute the central stalk of the synthase. Subunits b, d, F_6 and OSCP form the peripheral stalk. Protons pass from the intermembrane space to the matrix through F_o, which transfers the energy created by the proton electrochemical gradient to F_1, where ADP is phosphorylated to ATP.

3. Mitochondria and neurodegeneration

Mitochondria play an essential role in cell respiratory processes, and they are also involved in many other cellular functions, such as intracellular signaling, ROS production, cell cycle regulation, calcium homeostasis and apoptosis (Filosto et al., 2011). In literature, many evidences suggest that mitochondria can critically regulate cell death and survival, play a crucial role in aging and represent one of the key features in the pathogenesis of neurodegenerative disease (Golpich et al., 2017). The relationship between mitochondria and neurodegenerative diseases is not surprising if we consider that in neurons, as well as cardiac and skeletal muscle cells, the energy supply required for their functionality is highly dependent on these organelles, explaining why they are particularly vulnerable to energy-dependent defects resulting from mitochondrial alterations (Filosto et al., 2011).

Indeed, mitochondria impairments have been documented in many neurodegenerative diseases, including AD, Parkinson's disease (PD), Huntington's disease (HD) and amyotrophic lateral sclerosis (ALS).

Mitochondrial dysfunction may arise as a consequence of mutated mitochondrial DNA or mutated proteins that interact directly or indirectly with mitochondria. In most cases it is still unclear where mitochondria sit in relation to the overall disease cascade that ultimately causes neuronal dysfunction and death, and there is still a large discussion regarding the question of whether mitochondrial impairment is a necessary step in neurodegeneration (Lezi and Swerdlow, 2012). Before discussing in details what is the state of the art of mitochondria impairments and AD, let's see what has been reported until now about the most diffused neurodegenerative diseases.

3.1 Parkinson's disease (PD)

From the clinical point of view, PD is marked by progressive rigidity, bradykinesia and tremor, whereas the pathological features are loss of pigmented neurons in the substantia nigra and the presence of Lewy bodies.

Even if the cellular mechanisms that leads to cell death in the nigrostriatal system are still unclear, it is widely accepted the involvement of oxidative stress, chronic inflammation, aberrant protein folding, abnormal protein aggregation and mitochondrial dysfunction (Golpich et al., 2015; Greenamayre and Hastings, 2004; Ortega-Orellano et al., 2011).

Regarding the mitochondrial involvement, many hypothesis have been proposed; among them, it has been found, for example, a significant decrease in the complex I activity as well as in the coenzyme Q, ubiquinone and also in complex IV in postmortem studies of PD patients brains (Choi et al., 2006; Keeney et al., 2006; Nq et al., 2012).

It has been reported that mitochondrial dysfunction could be mediated by many proteins associated with PD, such as Parkin, PINK1, DJ1 and α-synuclein that regulate neuronal degeneration. Following mitochondrial depolarization, dynamin-related protein 1 (Drp1) and Parkin are co-recruited to mitochondria in proximity of PINK and Parkin prevents Drp 1 induced mitochondrial fission (Balog et al., 2106). Hence, loss/silencing of Parkin and PINK1 lead to mitochondrial fragmentation and early onset of PD (Lutz et al., 2009; Poole et al., 2008; Tan and Skipper, 2007; Valente et al., 2004) and furthermore, downregulation of PINK1 induces an

impairment in mitochondrial fusion/fission balance that can sensitize dopaminergic neurons to neurotoxins (Rojas-Charry et al., 2014).

Additionally, it has been reported that α-synuclein localizes to mitochondria because of its high affinity to mitochondrion-specific acidic phospholipids and cardiolipin (Devi et al., 2008) and this interaction is directly linked to mitochondrial fragmentation by shifting the dynamic equilibrium toward fission, finally inducing neuronal death (Nakamura et al., 2011).

3.2 Huntington's disease (HD)

HD is an inherited and an autosomal dominant disorder marked by psychiatric disturbances, cognitive deterioration and motor impairments. From the pathological point of view HD is characterized by loss of long projections neurons in cortex and striatum (Lin and Beal, 2006). The main cause of this disorder is the increased number of cytosine-adenine-guanine (CAG, translated in glutamine) triplet repeats in the huntingtin (HTT) gene and marked by accumulation of insoluble polyglutamine-containing Htt protein aggregates in affected neurons (Golpich et al., 2016; Yang et al., 2008).

Several evidences demonstrated that mitochondria alterations are involved also in this severe disorder (Chaturvedi et al., 2010; Chiang et al., 2011; Quintanilla et al., 2008). There are different mechanisms by which the mutation could affect the organelles activity.

For example, HTT may directly interact with mitochondria; in one study, it has been reported that lymphoblasts mitochondria from HD patients and brain mitochondria from YAC transgenic mice expressing HTT with 72 repeats present a lower mitochondria membrane potential and a depolarization at lower calcium concentration (Panov et al., 2002). Moreover, in late-stage HD patients, studies of mitochondria in striatal neurons revealed a decrease in the activity of several electron transport chain complexes, including complexes II, III and IV (Reddy et al., 2009).

Another possible pathway through which mutant HTT may alter mitochondrial functionality is by altering transcription. For example, it has been found a downregulation of PGC-1α, key factor for the regulation of different pathways such as mitochondrial biogenesis and electron transport chain activity (Cui et al.,2006); these data suggest that a deficiency in PGC-1α and downstream genes may lead to mitochondrial impairments in HD, especially in muscle (Chaturvedi et al., 2009), fat tissue (Phan et al., 2009) as well as brain (Weydt et al., 2006).

3.3 Amyotrophic lateral sclerosis (ALS)

ALS is a progressive adult-onset neurodegenerative disorder, clinically characterized by progressive weakness, atrophy and spasticity of muscle tissue, caused by the degeneration of upper and lower motor neurons in cortex, brainstem and spinal cord (Lin and Beal., 2006).

Similarly to AD, ALS consists in two different forms: the sporadic one, which is the most diffused, and the familial one, which represents 10% of cases (among these, about 20% of cases show mutations in the Cu/Zn-superoxide dismutase, SOD1)

In both sporadic and familial forms, postmortem and biopsy samples from the spinal cord, nerves and muscles show alterations in mitochondrial structure, number and localization. Additionally, defects in the ETC complexes have been reported in muscle and spinal cord (Lin and Beal, 2006).

However, it is still difficult to understand whether mitochondria contribute to the pathogenesis or are just bystanders; for this reason, the studies on ALS and these organelles have been focused on expression of mutant SOD1 in animal and cellular models of the disease.

In fact, even if SOD1 has traditionally been thought to be a cytoplasmic protein, immunoreactivity experiments reveal that the enzyme is concentrated inside vacuolated mitochondria (Lin and Beal, 2006). Of note, the SOD1 localization to mitochondria has been reported to occur only in affected tissues and this preferentially happens for the mutated enzyme (Liu et al., 2004).

Interestingly, interaction between SOD1 and mitochondria may lead to different pathways by which the organelles activity and cell survival could be affected.

Mitochondrial targeting of mutant SOD1 causes cytochrome *c* release and apoptosis, whereas targeting to the ER or nucleus do not cause the same effect (Takeuchi et al., 2002). Cleveland and coworkers suggest that mutant SOD1 may accumulates and aggregates at the OMM and congests the protein import machinery, eventually leading to mitochondrial impairment (Liu et al., 2004). Furthermore, mutant SOD1 has been proposed to promote aberrant ROS production. Indeed, in mice expressing mutant human SOD1, it has been found oxidative damage in mitochondrial lipids and proteins, followed by impaired respiration and ATP synthesis (Mattiazzi et al., 2002).

3.4 Mitochondria and AD

Nowadays, it is well known that during AD progression, tau pathology and Aβ impair neuronal cells affecting energy supply, antioxidant response and synaptic activity. Furthermore, as already said above, a growing body of evidences suggests that mitochondrial functionality could be affected by the presence of Aβ/tau pathology in terms of morphology or dynamics, bioenergetics and transport (Cabezas-Opazo et al., 2015) (figure 12).

It has been reported that impairments in fission/fusion proteins such as dynamin related protein1 (Drp1), Mitofusins 1 and 2 (Mfn 1 and Mfn 2) and optic atrophy protein (OPA1), can lead to defects in mitochondrial dynamics (DuBoff et al., 2013). In brain cells, a fine regulation of fission and fusion proteins is essential to keep a normal mitochondrial functionality (concerning energy supply, antioxidant defenses and calcium homeostasis) (Cabezas-Opazo et al., 2015).

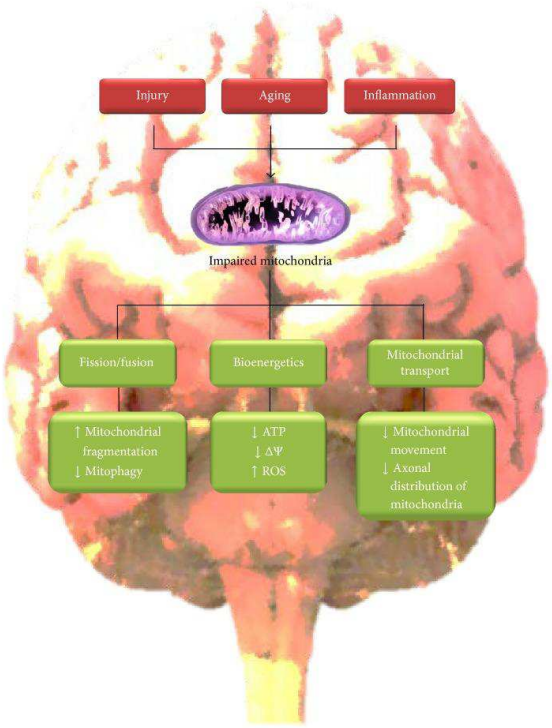

Figure 12: mitochondrial dysfunction in AD. Factors that contribute to AD such as injury, aging and inflammation can affect crucial mitochondrial features that are mitochondrial dynamics, bioenergetics and mitochondrial movement (modified from Cabezas-Opazo, 2015).

For example, it has been reported an altered mitochondrial morphology in brain samples of AD patients and these results have been further confirmed in cell lines in which WT and Swedish

mutant forms of APP protein were overexpressed. Mitochondria morphology changes from thin and elongated to a fragmented and rounded shape and this effect is more pronounced in the cells overexpressing the APP Swedish mutation (Wang et al., 2008). Other studies analyzed cortical samples from AD patients, finding high mRNA levels of Drp 1 and lower mRNA levels of fusion proteins such as OPA1, Mfn1 and Mfn2 (Manczak et al., 2011).

However, most of the data that shows mitochondrial dysfunctions in AD comes from studies in which Aβ directly impairs mitochondrial bioenergetics, including a decrease in ATP production, alteration of the electron transport chain complexes, mitochondrial membrane potential decrease and higher ROS production (Crouch et al., 2008). For instance, it has been reported that Aβ has a significant role in ROS production and it can also significantly impair the electron transport chain functionality (Crouch et al., 2008; Mao and Reddy, 2011). Additionally, it has been found that the exposure to increased Aβ reduces mitochondrial membrane potential and the respiration rate. Furthermore, several studies reported that Aβ addition leads to mitochondria swelling, apoptosis and mitochondrial permeability transition pore opening (Mao and Reddy, 2011).

Mitochondrial movements along the axon are mediated by microtubules, which are able to transport these organelles between the soma and the nerve terminals. The transport of molecules to the nerve terminal is called “anterograde” whereas the movement toward the soma is called “retrograde” (Wang et al., 2015). It has been reported that mouse hippocampal neurons treated with Aβ show a significant reduction in the anterograde mitochondrial transport, which seems to be related to synaptic failure and to the hallmark memory impairment of AD (Calkins and Reddy, 2011). Moreover, it seems that tau is involved in the axonal transport impairment mediated by Aβ and its reduction may protect against this Aβ-induced toxic effect (Vossel et al., 2010).

In addition to Aβ, increasing evidences suggest that oxidative stress is linked to mitochondrial dysfunction in AD. It is known that oxygen metabolism in the mitochondria and peroxisomes produces oxygen agents called reactive oxygen species (ROS) which comprise free radicals (small molecules with unpaired electrons in the outer shell, such as the hydroxyl radical OH^- and the superoxide radical O_2^-) and the hydrogen peroxide (H_2O_2) (Meraz-Dios et al., 2014). Although these molecules are necessary for biological functions, they show high reactivity with macromolecules such as membrane lipids, proteins, and DNA; this interaction could be detrimental and lead to cellular senescence. During the evolution, living organism have developed antioxidant mechanisms that can remove the reactive species, scavenging ROS or their precursor and binding trace

elements). However, an imbalance between oxidants and antioxidants agents could lead to oxidative stress, a phenomenon that is related to neurodegenerative diseases and aging processes.

Also from what concerns AD cases, it has been found that the oxidative damage occurs early in the brains, before the onset of significant plaque pathology and also before Aβ deposition in transgenic APP mice (Pratico et al., 2001; Nunomura et al., 2001).

Indeed, the brain is composed by several peroxidation-susceptible lipids and moreover, it is marked by a high demand of oxygen for its activities (Halliwell et al., 1992). For this reasons, oxidative stress on nervous tissue may seriously damage the brain via several interacting mechanisms, including an increase in intracellular free Ca^{2+}, release of excitatory amino acids and neurotoxicity (Bambrick et al., 2004).

Whether the oxidative stress causes mitochondrial dysfunction or if mitochondrial dysfunction induces oxidative stress remains to be elucidated (Wang et al., 2014). However, it is widely accepted that under physiological conditions, as well as in pathological processes, complex I and complex III are the main producers of ROS in the brain, (Hroudovà et al., 2014). Furthermore, it has been suggested that dysfunctional mitochondria are less efficient producers of ATP but more efficient producers of ROS, representing a major source of oxidative imbalance found in AD (Gibson et al., 1998; Castellani et al., 2002).

Given that mitochondria are the production site of a significant proportion of ROS, mtDNA is thought to be more susceptible to oxidative damage because of its proximity to the high concentration of ROS, the lack of efficient DNA repair mechanisms in the mitochondria (Croteau et al., 1999; Yakes and Houten, 1997), and the lack of DNA-protective histones (Richter et al., 1988), even if the latter two aspects have been recently questioned (Choi et al., 2011; Liu and Demple, 2010). Oxidative damage to DNA results in strand breaks, abasic sites (apurinic/apyrimidinic), base changes, and deletions (Phillips et al., 2014). Likely, mtDNA is not primary implicated in AD pathogenesis, but it can be involved subsequently (Mancuso et al., 2009). Moreover, changes have been reported in the expression of both mitochondrial and nuclear genes encoding parts of complex I and IV enzymes, which may contribute to alterations of oxidative metabolism in AD (Aksenov et al., 1999).

Mitophagy is another important feature of mitochondria that is altered in neurodegenerative diseases, including AD.

Mitophagy is a selective form of autophagy involved in the elimination of dysfunctional mitochondria and it is an essential quality control mechanism to protect mitochondria network's integrity and functionality (Rodolfo et al., 2017). A couple of years ago, it has been observed in brains from AD patients a strong induction of the Parkin-dependent mitophagy caused by a higher recruitment of Parkin to damaged mitochondria (Ye et al., 2015). Moreover, it has been found that Parkin over-expression in an AD mouse model is able to enhance the autophagic clearance of impaired mitochondria and prevent dysfunctions in these organelles (Khandelwal et al., 2011; Martin-Maestro et al., 2016).

Given that mitochondria dysfunction plays a crucial role in AD pathogenesis and seems to be present at early time of the disease, several groups suggest that rescuing mitochondrial functions through the improvement of mitochondrial dynamics, bioenergetic and transport should represent a useful target for an early therapeutic solution against neurodegeneration observed in AD (Cabezas-Opazo, 2015).

RESULTS

1 Properties of mitochondria isolated form brain cortex of wild type and FAD transgenic mice

1.1 *Oxygen consumption rate*

Mitochondria functionality can be easily evaluated directly in organelles isolated from the tissue of interest, or from cultured cells. To asses if brain mitochondria physiology is somehow influenced by the presence of mutated forms of the human proteins Presenilin 2 (hPS2m) and/or APP (APP/swe), and the time of onset of potential modifications, we isolated mitochondria from the cortex of wild type and transgenic animals of different ages, and measured the oxygen consumption rate, at basal, ADP-stimulated and uncoupled conditions by mean of a Clark electrode. Briefly, upon mitochondria isolation and protein quantification, the measurements were performed in a KCl-based saline containing rotenone, to inhibit respiratory chain complex I. After mitochondria addition into the electrode's chamber, the following injections were performed, as also described in figure 13 A:

- 5 mM Succinate (state 2 respiration)
- 100 μM ADP (state 3 respiration)
- 1 μg/ml Oligomycin (state 4 respiration)
- 100 nM FCCP (uncoupled state respiration)

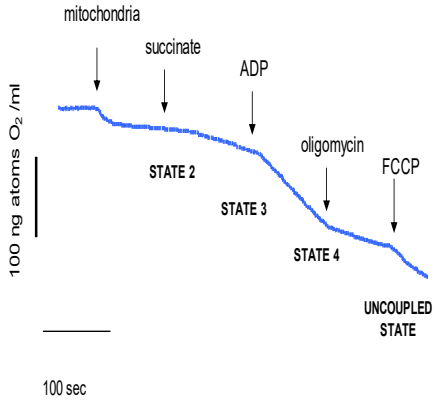

Figure 13 A: representative trace of OCR experiment. Where indicated by arrows mitochondria (1.5 mg/ml), succinate (5 mM), ADP 100 μM, oligomycin 2 μg/ml, and FCCP 100 nM were added.

The slope of the curve was measured after each addition and then translated into oxygen consumption rate. We evaluated the respiratory control, defined as the ratio between the ADP-stimulated respiration and state 4 respiration, and the respiratory capacity, defined as the ratio between uncoupled respiration and state 4 respiration. The figure 13 B shows the experiments performed with brain-cortex mitochondria isolated from WT, PS2 and PS2APP 6-month old mice.

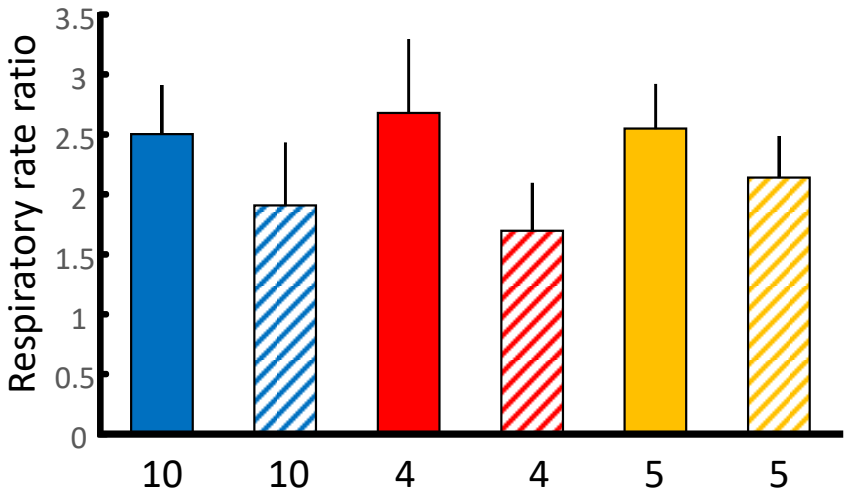

Figure 13 B: respiratory control (solid color bar) and respiratory capacity (hatched bar) of isolated brain-cortex mitochondria from 6-months-old mice WT (blue) PS2 (red), PS2APP (yellow). Mean ± SD. N=number of independent measurements, from least two different animals for genotype.

Since the alterations correlated with Alzheimer's disease could manifest late in the life of the individual we examined oxygen consumption rates also in mitochondria isolated from older animals, up to 24-month of age (figure 13 C).

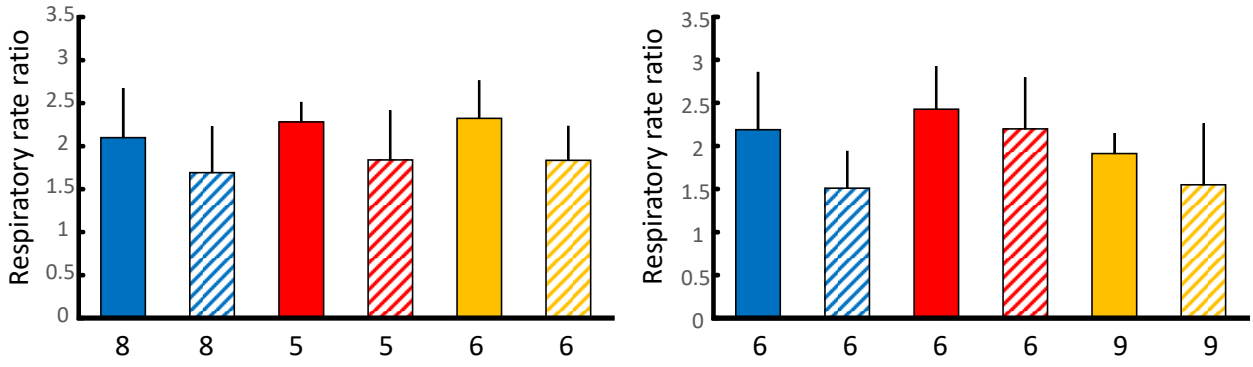

Figure 13 C: respiratory control (solid color bar) and respiratory capacity (hatched bar) of isolated brain-cortex mitochondria from 12-month-old (left) and 24-month old (right) mice. WT (blue), PS2 (red), PS2APP (yellow). Mean ± SD. N=number of independent measurements, from at least two different animals for genotype.

We observed that, under these experimental conditions, both the respiratory control and the respiratory capacity were similar among the three genotypes¸ and this prompted us to conclude that, most likely, the mitochondrial respiratory chain downstream complex I is not affected by the presence of the mutated human FAD proteins.

1.2 Mitochondria membrane potential

Mitochondria membrane potential was estimated using the fluorescent dye Rhodamine 123 (Rho 123), a cationic molecule that accumulates in the mitochondrial matrix driven by the negative membrane potential. Also in this case, the experiments were performed with rotenone to inhibit complex I. As shown in figure 14 A, the addition of succinate to de-energized mitochondria by stimulating mitochondria respiration allows the generation of the membrane potential, as a consequence Rho 123 is driven inside the matrix and the increase in concentration causes the quenching of its fluorescence (Emaus et al., 1986, Scaduto et al., 1999), on the other hand, the addition of FCCP disrupts the membrane potential, Rho 123 flows outside of the organelles, and the fluorescence values return close to initial values.

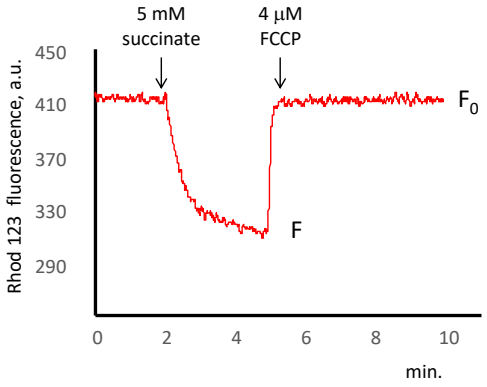

Figure 14 A: representative trace of mitochondria membrane potential measurement. Mitochondria and Rho 123 addition are not shown. Where indicated 5 mM succinate, and 4 µM FCCP were added.

The observed fluorescence variations can be translated into membrane potential values using the Nernst equilibrium potential equation

$$\Delta\Psi = 2.3\ RT/nF \ln \frac{[X^{n+}]_{out}}{[X^{n+}]_{in}}$$

where R is the universal gas constant, T the temperature in Kelvin, n the valence of the ion and F is the Faraday's constant. To adapt the equation to the usage of Rho 123, some assumptions have to be made. First, the non-specific binding of Rhodamine 123 to the mitochondria doesn't depend on the membrane potential and the resultant fluorescence value is assumed to correspond to 0 mV membrane potential. Second, the fluorescence of Rho 123 accumulated in the mitochondrial matrix is negligible when compared with the fluorescence of Rho 123 in the medium. And third, Rho 123 fluorescence varies linearly with the cation concentration. With the appropriate substitutions the following equation can be derived

$$\Delta\Psi = 59.2 \log_{10} [(\Delta F/F) \times (V_{ext}/V_{int})]$$

where ΔF is the difference between the fluorescence in the presence of FCCP, F_0 (0 mV membrane potential) and the fluorescence of the energized mitochondria F. Assuming that the mitochondrial matrix volume is 1 µl per mg of protein (V_{int}), and performing the experiments with 0.5 mg/ml of mitochondria in 2 ml total volume (V_{ext}) the equation becomes

$$\Delta\Psi = 59.2 \log_{10} [(\Delta F/F) \times 2000]$$

The validity of the above equation was verified through comparison with membrane potential values measured with the methyltriphenyl phosphonium ion ($TPMP^+$) electrode (Petronilli and Fontaine unpublished observation).

The mitochondrial membrane potential was evaluated for the three genotypes in animals 10 day-old, 6 and 12-month old (figure 14 B-C).

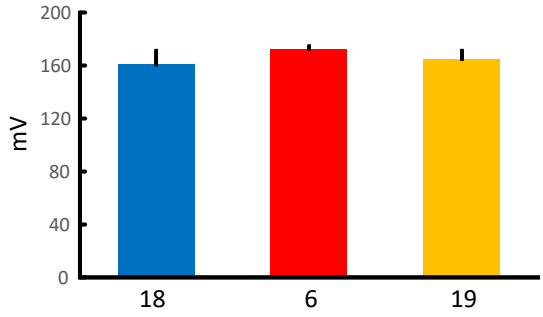

Figure 14 B: mitochondria membrane potential of 10-day-old WT (blue), PS2 (red) and PS2APP (yellow). Mean ± SD. N= number of measurements from at least three independent mitochondria preparation for each genotype.

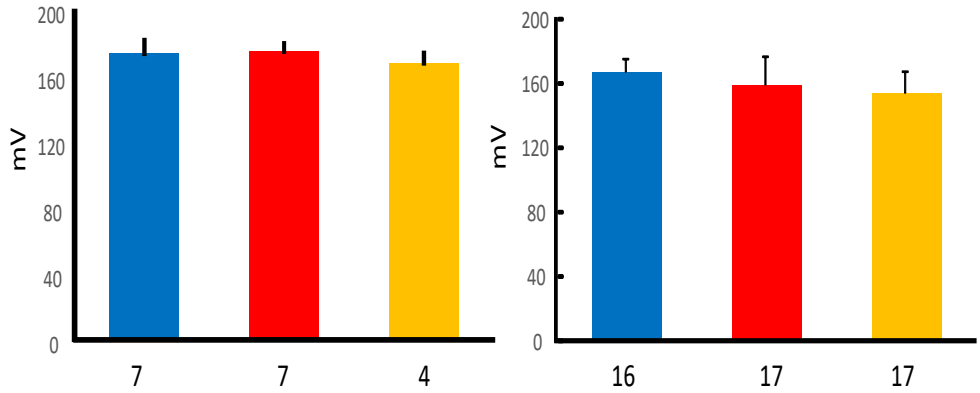

Figure 14 C: mitochondria membrane potential of (left) 6 month-old, and (right) 12-month-old mice WT (blue), PS2 (red) and PS2APP (yellow). Mean ± SD. N= number of measurements from at least three independent mitochondria preparation for each genotype.

The membrane potential values measured didn't differ significantly among the three genotypes, and this result, along with the OCR results, argue against a severe impairment of the respiratory chain downstream complex I in transgenic animals, at least for the ages examined.

1.3 Calcium retention capacity and PTP open probability

The calcium retention capacity (CRC), is the ability of mitochondria to accumulate Ca^{2+} in the matrix before the permeability transition (PT) ensues (Giorgio et al., 2013). Mitochondrial Ca^{2+} uptake was measured with Calcium Green 5N, a cell-impermeant fluorescent dye which changes its fluorescence upon calcium binding (figure 15 A).

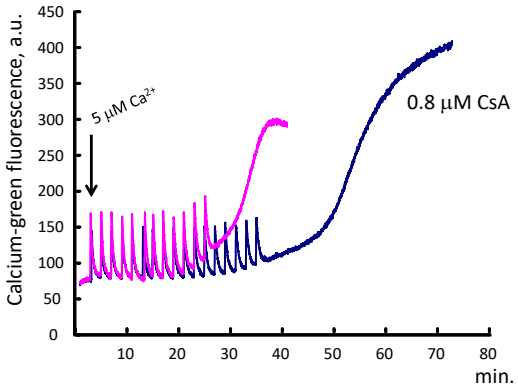

Figure 15 A: representative traces of CRC experiments. Mitochondria and Calcium green additions not shown. 5 μM Ca^{2+} was added every 2 minutes until PTP opening was observed as an increase in Ca-green fluorescence. Purple trace, without CsA, blue trace with 0.8 μM CsA.

The experiments were carried out in the presence of complex I inhibitor, rotenone, and succinate, as substrate for complex II activity. Known amounts of Ca^{2+} were added up to the opening of the PTP (visualized as a sustained increase in Calcium Green 5N fluorescence). The CRC was measured in isolated brain-cortex mitochondria of WT, PS2 and PS2APP mice from 10 days, up to 24-months of age. As elucidated in the figures 15 B, the measurements performed with mitochondria isolated from young (10 days, and 6-month-old) mice didn’t show any significant difference among the three genotypes, and the addition of CsA, a known PTP desensitizer, produced a comparable increase of CRC in all three genotypes.

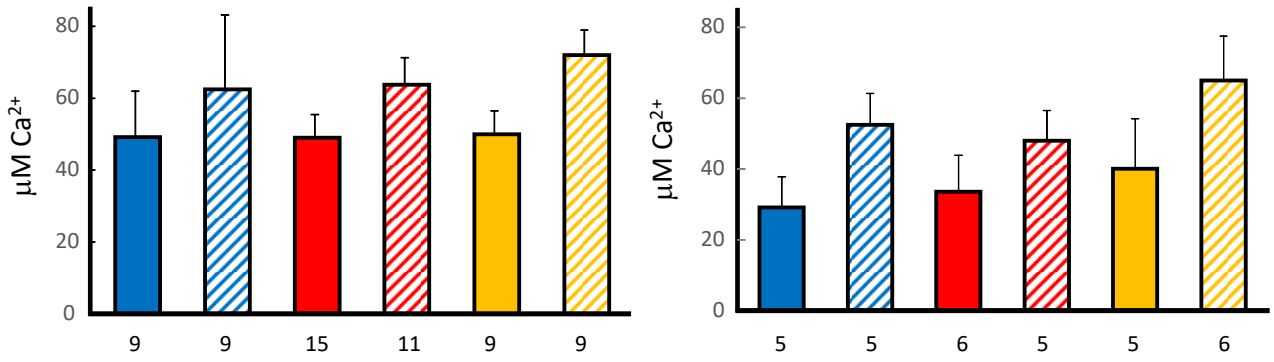

Figure 15 B: quantification of the CRC performed in mitochondria isolated from (left) 10-day-old, and (right) 6-month-old mice. Solid color bars: without CsA, hatched bars: with 0.8 µM CsA. Mean ± SD. N=number of independent measurements from at least 3 independent mitochondria preparation for each genotype.

Similar results were obtained in isolated mitochondria from 12-month-old mice (figure 15 C, left panel). In general, we observed that the CRC decreased with the increasing age of the animals, and this effect could be due to the natural process of aging of the animals. A more pronounced decrease in the CRC was observed in mitochondria isolated from 24-month-old PS2 and PS2APP mice compared to WT animals (figure C right panel), and this phenotype could be due to the fact that at this age transgenic animals already experience the effects of the disease caused by the presence of the mutated proteins. These outcomes suggest a possible effect due to the presence overtime of the mutated presenilin 2, rather than the accumulation of amyloid plaques, which is present only in the PS2APP mice (Ozmen et al., 2009; Fontana et a., 2017). Unfortunately, we were able to perform only few experiments with animals this old, because of the difficulties to keep them reasonably healthy up to this age. More experiments would be needed to assess the statistical significance of the observation.

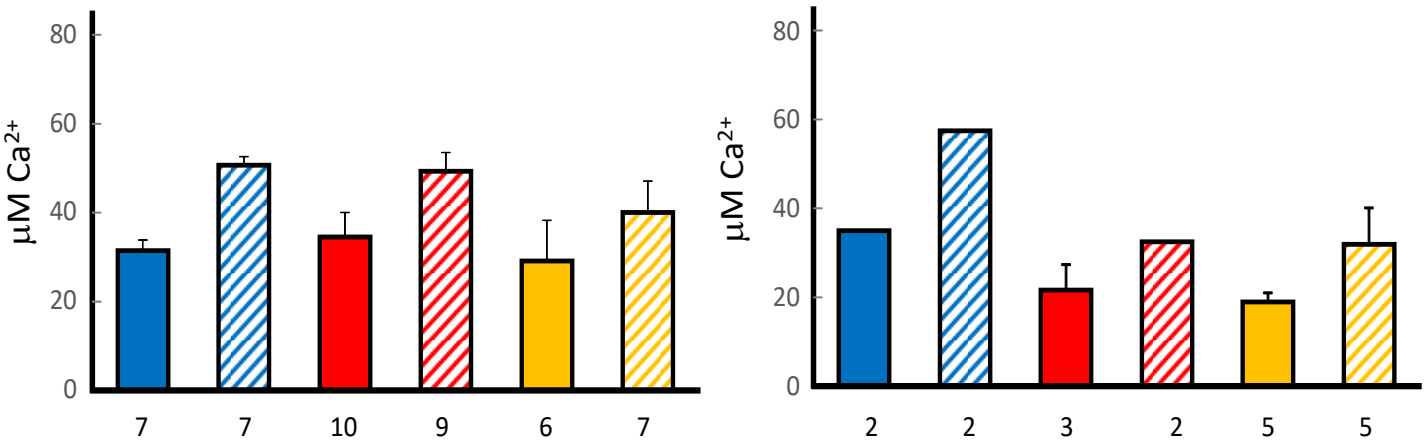

Figure 15 C: quantification of CRC measurements in mitochondria isolated from (left) 12-month-old, and (right) 24-month old mice. Solid color bars, without CsA; hatched bars, with 0.8 µM CsA. Mean ± SD. N=number of independent measurements from at least three independent mitochondria preparations for each genotype.

2 Primary neuronal cultures from mouse hippocampi

The experiments performed in isolated mitochondria didn't reveal overt defects in the mitochondria respiratory chain complexes, or a different sensitivity to matrix Ca^{2+} overload. This result could mean that the presence of the mutated FAD proteins doesn't per se impair the mitochondrial functionality; or could be due to the fact that mitochondria isolated from brain cortex derive from different type of cells (neurons and glia alike) and this complex composition could average the outcome masking possible defects present in more vulnerable cells. For this reason, and also to keep the mitochondria within their cellular contest and maintain their interactions with the rest of the cell, we decided to study mitochondria activity and cellular bioenergetics in primary neurons isolated from the hippocampus of newborn wt and transgenic mice. Briefly, after hippocampi dissection, the cells were mechanically and chemically dissociated and then plated on poly-L-lysine/laminin coated glass coverslips. Cells were grown for up to 12 days in 5 mM glucose to keep them in a condition that more closely mimics the composition of the extracellular cerebral fluid. The cultures were also treated with cytosine arabinoside (AraC, 2 µM) to inhibit astrocytes growth. Hippocampal cultures were characterized by immunofluorescence using antibodies directed against different cell markers to assess the composition of the culture (figure 16, upper part). As shown in the quantification the cultures were mainly composed by

neurons and astrocytes, nevertheless the presence of other types of cells, such as oligodendrocytes and fibroblasts cannot be excluded (histogram, figure 16).

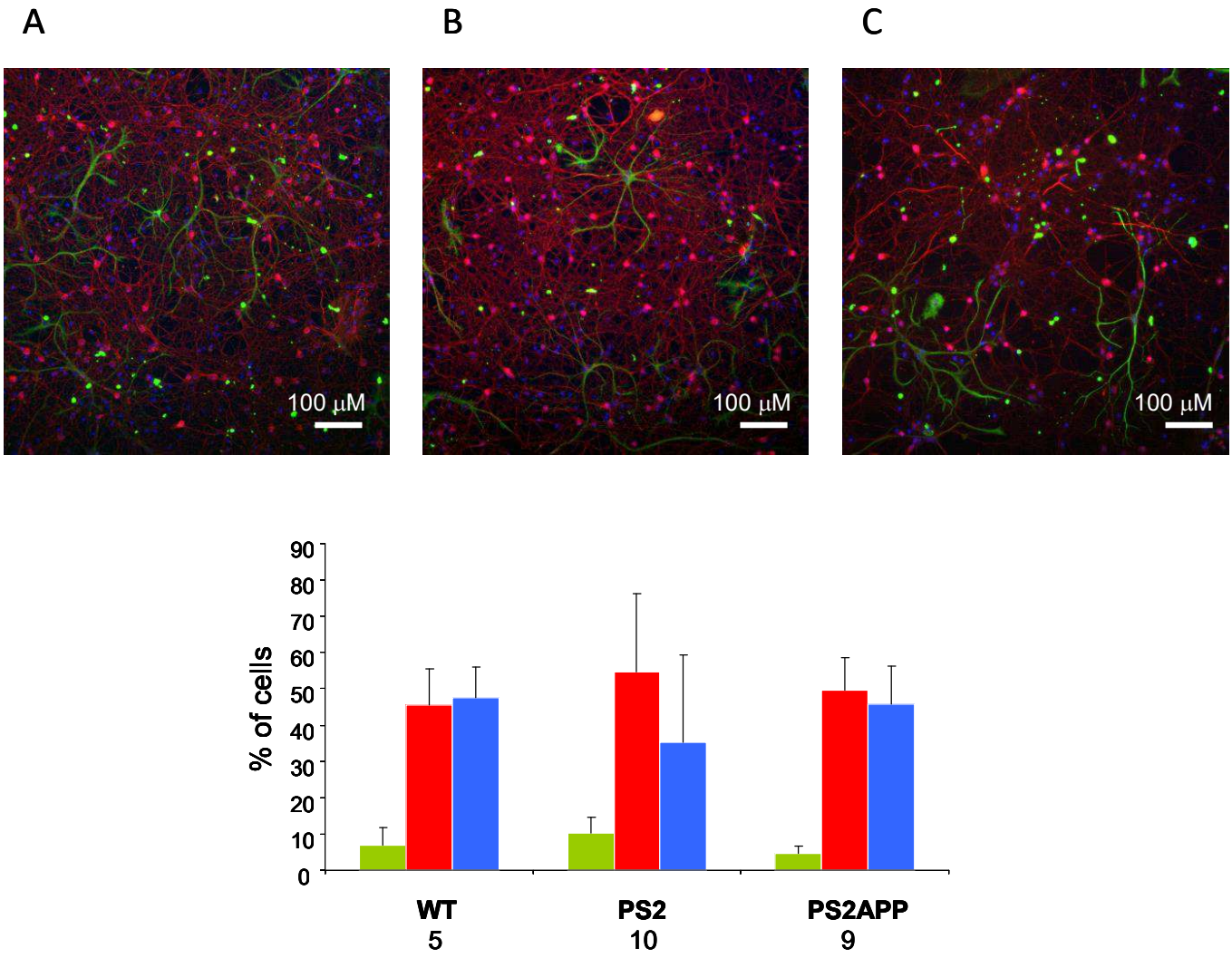

Figure 16: representative immunofluorescence on 12-day *in vitro* primary hippocampal cultures from, upper panel (A) WT, (B) PS2, and (C) PS2APP mice. Neurons, red, were stained with anti NF200, astrocytes, green, were stained with anti GFAP. Hoechst (in blue) was used to mark the cell nuclei. Lower panel, percentage of astrocytes (green), neurons (red) and cells not immunoreactive for NF200 and GFAP (blue), in the cultures examined. N= number of coverslips, from at least two independent cultures for each genotype. Mean ± SD.

2.1 Evaluation of OCR in intact neuronal culture

The Seahorse Extracellular Flux analyzer (XF Analyzer, Agilent Seahorse) is an innovative and very sensitive instrument able to simultaneously measure two crucial cellular energy pathways: glycolysis and mitochondrial respiration, directly in intact living cells.

During the measurement, the instrument can automatically and sequentially deliver up to 4 compounds of choice, allowing the analysis of different parameters, such as the basal respiration, the ATP-synthesis coupled respiration and the maximal respiratory capacity of the cultured cells (figure 17 A).

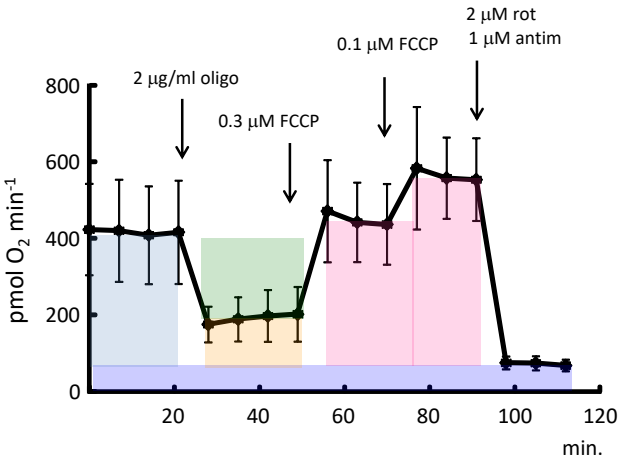

Figure 17 A: representative trace of a typical OCR experiment. As indicated by the arrows oligomycin (2 μg/ml), FCCP (0.3 μM and 0.1 μM, respectively) and rotenone (2 μM) plus antimycin (1μM) were sequentially added to the wells with the seeded cells. Light blue rectangle basal respiration; green rectangle ATP-synthesis coupled respiration; yellow rectangle proton leak oxygen consumption; pink rectangle uncoupled respiration; purple rectangle, non-mitochondrial respiration.

We observed that the basal respiration measured in 10-day *in vitro* neuronal cultures was similar among the three genotypes (figure 17 B).

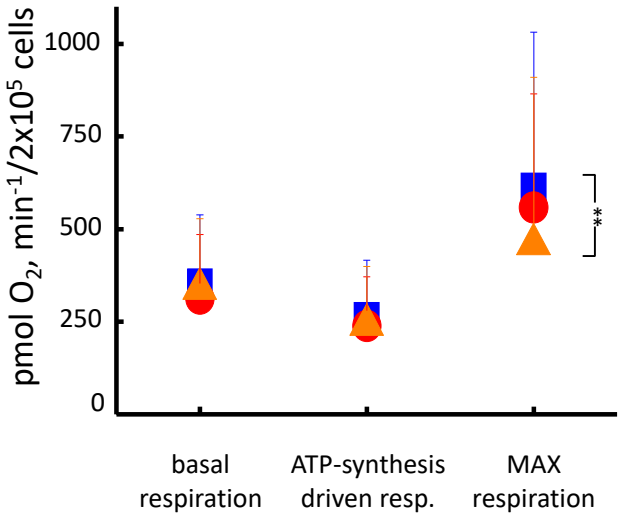

Figure 17 B: quantification of basal, ATP-synthesis driven, and maximal respiration of WT (blue squares), PS2 (red circles) and PS2APP (orange triangles) 10-day *in vitro* hippocampal cultures. Mean ± SD. N= number of wells for each conditions: WT 143; PS2 109; PS2APP 129 from at least three independent cultures for each genotype.

The addition of oligomycin to the culture inhibits the activity of the mitochondrial ATP synthase, allowing the determination of the fraction of the cellular respiration devoted to the synthesis of ATP, and of the oxygen consumed due to proton leakage across the mitochondrial inner membrane. Both ATP-synthesis coupled respiration and proton leak OCR were similar among the three genotypes.

The addition of carefully titrated FCCP concentrations depolarizes the mitochondria inner membrane, uncoupling the electron flow from the synthesis of ATP, and enabling the measurement of the maximal rate of mitochondrial respiration and the calculation of what is known as the respiratory reserve of the cells. Differences in the respiratory reserve could represent different ability of the cells to cope with challenging conditions that demand a higher energy production. We observed that WT type neurons have a higher spare respiratory capacity when compared to PS2 and PS2APP neurons and this difference becomes significant between WT and PS2APP cells. Since we didn't observe any significant difference in the FCCP-stimulated respiration of the mitochondria isolated from the cortex of transgenic animals, which could signify of an impairment within the respiratory chain complexes, this result suggests that in the double transgenic cells there might be an impairment in the supply of substrates to the mitochondria.

2.2 Extracellular acidification rate (ECAR) in intact cells

As previously mentioned, the Seahorse permit to simultaneously evaluate both oxygen consumption due to oxidative phosphorylation and the rate of glycolysis of the cells. The efficiency of the glycolysis can be deduced from the measurements of the acidification of the medium, the extracellular acidification rate (ECAR), which is mainly the due to the rate of lactic acid excretion, per unit of time, after its conversion from pyruvate (Wu et al., 2007; TeSIaa et al., 2014). Three parameters can thus be evaluated: the basal glycolysis, (ECAR of the active cells); the glycolytic capacity, which is the oligomycin-stimulated ECAR; and the glycolytic reserve, which can be calculated from the difference between the two previous parameters (figure 18, upper panel).

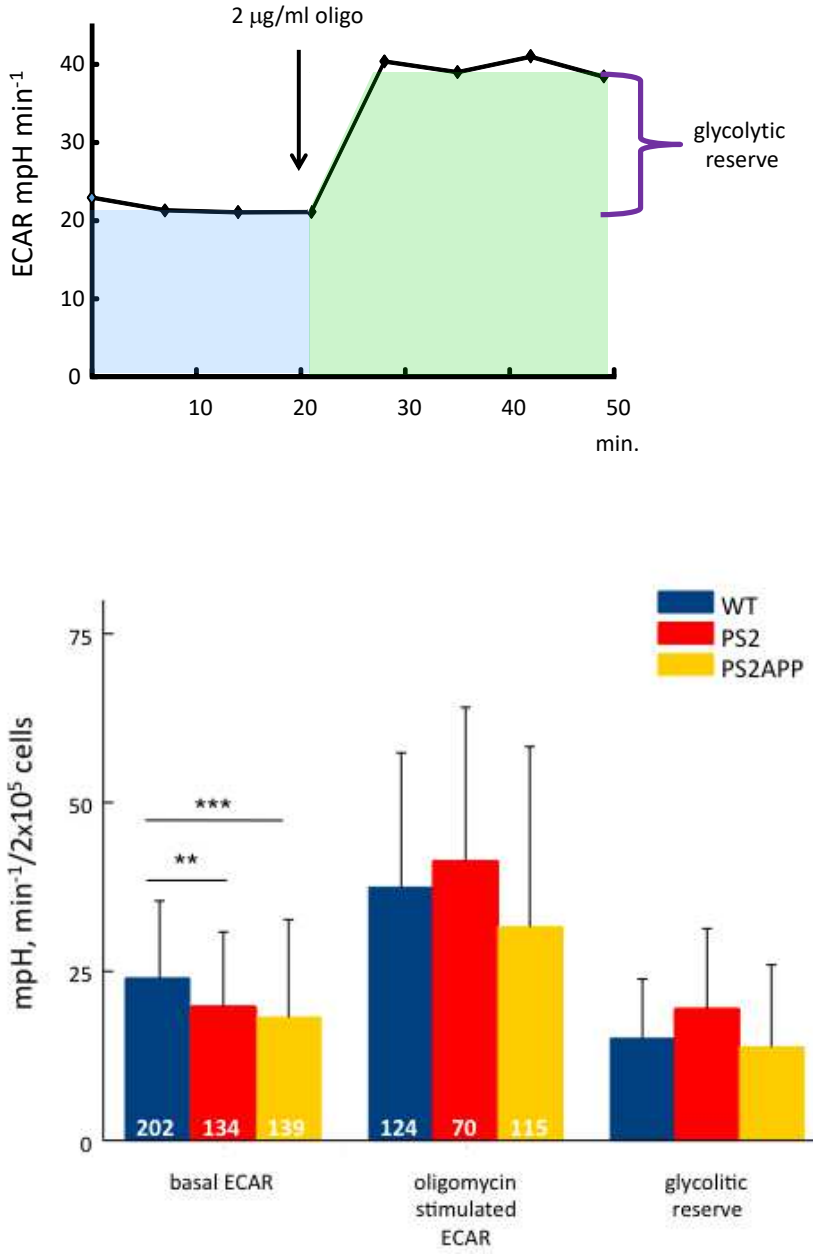

Figure 18: upper panel: representative trace of ECAR measurement, where indicated (arrow) 2μg/ml oligomycin was added. Light blue rectangle, basal glycolysis; green rectangle, glycolytic capacity. Lower panel: quantification of the basal, oligomycin stimulated ECAR, and of the glycolytic reserve of 10-day *in vitro* neuronal cultures. N= number of wells from at least three independent cultures for each genotype. Mean ± SD.

We observed a small, though significantly higher, basal ECAR in WT neuronal cultures compared with PS2 and PS2APP cultures, while the glycolytic capacity (oligomycin stimulated glycolysis), and the glycolytic reserve didn't show significant difference among the three genotypes, meaning that despite the different starting point these cells seem to have similar abilities to respond, via glycolysis, to an increased energetic demand (figure 18, lower panel).

2.3 Analysis of the expression of the respiratory chain complexes and ATP synthase in neuronal hippocampal cultures

Samples from at least four different hippocampal cultures for each genotype were collected for protein extraction and subsequent analysis of the relative protein levels of the electron transport chain complexes and ATP synthase by Western Blot (figure 19, upper panel).

As shown from the quantification, (figure 19, lower panel), the amount of the different respiratory chain complexes and of the ATP synthase is comparable among the three different genotypes, again arguing against major impairments of the oxidative phosphorylation machinery of the transgenic cultures.

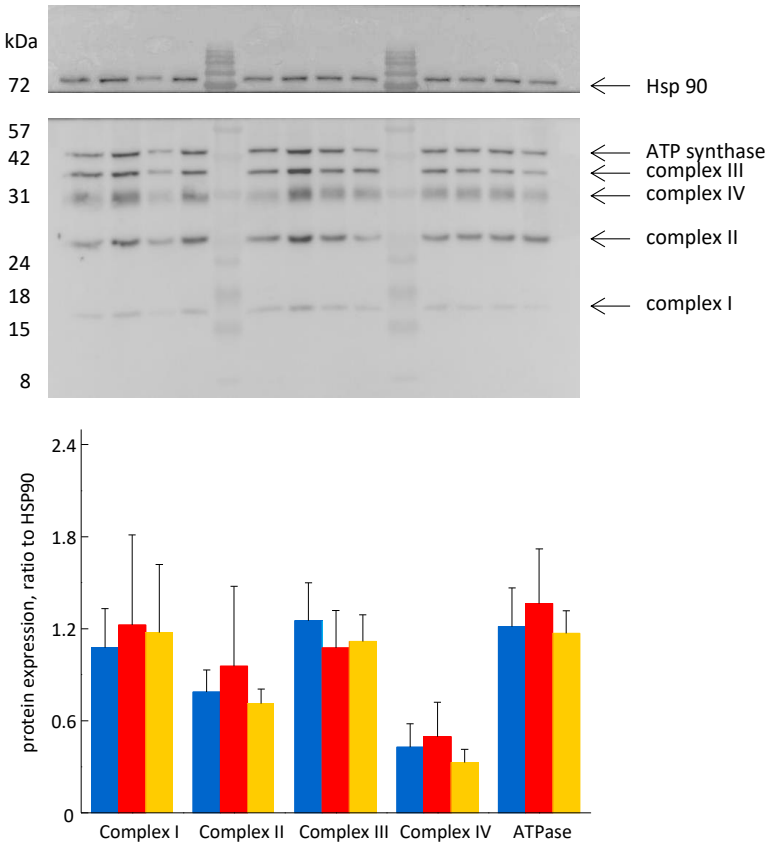

Figure 19: Western Blot and analysis of electron transport chain complexes expression in hippocampal cultures. Upper panel: Western blot of protein extracts from Wt, PS2, PS2APP neuronal cultures. Lower panel: Quantification of the bands' densitometry performed with ImageJ. Samples from at least 4 independent neuronal cultures for each genotype. Means ± SD

2.4 Mitochondrial membrane potential variations in hippocampal cultures

Loading cells with the voltage-sensitive fluorescent dye Tetramethylrhodamine Methyl Ester (TMRM), and challenging them with specific inhibitors of the respiratory chain, or of the ATP synthase, is a valuable approach to disclose possible hidden defects within the OXPHOS apparatus. With this purpose, 10-12-day *in vitro* neuronal cultures were treated with 10 nM TMRM at 37 °C for 30 minutes, off-line, (figure 20 A), and subsequent fluorescent image acquisitions were performed at the same temperature.

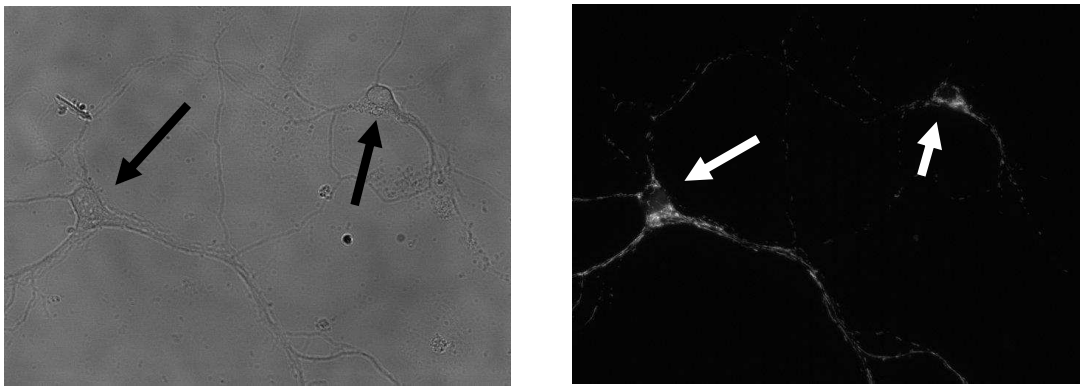

Figure 20 A: left panel: bright field image of primary hippocampal neurons (black arrows). Right panel: Fluorescence image of TMRM loaded neurons (white arrows) incubation condition as described in body text.

We observed that basal TMRM fluorescence was comparable among the three genotypes, excluding the possibility of different loading of the dye due to dissimilar plasma membrane or mitochondrial membrane potential (figure 20 B).

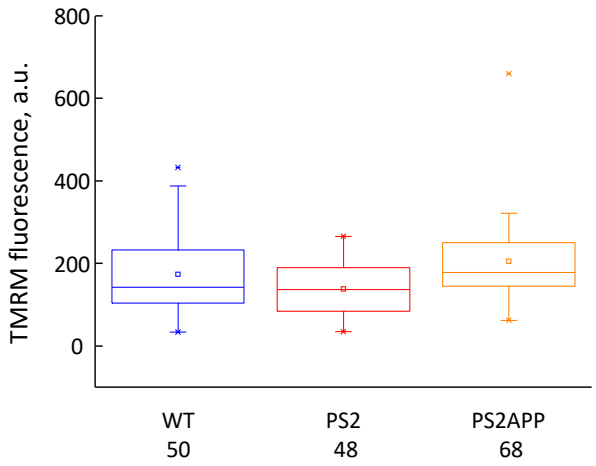

Figure 20 B: basal TMRM fluorescence values of WT (blue), PS2 (red) and PS2APP (orange) neuronal cultures. N= number of cells from at least three independent cultures for each genotype. Mean ± SD.

The addition of 2 μM rotenone caused the inhibition of Complex I activity, and a decrease in TMRM fluorescence indicative of a decrease in membrane potential was observed during the following 20 minutes (figure 20 C, left panel). As shown in the quantification, (figure 20 C right

panel), the induced depolarization is significantly more pronounced in PS2 and PS2APP neurons with respect to WT neurons. FCCP 4 μM was added to induce maximal membrane depolarization as a control for correct dye redistribution.

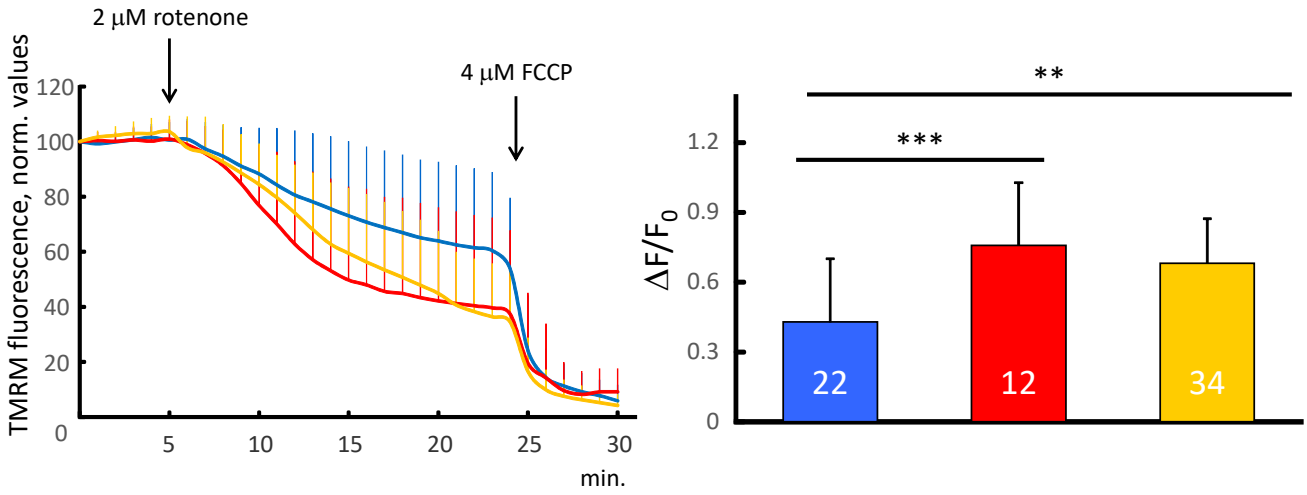

Figure 20 C: mitochondria TMRM fluorescence changes induced by rotenone. Left panel normalized, averaged TMRM traces. Where indicated by arrows 2 μM rotenone and 4 μM FCCP were added to the culture: WT (blue), PS2 (red), PS2APP (yellow). Right panel: quantification of the difference (ΔF) between basal fluorescence (F_0) and the fluorescence values reached 20 min after rotenone addition (F), (before FCCP addition), normalized to basal fluorescence values F_0. N= number of cells from at least three independent cultures for each genotype. Mean ± SD. **p< 0.01, ***p< 0.001.

The same type of experiments performed with Antimycin A, an inhibitor of Complex III of the respiratory chain, produced comparable results, with a higher degree of mitochondrial membrane depolarization in PS2 and PS2APP neurons with respect to WT neurons (figure 20 D).

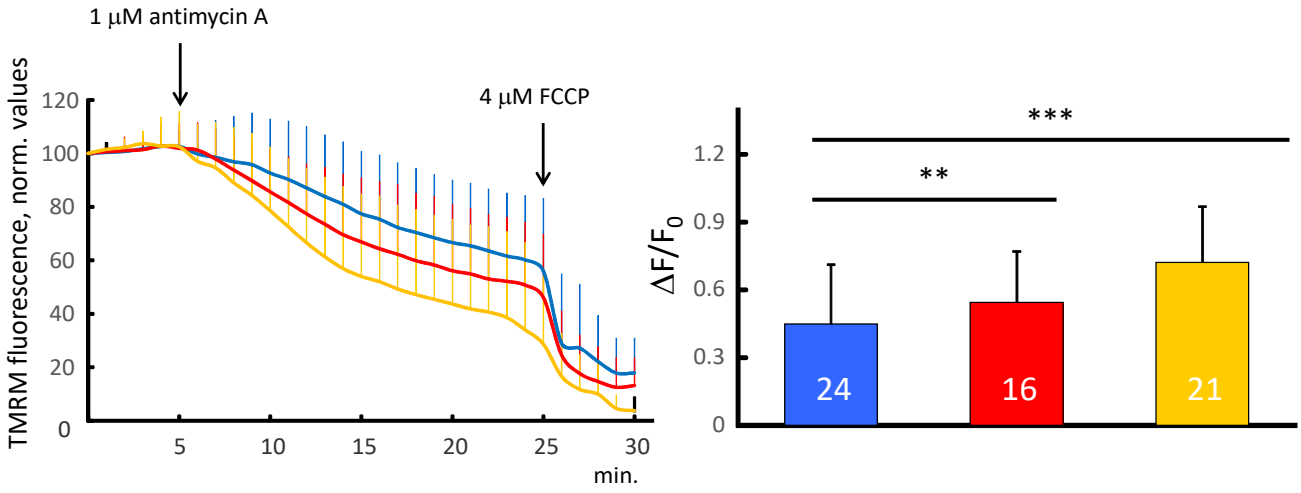

Figure 20 D: mitochondrial TMRM fluorescence changes induced by antimycin A addition. Left panel, normalized, averaged TMRM traces. Where indicated by arrows 1 μM Antimycin A, and 4 μM FCCP, respectively were added to the culture: WT (blue), PS2 (red), PS2APP (yellow). Left panel quantification of the difference, ΔF, between basal fluorescence, F_0 and the fluorescence values reached 20 min after antimycin A addition, F, (before FCCP addition), normalized to the basal fluorescence values F_0. N= number of cells from at least three independent cultures for each genotype. Mean ± SD. **p< 0.01, ***p< 0.001.

Taken together, these data suggested that when respiratory chain complexes I or III are blocked, mitochondria are not able to keep their membrane potential through the ATP synthase reverse activity, which hydrolyzes ATP pumping protons back into the medium. This outcome could possibly be due to impairment in the ATP synthase reverse activity, or to insufficient ATP supply to the synthase.

On the contrary, the addition of oligomycin, inhibitor of the ATP synthase, didn't affect the mitochondrial membrane potential, suggesting that the electron transport chain is not impaired and thus can sustain the membrane potential in both controls and transgenic neurons (figure 20 E).

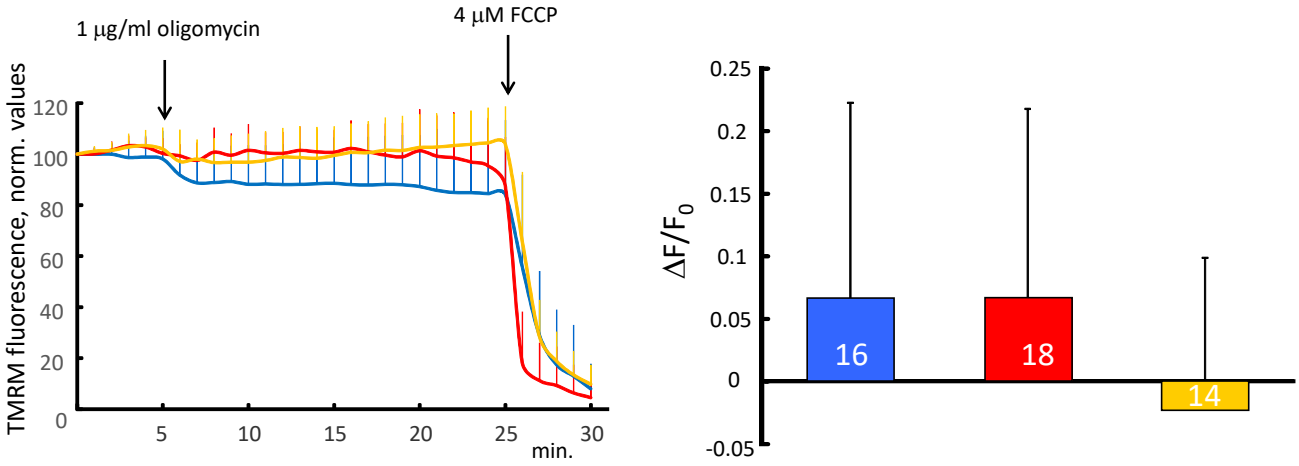

Figure 20 E: mitochondrial TMRM fluorescence changes induced by oligomycin addition. Left panel: normalized, averaged TMRM traces. Where indicated by arrows 2 μM oligomycin, and 4 μM FCCP, respectively were added to the culture: WT (blue), PS2 (red), PS2APP (yellow). Right panel: quantification of the difference, ΔF, between basal fluorescence and the fluorescence values reached 20 min after oligomycin addition, F, (before FCCP addition), normalized to the basal fluorescence values F_0. N= number of cells from at least three independent cultures for each genotype. Mean ± SD.

2.5 Effect of rotenone on mitochondrial membrane potential of control and FAD human fibroblasts

Transgenic animals are extremely useful models to investigate human diseases, but of course several drawbacks exist, and it would be advisable, whenever possible, to compare results obtained in the animal models with the closest available human counterpart. Having access to human fibroblasts from a FAD patient carrying the PS2-N141I mutation we sought to repeat the TMRM experiments also in these cells, using as controls fibroblast cultures obtained from healthy donors matched for age and sex. We observed that rotenone addition produces a mitochondrial membrane depolarization slightly higher in FAD-PS2 fibroblasts compared with control fibroblast, but overall the effect was not statistically significant (figure 21). The difference observed between human fibroblasts and mouse hippocampal neurons could be due to the fact that fibroblasts are mainly glycolytic cells, and rely less than neurons on oxidative metabolism. This result appears more consistent with a higher impact of defective mitochondria in neurons compared to fibroblasts.

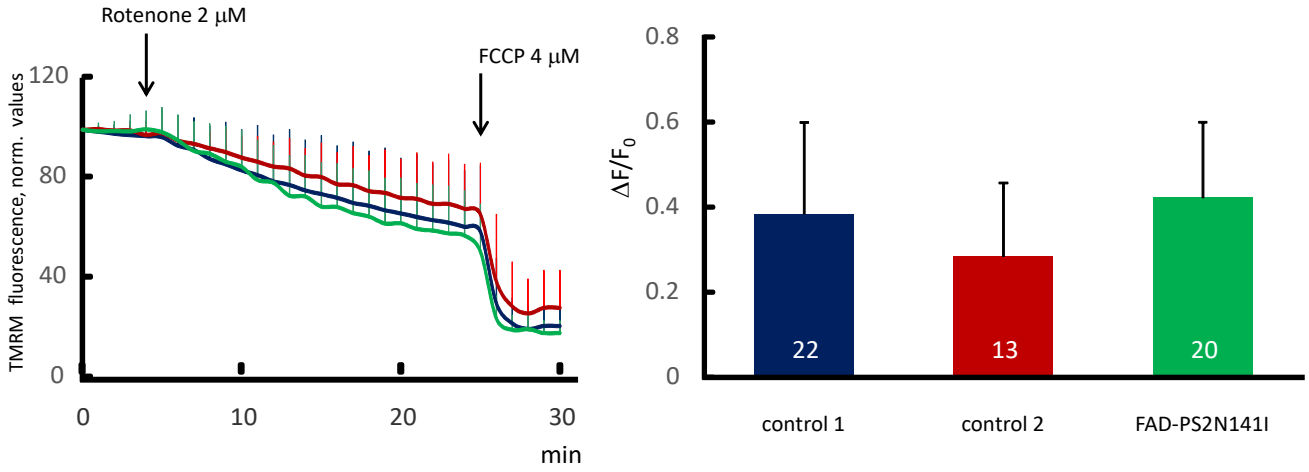

Figure 21: mitochondria TMRM fluorescence changes induced by rotenone. Left panel, normalized, averaged TMRM traces. Where indicated by arrows 2 μM rotenone and 4 μM FCCP were added to the culture: FAD-PS2 fibroblasts (green), control 1 (red), control 2 (blue). Right panel: quantification of the difference between initial fluorescence and the fluorescence values reached 20 min after rotenone addition ΔF (before FCCP addition) normalized to the basal fluorescence values F_0. N= number of cells from at least three independent cultures for each genotype. Mean ± SD.

3 ATP-synthase reverse activity

A defect in the ATP-synthase reverse activity could be a possible explanation for the stronger depolarization induced by rotenone or antimycin addition in PS2 and PS2APP neurons. To further investigate this hypothesis, we tested ATP hydrolysis by mean of ATP synthase in-gel activity. Isolated brain cortex mitochondria were treated with mild detergent to extract intact ATP synthase complexes (oligomers, dimers and monomers) that were subsequently separated by blue native gel electrophoresis (BNE) and identified by Coomassie Blue staining (figure 22, lanes 1-3). The gel was subsequently treated with a solution containing lead nitrate and the ATP-synthase reverse activity results in a whitish lead-phosphate precipitate in correspondence with the ATP synthase complexes. We observed a small precipitate in correspondence of the ATP synthase monomers, and a smaller, but still clearly visible, precipitate in correspondence of the ATP synthase monomers and dimers (figure 22, lanes 4-5). Furthermore, part of the gel was transferred onto a PVDF membrane, and probed with an ATP-synthase specific antibody (figure 22, lanes 6-7).

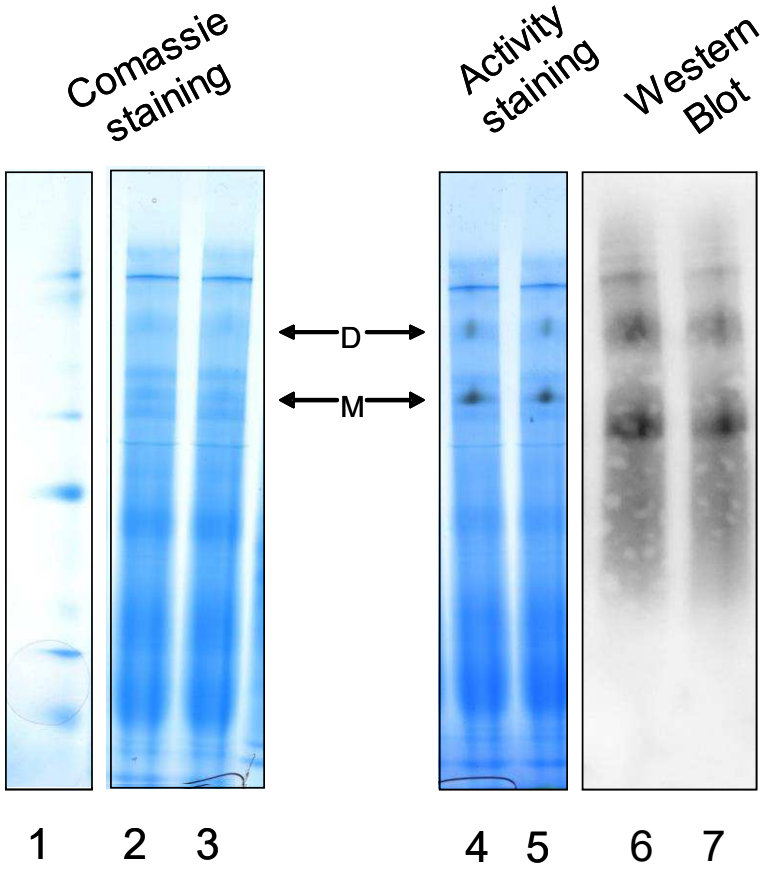

Figure 22: purification of F_oF_1 ATP synthase. The samples were subjected to BNE to separate dimers (D) and monomers (M) which were then identified by Coomassie Blue, lane 1 (marker) and lanes 2-3, and in-gel activity staining (lanes 4-5). Part of the gel was also probed with the anti ATP5B antibody (ab 1473) and used to test the ATP synthase by Western Blot (lanes 6-7).

The approach of the in-gel staining activity is not quantitative, and, in addition, its sensitivity is limited. Another method used to measure the ATP-synthase, hydrolytic activity is based on the reactions in which ATP hydrolysis is coupled to the oxidation of NADH (see the Discussion for a detailed description of the protocol). These measurements allow to evaluate the amount of hydrolyzed ATP per unit of time; as shown in figure 23, the ATP hydrolysis seems to be lower in WT mitochondria compared to PS2 and PS2APP ones, although the number of experiments is too low to establish whether the difference is significant.

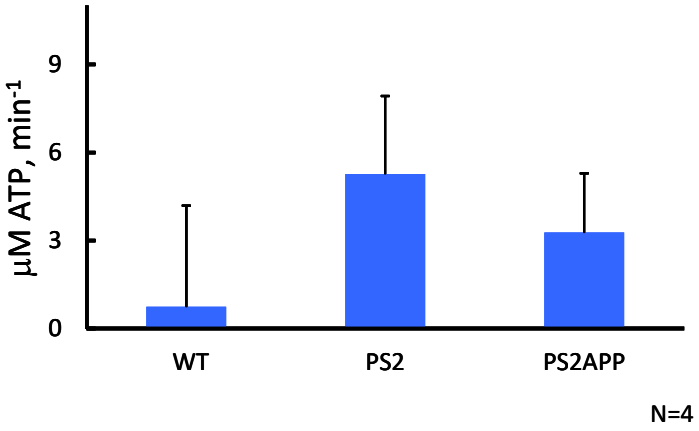

Figure 23: quantification of the rate of ATP hydrolysis in brain-cortex mitochondria from 3-month-old mice. N= number of experiments, at least 2 different animals for each genotype. Mean ± SD.

4 Effects of oligomycin or antimycin addition on cytosolic Ca^{2+} levels in hippocampal neurons

Tightly controlled Ca^{2+} homeostasis is crucial for all cells, and especially for neurons. The inhibition of the ATP synthase produced by oligomycin, or the inhibition of the respiratory chain complexes produced by selective inhibitors could have strong impacts on the ATP content of the cell, causing, in turn, cellular Ca^{2+} deregulation. For this reason, we wanted to ascertain whether the three genotypes have different ability in managing such challenges. Cytosolic Ca^{2+} concentration $[Ca^{2+}]_c$ was evaluated with Fura-2 AM. Precisely, 10-12-day-*in vitro* hippocampal cultures were loaded with Fura-2 AM at 37°C (figure 24 A, left panels), and the experiments were performed 40 minutes later at the same temperature. Oligomycin or antimycin were added 5 minutes after the beginning of image acquisition. At the end of the experiment, 30 mM KCl was added to induce a sustained depolarization of the plasma membrane, and a large Ca^{2+} entry into the cytoplasm (figure 24 A, right panel). We assessed $[Ca^{2+}]_c$ in resting conditions, and we didn't observe any significant differences among the three genotypes (figure 24 B, right panel). These data are consistent with what was previously observed in PS2 and PS2APP primary cortical neurons (Kipanyula et al., 2012).

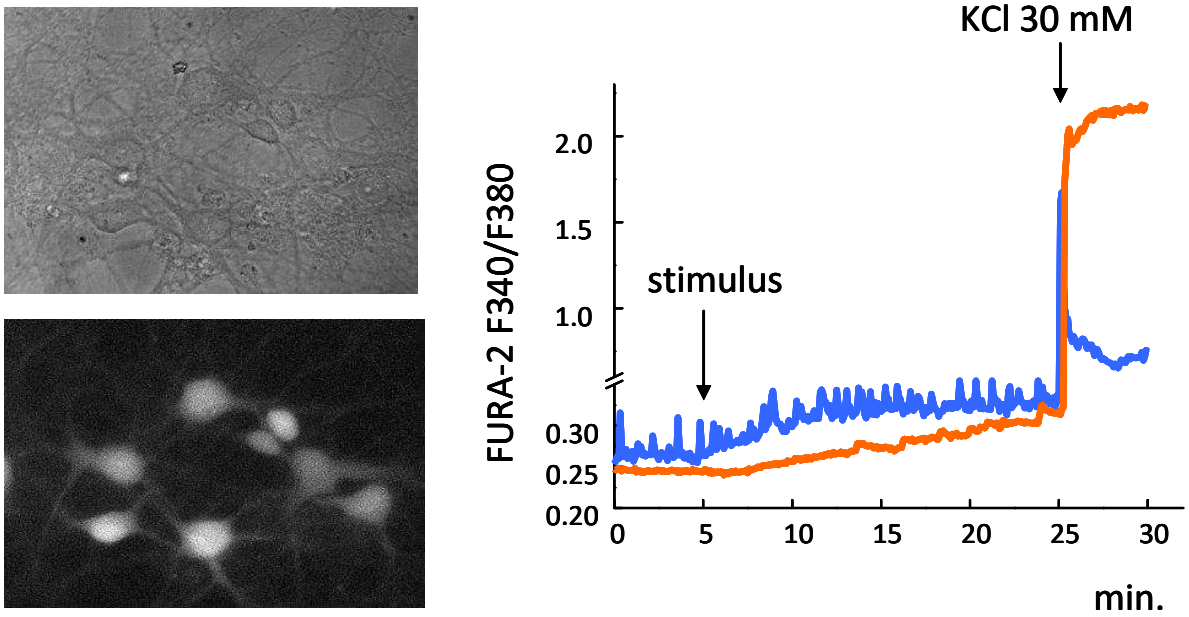

Figure 24 A: representative images of neuronal hippocampal culture. Left, top panel: bright field; bottom panel: Fura-2 loaded cells. Right panel: representative traces of a FURA-2 experiment. Where indicated by arrows a stimulus (antymicin A or oligomycin) and 30 mM KCl were added.

The addition of antimycin or oligomycin caused a small increase in the 340/380 FURA-2 fluorescence ratio indicative of an increase in $[Ca^{2+}]_c$. The value was calculated subtracting 340/380 ratio 15 minutes after drug addition from 340/380 basal ratio. Again, the three genotypes behaved in a similar way (figure 24 C).

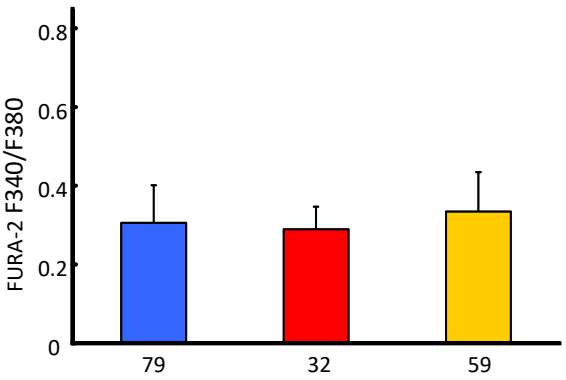

Figure 24 B: quantification of basal FURA-2 340/380 nm ratio representative of $[Ca^{2+}]_c$. WT (blue), PS2 (red), PS2APP (yellow) neuronal cultures. N= number of cells from at least three independent cultures for each genotype. Mean ± SD.

These results suggest that under these experimental conditions, the cells could equally handle a likely decrease in ATP content induced by the electron transport chain or the ATP synthase blockade. It is reasonable to think that a stronger and prolonged stimulus may reveal differences in the ability of the cells to deal with larger $[Ca^{2+}]_c$. increase. Indeed, we noticed that after KCl addition, a higher percentage of PS2 and PS2APP neurons were not able to actively extrude the excess of Ca^{2+}. We observed that 18% of WT neurons failed to actively extrude excess Ca^{2+} compared with 29 % of PS2, and 24% of PS2APP cells. These differences are small, but this could be an aspect worth investigating in the future.

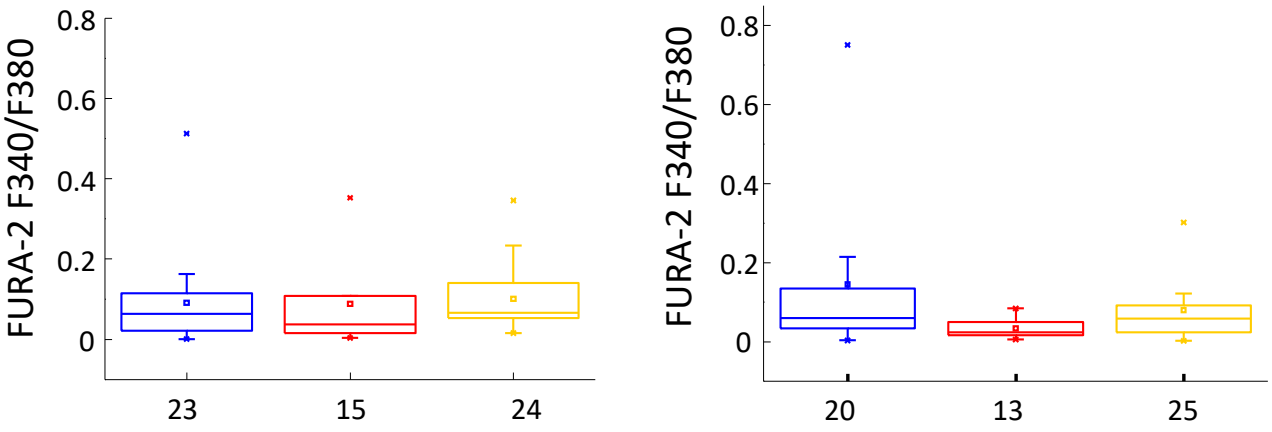

Figure 24 C: quantification of the increase in the FURA 2 340/380 nm ratio after the addition of (left panel) 1 μM antimycin A, and (right panel) 2 μg/ml oligomycin. N= number of cells from at least three independent cultures for each genotype. Mean ± SD.

5 Evaluation of reactive oxygen species production (ROS) in hippocampal cultures

The imbalance between cellular production of reactive oxygen species (ROS) and the action of antioxidant mechanisms leads to oxidative stress which is known to cause damages to many cellular components such as DNA, proteins, and lipids. The brain, with its high oxygen consumption, and the presence of a large lipid fraction, is particularly vulnerable, and in fact oxidative stress has been implicated in many neurodegenerative diseases. Even a slight mitochondria dysfunction may change ROS production, which could lead to altered Ca^{2+} homeostasis, excitotoxicity and cell death. For these reasons, we decided to evaluate ROS levels in

hippocampal cultures, to establish if the three different genotypes exhibit a different production of ROS at the resting levels. MitoSOX Red is a fluorescent cationic dye selectively targeted to mitochondria in living cells. Once in the matrix, the sensor is rapidly oxidized by superoxide, but not by other ROS or by reactive nitrogen species (RNS), and the oxidation product becomes highly fluorescent upon binding to nucleic acids. We loaded 12-day *in vitro* neuronal cultures with MitoSOX Red but, we didn't observe any remarkable difference between WT and PS2APP neurons in basal conditions (figure 25). Basal fluorescent levels were always very low, perhaps because of a low superoxide production of these cells in resting conditions, or for insufficient sensitivity of the detection system used. We could not boost ROS production in the cells by treating the cultures with respiratory chain inhibitors (rotenone or antimycin) because they induce depolarization of the mitochondrial membrane potential which would cause leakage of the probe from the organelles.

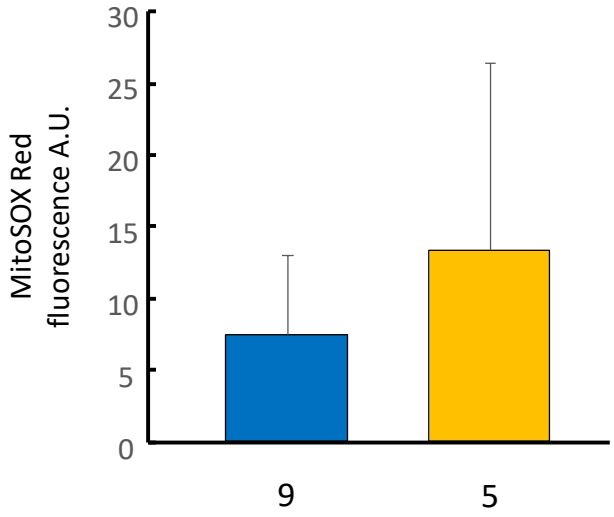

Figure 25: quantification of basal fluorescence levels of MitoSOX Red in WT (blue) and PS2APP (yellow) neurons. N= number of cells, at least two independent neuronal cultures for each genotype. Mean ± SD.

DISCUSSION

Alzheimer's Disease (AD) is the most common form of dementia in developed countries; the outcomes of the disease are severe memory impairment and cognitive dysfunctions. Despite strong efforts, available treatments aimed at stopping, or slowing the disease progression are still insufficient, mainly because the understanding of causes or factors contributing to the disorder are still vastly incomplete (Cadonic et al., 2016).

The main hypothesis regarding AD etiology are focused on either genetic heritability (Gatz et al., 2006), impaired acetylcholine synthesis (Francis et al., 1999), accumulation of neurotoxic protein forming plaques (Hardy et al., 1991) and neurofibrillary tangles (Mudher et al., 2002), but also on defects in mitochondria functionality and dynamics (Swerdlow and Khan, 2004; Swerdlow et al., 2014).

For many cell types, mitochondria are central in providing the necessary energy supply to the cells, and also are crucial for several cellular functions such as calcium homeostasis, cell signaling, ROS production and apoptosis. Neurons, in particular, are highly dependent on the mitochondria to generate the ATP necessary to maintain normal physiological activities. In fact, not surprisingly, mitochondrial dysfunctions have been related to the onset and progression of several neurodegenerative diseases, such as Parkinson's disease, Huntington's disease, amyotrophic lateral sclerosis and AD (Lin et al., 2006; Esteves et al., 2009; Cadonic et al. 2016).

For these reasons, we set to assess whether the presence of the FAD-linked PS2-N141 mutation, and the APP Swedish mutation would affect mitochondria and cellular physiology.

Mitochondria isolated from tissues or cell cultures have the advantage of a tight control over the experimental conditions, permitting the direct delivery of substrates or reagents otherwise impermeant to the cellular membrane (Brand et al., 2011).

We assessed the oxygen consumption rate of mitochondria isolated from the brain cortex of animals at different ages and we didn't observe major differences in the basal, ADP-stimulated or uncoupled respiration of the mitochondria of transgenic animals when compared with WT age-matched controls. In line with this result, also the mitochondrial membrane potential was similar among the different genotypes for the stages of life examined.

Moreover, the CRC experiments performed in isolated-brain mitochondria of 8-10 days, 6 and 12 month-old mice, didn't reveal different sensitivity of the PTP to matrix calcium overload among the three genotypes. We observed that the amount of Ca^{2+} accumulated by the mitochondria tended to decrease with the age of the animals, but this phenotype was similar among the three genotypes up to 12-month of age. Instead we observed a tendency toward a decreased CRC in 24 month-old PS2 and PS2APP mice compared with WT animals. Though the number of measurements we performed was low, and more experiments would be needed to determine a statistical difference, nevertheless, this effect could be due to the macroscopic damages already suffered by the brains of transgenic animals of this age (Hwang et al., 2002, Richards et al 2003; Ozmen et al., 2007). Since we didn't observe significant differences in the respiratory chain functionality, and in the sensitivity to matrix Ca^{2+} overload, we would conclude that these FAD-linked mutations do not cause evident primary mitochondrial dysfunctions in the transgenic animals up to 12-month of age.

Of note, in these sets of experiments we blocked complex I with rotenone and used succinate as substrate for the respiratory chain. For this reason, we cannot unequivocally exclude impairments in complex I activity, nevertheless the absence of difference in basal and ATP-synthesis driven respiration, as well as in mitochondria membrane potential of oligomycin-treated hippocampal neurons, argues against a complex I defect caused by the presence of PS2 and PS2APP mutated proteins.

A more thorough analysis of mitochondrial functionality would require to examine the organelles within the cellular environment, we choose to culture neurons isolated from the hippocampus of newborn mice, since this brain region is one early affected by the disease (Selkoe and Hardy 2016, Pini et al 2016). The cultures were analyzed by immunofluorescence, using antibodies against proteins characteristic of different cell types and the proportion of neurons compared to glial cells was about 5 to 1, moreover the cultures from the different genotypes manifested the same viability (data not shown).

The measurements of the oxygen consumption rate in intact cell, by the mean of the Extracellular Flux Analyzer (Agilent Seahorse), were comparable among the three genotypes concerning basal, and ATP-synthesis coupled respiration, suggesting that at resting conditions the cells have comparable metabolism. When challenged with FCCP, to uncouple the oxidative phosphorylation, and stimulate the mitochondria to respire at their maximal capacity, we observed that PS2 and

PS2APP transgenic lines had a lower spare respiratory capacity, compared with WT cultures, and the difference was statistically significant between WT and double transgenic cultures. Since we didn't observe major impairments in the functionality of respiratory chain complexes in isolated mitochondria, we would speculate that the difference in maximal respiration observed in intact cells could be due to a defective delivery of respiratory substrates to the mitochondria. The decrease of the respiratory reserve in transgenic cultures would be of major implication for the ability of the cells to cope with an augmented energetic demand (Lewerenz and Maher, 2015; Ong et al., 2013), and could account for the increased vulnerability of hippocampal neurons in Alzheimer's disease (Saxena and Caroni, 2011; Palop et al., 2007).

Latent defects of the respiratory chain or of the ATP synthase could be unmasked by challenging the complexes with appropriate inhibitors, and monitoring the ability of mitochondria to sustain the membrane potential (Irwin et al., 2003; Angelin et al., BBA 2008). We observed that the addition of rotenone or antimycin A, to block respectively Complex I or Complex III of the respiratory chain, produce a decrease in the TMRM fluorescence indicative of a decrease in the mitochondrial membrane potential, which was significantly larger in single and double transgenic cultures, compared with control cells. This result could be symptomatic of an inability of the ATP synthase to sustain the mitochondrial membrane potential through its reverse activity, the hydrolysis of ATP and the pumping of protons into the intermembrane space; or, in alternative, it could be due to an inefficient supply of ATP to the synthase.

On the other hand, the ATP-synthase blockade induced by oligomycin, didn’t lead to mitochondrial membrane potential variations, suggesting that the electron transport chain doesn't bear major defects.

Corresponding experiments where performed on human fibroblasts from a FAD patient carrying the PS2-N141I mutation (Zatti et al., 2006). We observed a slightly higher mitochondrial membrane depolarization in fibroblasts isolated from a FAD patient, compared to what observed in cells of healthy donors, age and sex matched, thought the differences were not statistically significant. The different sensitivity to respiratory chain inhibition between fibroblast and neurons could be due mainly to their different metabolism. In fact, fibroblasts are prevalently glycolytic cells, less dependent than neurons on oxidative metabolism, (Ghesquiere et al., 2014) and thus, they could be less sensitive to challenges that might reduce oxidative phosphorylation-produced ATP (De Bock et al., 2013).

The hydrolytic activity of the ATP synthase can be visualized *in situ* by the mean of lead phosphate precipitates, after the separation of the synthase complexes on native gel (Wittig et al., 2006; Bisetto et al., 2007). We choose this approach to investigate if the hydrolytic capacity of the ATP synthase in PS2 and PS2 APP mitochondria was lower than that of the Wt mitochondria. This semiquantitative method didn't produce clear-cut results, and the average size of the lead phosphate precipitates observed was similar among the three genotypes. Another, quantitative, though indirect approach to investigate the ATP synthase hydrolytic activity is through the measurements of the NADH oxidation based on the reaction

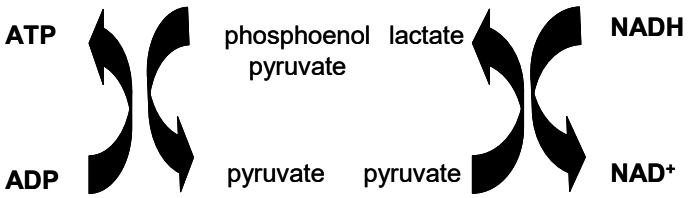

Briefly, after each cycle of ATP hydrolysis, the pyruvate kinase converts one molecule of phosphoenolpyruvate to pyruvate phosphorilating ADP back to ATP. In turn, pyruvate is reduced to lactate by the L-lactate dehydrogenase resulting in the oxidation of one NADH molecule to NAD^+. The constant regeneration of ATP allows the indirect measurement of ATP hydrolysis rate by the mean of the rate of NADH absorbance decrease.

We observed a slightly smaller hydrolytic activity in WT brain cortex mitochondria, compared with PS2 and PS2APP mitochondria, but due to the low number of measurements performed thus far the difference is not yet statistically significant. Again, we are aware that the results obtained with this approach could also be blunted by the fact that we are examining a pool of mitochondria coming from the different types of cells present in the mouse brain cortex.

The inhibition of complex III and ATP-synthase, induced respectively by antimycin and oligomycin, may cause a reduction in the ATP content of the cell, in turn leading to cellular Ca^{2+} dysregulation. Ca^{2+} dysregulation can precipitate cellular stress conditions, since the ion controls a wide range of fundamental cellular functions (Berridge 1998, Bezprozvanny 2017).

For this reason, we decided to check what happens in $[Ca^{2+}]_c$ under conditions of impaired oxidative phosphorylation.

We observed that resting levels of $[Ca^{2+}]_c$ were similar among the three genotypes, confirming results obtained in cortical neurons (Kypanyula et al., 2012).

We evaluated the increase in the FURA-2 340/380 fluorescence ratio consequent on the addition of antimycin or oligomycin to the cells. No differences were observed among the three genotypes and we concluded that under these specific experimental conditions, and for the length of time the cells were challenged, neurons of the different genotypes could equally handle a possible decrease in ATP content due to mitochondria impairment. It could be envisaged that a stronger, and prolonged stimulus would be necessary to disclose differences in the ability of neurons to deal with a higher cytosolic calcium content. In fact, we observed that a higher percentage of PS2 and PS2APP than WT neurons couldn't extrude the excess of cytosolic calcium caused by KCl addition.

The results obtained with isolated mitochondria first, and with neuronal culture second, point toward a defect in PS2 and PS2APP hippocampal neurons, observable when the cells are challenged with high metabolic demand, that could impair their response to stressful conditions and make them more vulnerable to external insults.

MATERIALS AND METHODS

Mouse strains and isolation of brain cortex mitochondria

The transgenic mouse lines PS2.30H and B6.152H were kindly donated by Dr. L. Ozmen (F. Hoffmann-La Roche Ltd, Basel, Switzerland) (Richards et al., 2003; Ozmen et al., 2009; Rhein et al., 2009). Both lines have the background strain of C57BL ⁄ 6 mice, which were used as wt controls and purchased from Charles River (Lecco, Italy). All procedures involving animals were carried out in strict adherence to the Italian regulations on animal protection and care and with the explicit approval of the local veterinary authority. Animals up to 8-day of age were sacrificed by decapitation, animals above 1-month of age were sacrificed by cervical dislocation, the procedures were performed by authorized personnel of the animal care facility. Brains were excised from the skulls, and the cortices were separated from olfactory bulbs, cerebellum and brainstem. The cortices were then rapidly transferred in an ice-cold solution of 225 mM mannitol, 50 mM sucrose, 10 mM Hepes, 1 mM P_i, 1 mM $MgCl_2$, 1 mM EGTA, 0.2% bovine serum albumin fatty acid free and 2 μM Tpen (pH: 7.4) (dissection medium 1), minced with scissors, and homogenized with few strokes in a glass potter. The homogenates were centrifuged at 2000 *g* for 3-minutes. The resulting supernatant was centrifuged at 12000 g for 6-minutes; the pellet obtained was resuspended with a large volume of the dissection medium with EGTA 20 μM and without BSA (dissection medium 2) and centrifuged as above. The resulting pellet was resuspended with a low volume of dissection medium 2, and the amount of protein obtained was quantified using the bicinchoninic acid assay (Euroclone). For all the experiments performed with isolated mitochondria, a basic isosmotic saline composed by 120 mM KCl, 10 mM NaCl, 20 mM Hepes, 1 mM P_i, and 1 mM $MgCl_2$. was used.

Mitochondrial calcium retention capacity (CRC) and membrane potential measurements

Kinetic, fluorimetric measurements of the mitochondria membrane potential and Ca^{2+} uptake were carried out at 25 °C with a Perkin-Elmer 650-40 spectrofluorimeter equipped with magnetic stirring and thermostatic control (Fontaine et al., 1998, Giorgio et al., 2013). Membrane potential was evaluated using 100 nM Rhodamine 123 (excitation-emission, 503-527 nm). During the experiments, upon mitochondria addition (0.5 mg/ml), 5 mM succinate and 4 μM FCCP were

sequentially added, and the fluorescence reached at equilibrium after each was registered. Extramitochondrial Ca^{2+} was measured after mitochondria addition (1 mg/ml) in the presence of 1 μM Calcium Green 5N (excitation-emission 505-532 nm). Known amount of Ca^{2+} (5 μM) were added every 2-minutes until the opening of the PTP, visualized as an increase in the Calcium Green fluorescent emission due to Ca^{2+} released from the mitochondrial matrix. These measurements were carried out in the absence or in the presence of 0.8 μM Cyclosporin A (CsA).

Oxygen consumption rate (OCR)

Mitochondrial OCR was evaluated polarographically at 25° C using a Clark-type electrode. The experiments were performed with 5 mM succinate as respiratory substrate, 100 μM ADP to measure the ADP-dependent OCR (state 3), 2μg/ml oligomycin to establish the state 4 and 100 nM FCCP to achieve the uncoupled respiration.

Cell Culture

Human fibroblasts (obtained from Coriell Institute for medical research): FAD-PS2-N141I (AG09908); and control fibroblasts (AG08525)) were grown in DMEM containing 15% FCS, supplemented with 2 mM L-glutamine, 100 U/ml penicillin and 100 μg/ml streptomycin, at 37° C, in a humidified atmosphere containing 5% CO2.

Transgenic mouse lines PS2.30H and B6.152H

- The C57BL/6J WT mice share the prevalent (> 90%) genetic background of the other lines and they were used as control.
- PS2.3OH (PS2): homozygous single transgenic line expressing the FAD-linked PS2-N141I under the prion promoter control and it is ubiquitously expressed.
- B6.152H (PS2APP): homozygous for both the human FAD-linked PS2-N141I mutation and the human APP K670N, M671L mutant (Swedish familial mutation). Mutated human APP is under the control of the Thy-1 promoter that is expressed only in neurons.

Primary neuronal cultures

Mouse primary hippocampal cultures were obtained from the brain of 0-1-day old newborn mice. After the brain dissection from mice, all the steps were performed in a saline with 10% Krebs buffer (composed by 124 mM NaCl, 14.4 glucose, 10 mM Hepes, 5.5 mM KCl, 1 mM NaH_2PO_4 and μM 2.8 Phenol Red, pH 7.4), 3% BSA fatty acid free and 465 μM $MgCl_2$. Cells were dissociated in 0.8 mg/ml trypsin for 10 min at 37° C, and digestion was blocked by the addition of 6.3 μg/ml trypsin inhibitor plus 40 μg/ml DNAse (protocol adapted from Zatti et al., 2006). Dissociated cells were plated on poly-L-lysine/laminin (30 μg/ml and 2 μg/ml, respectively) coated glass coverslips in MEM (Gibco, 32360-026) containing glucose (20 mM), and added with 0.5 mM L-glutamine, 1% N2 supplement, 0.5% B27 supplement, 3.6 μM biotin, 1 mM pyruvic acid, 25 μg/ml penicillin, 25 μg/ml streptomycin, and 10% horse serum. 24 h after cell plating the complete MEM was replaced with serum- and antibiotic-free Basal Medium Eagle (BME from Gibco, 42010-026) containing 2 % B27, 2 mM L-glutamine, and 0.23 mM sodium pyruvate. Fresh medium was added (1/5 of total plating volume) every 4^{th} day. Cultures were routinely treated with 2 μM cytosine arabinoside (AraC) to limit astrocytes growth.

Immunofluorescence

10-12 day *in vitro* hippocampal neurons were fixed with a medium containing 4 % PFA and 20% sucrose, for 10-minutes at RT. Glass coverslips were then washed for 5-min x 3 times with PBS and incubated with quenching solution (0.24% NH_4Cl in PBS) for 20 minutes; at the end of the incubation time were again washed for 5-min x 3 times. Cells were then treated with 0.1% TRITON-X 100 in PBS (permeabilization solution) for 3-minutes, and subsequently with 10% Goat serum, 2% BSA, 0.2% gelatin, in PBS (blocking solution) for 30 minutes. Primary antibodies were dissolved in blocking solution at the specified concentration and incubated with the cells for 1 hour at RT. The coverslips were then washed three times with PBS. Secondary Alexa-conjugated antibodies (diluted at recommended concentration in blocking solution) were incubated for 45 minutes at RT, and coverslips were then washed with PBS, stained with 100 μg/ml Hoechst and mounted on glass slides using Mowiol 4-88 (Calbiochem, 475904). Neurons were stained in red with neurofilament 200 (NF200) antibody (Sigma, N5389) whereas astrocytes in green with the glial fibrillary acidic protein (GFAP) antibody (Dako, Z0334). Images were collected by a DMI 6000

inverted microscope, with ORCA FLASH 4.0 (Hamamatsu) camera and then elaborated with ImageJ program (National Institutes of Health, US).

Cytosolic Ca^{2+} imaging with Fura-2

Cells were incubated with 1 μM Fura-2 AM, 0.02 % pluronic F-127 and 200 μM sulfinpyrazone for 40 minutes at 37 °C in physiologic saline composed by 140 mM NaCl, 2.8 mM KCl, 10 mM Hepes,2 mM $MgCl_2$ and supplemented with 5 mM glucose and 2 mM Ca^{2+} (pH 7.4). After the incubation the cells were washed with the saline. Fura-2–fluorescence images were captured using an inverted microscope (Zeiss Axiovert 100, Jena, Germany) with a 40X oil ultraviolet-permeable objective (Fluar, NA 1.30). Alternating excitation wavelengths of 340 and 380 nm were obtained by a monochromator (polychrome V, TILL-Photonics) controlled by a custom-made software package, Roboscope (developed by Catalin Ciubotaru, at VIMM, Padua, Italy). A neutral density filter, UVND 0.6 (Chroma, USA), was used in the excitation pathway. The emitted fluorescence was measured at 510 nm. Images were acquired every 5 seconds, with 200 ms exposure, by a PCO SensiCam QE (Kelheim, Germany) camera controlled by the Roboscope software. Regions of interest, corresponding to the entire soma, were selected for Ca^{2+} imaging. Coverslips were mounted in open-topped chamber, and bathed with the physiologic saline, all the experiments were performed at 37° C. After 5 minutes of basal acquisition, cells were challenged with 2 μg/ml oligomycin, or 1 μM antimycin A. The addition of 30 mM KCl at the end of each acquisition was used to depolarize the membrane potential and allow sustained Ca^{2+} entry in the cells.

In-situ mitochondrial membrane potential imaging with TMRM

Cells (hippocampal cultures or human fibroblasts) were incubated for 30 minutes at 37° C in the physiological saline with 10 nM TMRM and 2 μg/ml Cyclosporin H (CsH) to inhibit multidrug-resistance pumps, which could affect TMRM loading. TMRM-loaded cells were visualized using an inverted microscope (Zeiss Axiovert 100) with a 40X oil objective (Fluar, NA 1.30). Excitation light at 540±7.5 nm was produced by a monochromator (polychrome V; TILL Photonics) and passed through a Zeiss TRITC filter (Emission 573-613 nm) and a dichroic mirror (565 DCXR). Images were acquired using a cooled CCD camera (SensicamQE PCO, Kelheim, Germany). All filters and dichroic mirrors were from Chroma Technologies (Bellow Falls, VT, USA). The experiments were performed

at 37 °C, with one acquisition every minute and 50 ms exposure time. Complex I, and complex III of the respiratory chain, or the ATP synthase were selectively inhibited respectively by 2 μM rotenone, 1 μM antimycin or 2 μg/ml oligomycin. At the end of each experiment, 3 μM FCCP was added to assess the correct distribution of the dye.

Reactive Oxygen Species (ROS) measurements with MitoSOX Red

Hippocampal cultures were loaded with 200 nM MitoSOX Red (Invitrogen, M36008) in the physiological saline for 30 minutes at 37° C. MitoSOX red fluorescence images were acquired with an inverted microscope (Zeiss Axiovert 100) with a 40X oil objective (Fluar, NA 1.30). Excitation light at 510 nm was produced by a monochromator (polychrome V; TILL Photonics) and passed through a Zeiss TRITC filter (Emission 573-613 nm) and a dichroic mirror (565 DCXR). Images were acquired using a cooled CCD camera (SensicamQE PCO, Kelheim, Germany). All filters and dichroics were from Chroma Technologies (Bellow Falls, VT, USA). We compared the basal MitoSOX fluorescence at the beginning of each experiment, right after cell loading, with the fluorescence values reached after 1-hour 2 μg/ml oligomycin treatment.

Mitochondrial ATP hydrolysis

This assay is based on the reaction in which the hydrolysis of ATP is coupled to the oxidation of NADH. The experiments were carried out with 0.5 mg/ml of isolated mouse brain mitochondria, suspended in a saline containing 120 mM KCl, 10 mM NaCl, 20 mM Hepes, 1 mM P_i, 1 mM $MgCl_2$, 4 mM phospoenolpyruvate (PEP), 4 U/ml pyruvate kinase, 3 U/ml LDH (lactic dehydrogenase), 0.2 mM NADH and 2 mM ATP. Furthermore, 10 μM ouabain octahydrate, 10 μM vanadate and 2 μg/ml oligomycin were added to respectively inhibit the Na^+/K^+-ATPase, some plasma membrane ATPases (such as Na^+/K^+-ATPase and Ca^{2+}-ATPase) and the ATP synthase. The measurements were performed with a Cary Series UV-Vis spectrophotometer and the absorbance measured at 340 nm. The rate of NADH oxidation was measured and converted into NADH concentration using the NADH extinction coefficient ε= 6220 M^{-1}, cm^{-1}. Hydrolyzed ATP concentration was obtained knowing that 1 mole of ATP is hydrolyzed for every mole of NADH oxidized.

Blue native gel electrophoresis (BNE) and activity assay

Isolated mouse brain mitochondria were suspended at 10 mg/ml in 1 mM aminocaproic acid and 50 mM Bis-Tris, pH 7.0 (Giorgio et al., 2009), solubilized with 2 % digitionin, and immediately centrifuged at 58000 rpm for 25 minutes at 4°C (Beckman TL-100 Ultracentrifuge, TLA 120.1 rotor). The supernatants were supplemented with 0.35% Coomassie Blue G-250 (5% stock solution) and loaded in a 3-12% polyacrylamide gradient BNE (Invitrogen, BN1001BOX).

After the electrophoretic separation the gel was either stained with Comassie Blue, blotted onto PVDF Transfer membrane (GE Healthcare, RPN 303F) and probed with the anti ATP5B antibody (Abcam, ab1473) or used to detect ATPase activity *in situ*. For the latter assay, the gel was incubated overnight in a 35 mM Tris and 270 mM glycin buffer containing 0.2 M ATP, 0.3 M $MgSO_4$ and $Pb(NO_3)_2$ (about 20 mg every 10 ml of solution).

OCR measurements in intact cells

Isolated hippocampal cells were directly seeded ($2x10^5$ per well) onto 24 XF assay plate (Agilent Seahorse XF Technology), and after 10-12 days *in vitro*, the OCR was measured by the mean of the Extracellular Flux Analyzer (Agilent Seahorse). Two different protocols were followed. The first one was characterized by subsequent addition of 2 μg/ml oligomycin, 0.4 μM FCCP, and 2 μM rotenone together with plus 1 μM antimycin to evaluate the basal respiration rate, and the ATP synthesis coupled respiration rate. The same experiments were used to measure the extracellular acidification rate (ECAR). The other protocol employed subsequent FCCP additions (up to 0.4 μM), before rotenone/antimycin, to evaluate the maximal respiration rate achieved by the cells. The experiments were performed at 37°C, in a physiological saline in presence of 5 mM glucose and 2 mM Ca^{2+}.

Preparation of protein extracts and Western blot analysis

Hippocampal cultures from WT, PS2 and PS2APP mice were harvested and treated as follow: cells were homogenized and solubilized in RIPA buffer composed by 50 mM Tris, 150 mM NaCl, 1% Triton X-100, 0.5% deoxycholic acid, 0.1% SDS, protease inhibitor cocktail (Roche, 04693132001), phosphatase inhibitor cocktail (Roche, 04906837001), *as per* manufacturer instruction (pH 7.5)

and incubated on ice for 30 minutes. Un-solubilized material was spun down at 15000 g for 15 minutes at 4°C. Supernatant was collected and protein concentration quantified using the BCA assay kit (EuroClone). Proteins were loaded onto polyacrylamide gels (12%) and subsequently blotted onto nitrocellulose membrane (GE Healthcare, Amersham™ Protran™ 0.2 μM NC, 10600001).

The membranes were probed with MitoProfile total OXPHOS Rodent WB antibody Cocktail (Abcam ab110413) or Hsp 90 antibody (BD Biosciences, 610418).

Immuno-bands were visualized with the chemiluminescence reagent Westear Supernova (Cyanogen) on a Uvitec Mini HD9 (Eppendorf) instrument. Band intensities were analysed using ImageJ software (National Institute of Health, US).

Statistical analysis

Data were analyzed using Origin 8.0 SR5 (OriginLab Corporation), Microsoft Excel 2010 (Microsoft Corporation, Redmond, WA, USA) and ImageJ (National Institutes of Health,US) softwares.

Unless otherwise stated, numerical values presented throughout the text refer to mean ± standard deviation (DS).

(N=number of independent experiments, cells or wells as stated in the figure legends; * = $p < 0.05$, **=$p<0.01$, *** = $p < 0.001$, unpaired Student's *t* test or ANOVA test).

REFERENCES

1. Ables, J. L., Breunig, J. J., Eisch, A. J. & Rakic, P. Not(ch) just development: Notch signalling in the adult brain. *Nat. Rev. Neurosci.* (2011).

2. Abrahams, J. P., Leslie, A. G. W., Lutter, R. & Walker, J. E. Structure at 2.8 Â resolution of F1-ATPase from bovine heart mitochondria. *Nature* (1994).

3. Aisen, P. S. *et al.* On the path to 2025: understanding the Alzheimer's disease continuum. *Alzheimers. Res. Ther.* (2017).

4. Araki, W. *et al.* Trophic effect of β-amyloid precursor protein on cerebral cortical neurons in culture. *Biochem. Biophys. Res. Commun.* (1991).

5. Arispe, N., Diaz, J., Durell, S. R., Shafrir, Y. & Guy, H. R. Polyhistidine peptide inhibitor of the Aβ calcium channel potently blocks the Aβ-induced calcium response in cells. Theoretical modeling suggests a cooperative binding process. *Biochemistry* (2010).

6. Arnerić, S. P. *et al.* Cerebrospinal fluid biomarkers for Alzheimer's disease: A view of the regulatory science qualification landscape from the coalition against major diseases CSF biomarker team. *Journal of Alzheimer's Disease* (2016).

7. Balog, J., Mehta, S. L. & Vemuganti, R. Mitochondrial fission and fusion in secondary brain damage after CNS insults. *Journal of Cerebral Blood Flow & Metabolism* (2016).

8. Bambrick, L., Kristian, T. & Fiskum, G. Astrocyte Mitochondrial Mechanisms of Ischemic Brain Injury and Neuroprotection. *Neurochemical Research* (2004).

9. Barage, S. H. & Sonawane, K. D. Amyloid cascade hypothesis: Pathogenesis and therapeutic strategies in Alzheimer's disease. *Neuropeptides* (2015).

10. Basso E., Petronilli V., Forte MA., Bernardi P. Phosphate is essential for inhibition of the mitochondrial permeability transition pore by cyclosporin A and by cyclophilin D ablation. J *Biol Chem*. (2008)

11. Beck, S. J. *et al.* ARTICLE Deregulation of mitochondrial F1FO-ATP synthase via OSCP in Alzheimer's disease. *Nature Communications* (2016).

12. Beher, D., Hesse, L., Masters, C. L. & Multhaup, G. Regulation of amyloid protein precursor (APP) binding to collagen and mapping of the binding sites on APP and collagen type I. *J. Biol. Chem.* (1996).

13. Bernardi, P., Di Lisa, F., Fogolari, F. & Lippe, G. From ATP to PTP and back: A dual function for the mitochondrial ATP synthase. *Circulation Research* (2015).

14. Bernardi, P. *et al.* The mitochondrial permeability transition from in vitro artifact to disease target. *FEBS Journal* (2006).

15. Berridge, M. J. Neuronal calcium signaling. *Neuron* (1998).

16. Bisetto, E., Di Pancrazio, F., Simula, M. P., Mavelli, I. & Lippe, G. Mammalian ATPsynthase

monomer versus dimer profiled by blue native PAGE and activity stain. *Electrophoresis* (2007).

17. Bolmont, T. *et al.* Induction of Tau Pathology by Intracerebral Infusion of Amyloid-β-Containing Brain Extract and by Amyloid-β Deposition in APP × Tau Transgenic Mice. *Neurobiology* (2007).

18. Boyer, P. D. The ATP synthase-a splendid molecular machine. *Annu. Rev. Biochem.* (1997).

19. Braak, F., Braak, H. & Mandelkow, E. M. A sequence of cytoskeleton changes related to the formation of neurofibrillary tangles and neuropil threads. *Acta Neuropathol.* (1994).

20. Braak, H. & Braak, E. Frequency of stages of Alzheimer-related lesions in different age categories. *Neurobiol. Aging* (1997).

21. Braak, H., Alafuzoff, I., Arzberger, T., Kretzschmar, H. & Tredici, K. Staging of Alzheimer disease-associated neurofibrillary pathology using paraffin sections and immunocytochemistry. *Acta Neuropathol.* (2006).

22. Braak, H. & Del Tredici, K. Where, when, and in what form does sporadic Alzheimer's disease begin? *Curr. Opin. Neurol.* (2012).

23. Braak, H. & Del Tredici, K. Alzheimer's pathogenesis: Is there neuron-to-neuron propagation? *Acta Neuropathologica* (2011).

24. Braak, H. & Del Tredici, K. The preclinical phase of the pathological process underlying sporadic Alzheimer's disease. *Brain* (2015).

25. Braak, H., Zetterberg, H., Del Tredici, K. & Blennow, K. Intraneuronal tau aggregation precedes diffuse plaque deposition, but amyloid-β changes occur before increases of tau in cerebrospinal fluid. *Acta Neuropathologica* (2013).

26. Brand, M. D. & Nicholls, D. G. Assessing mitochondrial dysfunction in cells. *Biochem. J.* (2011).

27. Brunello, L. *et al.* Presenilin-2 dampens intracellular Ca^{2+} stores by increasing Ca^{2+} leakage and reducing Ca^{2+} uptake. *J. Cell. Mol. Med.* (2009).

28. Busche, M. A. & Konnerth, A. Impairments of neural circuit function in Alzheimer's disease. *Philos. Trans. R. Soc. B Biol. Sci.* (2016).

29. Cadonic, C., Sabbir, M. G. & Albensi, B. C. Mechanisms of Mitochondrial Dysfunction in Alzheimer's Disease. *Mol. Neurobiol.* (2016).

30. Cadonic, C., Sabbir, M. G. & Albensi, B. C. Mechanisms of Mitochondrial Dysfunction in Alzheimer's Disease. *Mol. Neurobiol.* (2016).

31. Campanella, M., Parker, N., Tan, C. H., Hall, A. M. & Duchen, M. R. IF1: setting the pace of the F1Fo-ATP synthase. *Trends in Biochemical Sciences* (2009).

32. Campion, D. *et al.* A novel presenilin 1 mutation resulting in familial Alzheimer's disease with an onset age of 29 years. *Neuroreport* (1996).

33. Cárdenas, C. *et al.* Essential Regulation of Cell Bioenergetics by Constitutive InsP3 Receptor Ca^{2+} Transfer to Mitochondria. *Cell* (2010).

34. Castellani, R. *et al.* Role of mitochondrial dysfunction in Alzheimer's disease. *J. Neurosci. Res.* (2002).

35. Castellani, R. *et al.* Role of mitochondrial dysfunction in Alzheimer's disease. *Journal of Neuroscience Research* (2002).

36. Cenquizca, L. A. & Swanson, L. W. Spatial organization of direct hippocampal field CA1 axonal projections to the rest of the cerebral cortex. *Brain Research Reviews* (2007).

37. Chan, S. L., Mayne, M., Holden, C. P., Geiger, J. D. & Mattson, M. P. Presenilin-1 mutations increase levels of ryanodine receptors and calcium release in PC12 cells and cortical neurons. *J. Biol. Chem.* (2000).

38. Chaturvedi, R. K. *et al.* Impaired PGC-1a function in muscle in Huntington's disease. *Human Molecular Genetics* (2009).

39. Chételat, G. *et al.* Amyloid imaging in cognitively normal individuals, at-risk populations and preclinical Alzheimer's disease. *NeuroImage: Clinical* (2013).

40. Cheung, K.-H. *et al.* Mechanism of Ca^{2+} Disruption in Alzheimer's Disease by Presenilin Regulation of InsP 3 Receptor Channel Gating. *Neuron*. (2008).

41. Chiang, M. C., Chern, Y. & Huang, R. N. PPARgamma rescue of the mitochondrial dysfunction in Huntington's disease. *Neurobiol. Dis.* (2012).

43. Chiang, P. M., Fortna, R. R., Price, D. L., Li, T. & Wong, P. C. Specific domains in anterior pharynx-defective 1 determine its intramembrane interactions with nicastrin and presenilin. *Neurobiol. Aging* (2012).

44. Choi, H. J. *et al.* Tetrahydrobiopterin causes mitochondrial dysfunction in dopaminergic cells: Implications for Parkinson's disease. *Neurochem. Int.* (2006).

45. Choi, Y.-S. *et al.* Shot-gun proteomic analysis of mitochondrial D-loop DNA binding proteins: identification of mitochondrial histonesw. *Mol. BioSyst. Mol. BioSyst* (2011).

46. Chyung, J. H., Raper, D. M. & Selkoe, D. J. γ-secretase exists on the plasma membrane as an intact complex that accepts substrates and effects intramembrane cleavage. *J. Biol. Chem.* (2005).

47. Clarris, H. J. *et al.* Identification of Heparin-Binding Domains in the Amyloid Precursor Protein of Alzheimer's Disease by Deletion Mutagenesis and Peptide Mapping. *J. Neurochem.* (2002).

48. Crompton, M., Ellinger, H. & Costi, A. Inhibition by cyclosporin A of a Ca^{2+}-dependent pore in heart mitochondria activated by inorganic phosphate and oxidative stress The capacity of cyclosporin A to inhibit opening of a Ca^{2+}-dependent pore in the inner membrane of heart. *Biochem. J* (1988).

49. Croteau, D. L., Stierum, R. H. & Bohr, V. A. Section I. Damage and repair in mitochondria Mitochondrial DNA repair pathways. *Mutat. Res.* (1999).

50. Crous-Bou, M., Minguillón, C., Gramunt, N. & Molinuevo, J. L. Alzheimer's disease prevention: from risk factors to early intervention. *Alzheimers Res Ther*. (2017).

51. Crystal, A. S. *et al.* Membrane topology of γ-secretase component PEN-2. *J. Biol. Chem.*

(2003).

52. Cui, L. *et al.* Transcriptional Repression of PGC-1α by Mutant Huntingtin Leads to Mitochondrial Dysfunction and Neurodegeneration. *Cell* (2006).

53. Davies, K. M. *et al.* Macromolecular organization of ATP synthase and complex I in whole mitochondria. *Proc. Natl. Acad. Sci.* (2011).

54. Dawkins, E. & Small, D. H. Insights into the physiological function of the β-amyloid precursor protein: Beyond Alzheimer's disease. *Journal of Neurochemistry* (2014).

55. De Bock, K. *et al.* Role of PFKFB3-driven glycolysis in vessel sprouting. *Cell* (2013).

56. De Strooper, B. *et al.* Deficiency of presenilin-1 inhibits the normal cleavage of amyloid precursor protein. *Nature* (1998).

57. De Strooper, B. Aph-1, Pen-2, and Nicastrin with Presenilin generate an active γ-Secretase complex. *Neuron* (2003).

58. De Strooper, B. *et al.* A presenilin-1-dependent g-secretase-like protease mediates release of Notch intracellular domain. *Nature* (1999)

59. De Strooper, B., Iwatsubo, T. & Wolfe, M. S. Presenilins and γ-secretase: structure, function, and role in Alzheimer Disease. *Cold Spring Harbor perspectives in medicine* (2012).

60. De Strooper, B. & Karran, E. The Cellular Phase of Alzheimer's Disease. *Cell* (2016).

61. Demehri, S., Turkoz, A. & Kopan, R. Epidermal Notch1 loss promotes skin tumorigenesis by impacting the stromal microenvironment. *Cancer Cell* (2009).

62. Devi, L., Raghavendran, V., Prabhu, B. M., Avadhani, N. G. & Anandatheerthavarada, H. K. Mitochondrial import and accumulation of α-synuclein impair complex I in human dopaminergic neuronal cultures and Parkinson disease brain. *J. Biol. Chem.* (2008).

63. Duara, R. *et al.* A comparison of familial and sporadic Alzheimer's disease 813. *Neurology* (1993).

64. Dubois, B. *et al.* Preclinical Alzheimer's disease: Definition, natural history, and diagnostic criteria. *Alzheimer's and Dementia* (2016).

65. Edland, S. D. *et al.* Increased risk of dementia in mothers of Alzheimer's disease cases: evidence for maternal inheritance. *Neurology* (1996).

66. Emaus, R. K., Grunwald, R. & Lemasters, J. J. Rhodamine 123 as a probe of transmembrane potential in isolated rat-liver mitochondria: spectral and metabolic properties. *BBA - Bioenerg.* (1986).

67. Ertekin-Taner, N. Genetics of Alzheimer's Disease: A Centennial Review. *Neurologic Clinics* (2007).

68. Espuny-Camacho, I. *et al.* Hallmarks of Alzheimer's Disease in Stem-Cell-Derived Human Neurons Transplanted into Mouse Brain. *Neuron* (2017).

69. Fanselow, M. S. & Dong, H. W. Are the Dorsal and Ventral Hippocampus Functionally Distinct Structures? *Neuron* (2010).

70. Filosto, M. *et al.* The role of mitochondria in neurodegenerative diseases. *J. Neurol.* (2011).

71. Fontaine, E., Eriksson, O., Ichas, F. O. & Bernardi, P. Regulation of the Permeability Transition Pore in Skeletal Muscle Mitochondria. *The Journal of Biological Chemistry* (1998).

72. Fontana, R. *et al.* Early hippocampal hyperexcitability in PS2APP mice: role of mutant PS2 and APP. *Neurobiol. Aging* (2017).

73. Forstl, H. & Kurz, A. Clinical features of Alzheimer's disease. *Eur. Arch. Psychiatry Clin. Neurosci.* (1999).

74. Fortna, R. R. *et al.* Membrane Topology and Nicastrin-enhanced Endoproteolysis of APH-1, a Component of the γ-Secretase Complex. *J. Biol. Chem.* (2004).

75. Foster, N. L. *et al.* Brain choline acetyltransferase activity and neuropeptide Y concentrations in Alzheimer's disease. *Neurosci. Lett.* (1986).

76. Francis, P. T., Palmer, A. M., Snape, M. & Wilcock, G. K. The cholinergic hypothesis of Alzheimer's disease: a review of progress. *J Neurol Neurosurg Psychiatry* (1999).

77. Fuenzalida, K. *et al.* Peroxisome proliferator-activated receptor γ up-regulates the Bcl-2 anti-apoptotic protein in neurons and induces mitochondrial stabilization and protection against oxidative stress and apoptosis. *J. Biol. Chem.* (2007).

78. Futai, M., Nakanishi-Matsui, M., Okamoto, H., Sekiya, M. & Nakamoto, R. K. Rotational catalysis in proton pumping ATPases: From E. coli F-ATPase to mammalian V-ATPase. in *Biochimica et Biophysica Acta - Bioenergetics* (2012).

79. Gatz, M. *et al.* Role of Genes and Environments for Explaining Alzheimer Disease. *Arch. Gen. Psychiatry* (2006).

80. Ghesquière, B., Wong, B. W., Kuchnio, A. & Carmeliet, P. Metabolism of stromal and immune cells in health and disease. *Nature* (2014).

81. Giacomello, M., Drago, I., Pizzo, P. & Pozzan, T. Mitochondrial Ca^{2+} as a key regulator of cell life and death. *Cell Death Differ.* (2007).

82. Gibson, G. E., Sheu, K. F. R. & Blass, J. P. Abnormalities of mitochondrial enzymes in Alzheimer disease. *J. Neural Transm.* (1998).

83. Giorgio, V. *et al.* Cyclophilin D modulates mitochondrial F0F1-ATP synthase by interacting with the lateral stalk of the complex. *J. Biol. Chem.* (2009).

84. Giorgio, V. *et al.* Dimers of mitochondrial ATP synthase form the permeability transition pore. *Proc Natl Acad Sci U S A.* (2013)

85. Goedert, M., Wischik, C. M., Crowther, R. A., Walker, J. E. & Klug, A. A. Cloning and sequencing of the cDNA encoding a core protein of the paired helical filament of Alzheimer disease: Identification as the microtubule-associated protein tau. *Med. Sci.* (1988).

86. Golpich, M. *et al.* Glycogen synthase kinase-3 beta (GSK-3β) signaling: Implications for Parkinson's disease. *Pharmacological Research* (2015).

87. Golpich, M. *et al.* Mitochondrial Dysfunction and Biogenesis in Neurodegenerative diseases: Pathogenesis and Treatment. *CNS Neuroscience and Therapeutics* (2017).

88. Gong, B. *et al.* Ubiquitin Hydrolase Uch-L1 Rescues β-Amyloid-Induced Decreases in Synaptic Function and Contextual Memory. *Cell* (2006).

89. Haass, C. & Selkoe, D. J. Cellular processing of β-amyloid precursor protein and the genesis of amyloid β-peptide. *Cell* (1993).

90. Haass, C. & Selkoe, D. J. Soluble protein oligomers in neurodegeneration: lessons from the Alzheimer's amyloid β-peptide. *Nat. Rev. Mol. Cell Biol.* (2007).

91. Habersetzer, J. *et al.* ATP synthase oligomerization: From the enzyme models to the mitochondrial morphology. *International Journal of Biochemistry and Cell Biology* (2013).

92. Halliwell, B. Reactive oxygen species and the central nervous system. *Journal of Neurochemistry* (1992).

93. Hardy, J. The Amyloid Hypothesis of Alzheimer's Disease: Progress and Problems on the Road to Therapeutics. *Science* (2002).

94. Hardy, J. & Higgins, G. Alzheimer's disease: the amyloid cascade hypothesis. *Science* (1992).

95. Hardy, J. & Allsop, D. Amyloid deposition as the central event in the aetiology of Alzheimer's disease. *Trends in Pharmacological Sciences* (1991).

96. Hébert, S. S. *et al.* Coordinated and widespread expression of gamma-secretase in vivo: Evidence for size and molecular heterogeneity. *Neurobiol. Dis.* (2004).

97. Henricson, A., Käll, L. & Sonnhammer, E. L. L. A novel transmembrane topology of presenilin based on reconciling experimental and computational evidence. *FEBS J.* (2005).

98. Herreman, A. *et al.* Presenilin 2 deficiency causes a mild pulmonary phenotype and no changes in amyloid precursor protein processing but enhances the embryonic lethal phenotype of presenilin 1 deficiency. *Proc Natl Acad Sci U S A.* (2003).

99. Hoffmann, J., Twiesselmann, C., Kummer, M. P., Romagnoli, P. & Herzog, V. A. Possible role for the Alzheimer amyloid precursor protein in the regulation of epidermal basal cell proliferation. *Eur J Cell Biol*. (2000).

100. Holtzman, D. M., John, C. M. & Goate, A. Alzheimer's Disease: The Challenge of the Second Century. *Sci Transl Med*. (2011).

101. Hroudová, J., Singh, N. & Fišar, Z. Mitochondrial dysfunctions in neurodegenerative diseases: Relevance to alzheimer's disease. *BioMed Research International* (2014).

102. Hu, H., Tan, C.-C., Tan, L. & Yu, J.-T. A Mitocentric View of Alzheimer's Disease. *Mol Neurobiol*. (2017).

103. Irwin, W. *et al.* Mitochondrial dysfunction and apoptosis in myopathic mice with collagen VI deficiency. *Nat. Genet.* (2003).

104. Jack, C. R. *et al.* Brain β-amyloid load approaches a plateau. *Neurology* (2013).

105. Jarrett, J. T., Berger, E. P. & Lansbury, P. T. The Carboxy Terminus of the β Amyloid Protein Is Critical for the Seeding of Amyloid Formation: Implications for the Pathogenesis of Alzheimer's Disease. *Biochem. &copy* (1993).

106. Jin, L.-W. *et al.* Peptides Containing the RERMS Sequence of Amyloid ,β/A4 Protein

Precursor Bind Cell Surface and Promote Neurite Extension. *J. Neurosci.* (1994).

107. Kaasik, A., Safiulina, D., Zharkovsky, A. & Veksler, V. Regulation of mitochondrial matrix volume. *AJP Cell Physiol.* (2006).

108. Kaether, C., Haass, C. & Steiner, H. Assembly, trafficking and function of γ-secretase. in *Neurodegenerative Diseases* (2006).

109. Kaether, C., Schmitt, S., Willem, M. & Haass, C. Amyloid precursor protein and Notch intracellular domains are generated after transport of their precursors to the cell surface. *Traffic* (2006).

110. Kang, D. E. *et al.* Presenilin couples the paired phosphorylation of β-catenin independent of axin: Implications for β-catenin activation in tumorigenesis. *Cell* (2002).

111. Karran, E. & De Strooper, B. The amyloid cascade hypothesis: are we poised for success or failure? *J. Neurochem.* (2016).

112. Kathrin Lutz, A. *et al.* Loss of parkin or PINK1 function increases Drp1-dependent mitochondrial fragmentation. *J. Biol. Chem.* (2009).

113. Keeney, P. M. Parkinson's Disease Brain Mitochondrial Complex I Has Oxidatively Damaged Subunits and Is Functionally Impaired and Misassembled. *J. Neurosci.* (2006).

114. Kehoe, P. G., Miners, S. & Love, S. Angiotensins in Alzheimer's disease - friend or foe? *Trends in Neurosciences* (2009).

115. Khandelwal, P. J., Herman, A. M., Hoe, H. S., Rebeck, G. W. & Moussa, C. E. H. Parkin mediates beclin-dependent autophagic clearance of defective mitochondria and ubiquitinated Aβ in AD models. *Hum. Mol. Genet.* (2011).

116. Kibbey, M. C. *et al.* β-Amyloid precursor protein binds to the neurite-promoting IKVAV site of laminin. *Cell Biol.* (1993).

117. Kim, J. *et al.* Beta-amyloid oligomers activate apoptotic BAK pore for cytochrome c release. *Biophys. J.* (2014).

118. Kim, T. K. & Eberwine, J. H. Mammalian cell transfection: The present and the future. *Anal. Bioanal. Chem.* (2010).

119. Kimberly, W. T., Zheng, J. B., Guénette, S. Y. & Selkoe, D. J. The Intracellular Domain of the β-Amyloid Precursor Protein Is Stabilized by Fe65 and Translocates to the Nucleus in a Notch-like Manner. *J. Biol. Chem.* (2001).

120. Kinnally, K. W., Campo, M. L. & Tedeschi, H. Mitochondrial channel activity studied by patch-clamping mitoplasts. *J. Bioenerg. Biomembr.* (1989).

121. Kipanyula, M. J. *et al.* Ca^{2+} dysregulation in neurons from transgenic mice expressing mutant presenilin 2. *Aging Cell* (2012).

122. Kovacs, D. M. *et al.* Alzheimer-associated presenilins 1 and 2: neuronal expression in brain and localization to intracellular membranes in mammalian cells. *Nat. Med.* (1996).

123. La Ferla, F. M. Pathways linking Abeta and tau pathologies. *Biochem Soc Trans*. (2010).

124. LaFerla, F. M., Green, K. N. & Oddo, S. Intracellular amyloid-β in Alzheimer's disease. *Nat.*

Rev. Neurosci. (2007).

125. LaVoie, M. J. *et al.* Assembly of the γ-secretase complex involves early formation of an intermediate subcomplex of Aph-1 and nicastrin. *J. Biol. Chem.* (2003).

126. Lazarov, O. & Hollands, C. Hippocampal neurogenesis: Learning to remember. *Progress in Neurobiology* (2016).

127. Lazarov, O. & Marr, R. A. Of mice and men: Neurogenesis, cognition, and Alzheimer's disease. *Frontiers in Aging Neuroscience* (2013).

128. Leissring, M. A., Parker, I. & LaFerla, F. M. Presenilin-2 mutations modulate amplitude and kinetics of inositol 1,4,5-trisphosphate-mediated calcium signals. *J. Biol. Chem.* (1999).

129. Leissring, M. A., Paul, B. A., Parker, I., Cotman, C. W. & Laferla, F. M. Alzheimer's presenilin-1 mutation potentiates inositol 1,4,5- trisphosphate-mediated calcium signaling in Xenopus oocytes. *J. Neurochem.* (1999).

130. Leissring, M. A. *et al.* Brief Report Capacitative Calcium Entry Deficits and Elevated Luminal Calcium Content in Mutant Presenilin-1 Knockin Mice. *J. Cell Biol.* (2000).

131. Lewerenz, J. & Maher, P. Chronic glutamate toxicity in neurodegenerative diseases-What is the evidence? *Frontiers in Neuroscience* (2015).

132. Lewis, J. Enhanced Neurofibrillary Degeneration in Transgenic Mice Expressing Mutant Tau and APP. *Science* (2001).

133. Lezi, E. & Swerdlow, R. H. Mitochondria in neurodegeneration. *Adv. Exp. Med. Biol.* (2012).

134. Li, T., Ma, G., Cai, H., Price, D. L. & Wong, P. C. Nicastrin Is Required for Assembly of Presenilin/γ-Secretase Complexes to Mediate Notch Signaling and for Processing and Trafficking of β-Amyloid Precursor Protein in Mammals. *J Neurosci*. (2003).

135. Lin, M. T. & Beal, M. F. Mitochondrial dysfunction and oxidative stress in neurodegenerative diseases. *Nature* (2006).

136. Liu, J. *et al.* Toxicity of familial ALS-linked SOD1 mutants from selective recruitment to spinal mitochondria. *Neuron* (2004).

137. Liu, L. *et al.* Trans-synaptic spread of tau pathology in vivo. *PLoS One* (2012).

138. Liu, P. & Demple, B. DNA repair in mammalian mitochondria: Much more than we thought? *Environ. Mol. Mutagen.* (2010).

139. Mamelak, M. Energy and the Alzheimer brain. *Neuroscience and Biobehavioral Reviews* (2017).

140. Mancuso, M., Calsolaro, V., Orsucci, D., Siciliano, G. & Murri, L. Is there a primary role of the mitochondrial genome in Alzheimer's disease? *Journal of Bioenergetics and Biomembranes* (2009).

141. Marambaud, P. *et al.* A presenilin-1/γ-secretase cleavage releases the E-cadherin intracellular domain and regulates disassembly of adherens junctions. *EMBO J.* (2002).

142. Marchetti, M. & Marie, H. Hippocampal synaptic plasticity in Alzheimer's disease: What have we learned so far from transgenic models? *Reviews in the Neurosciences* (2011).

143. Martin, J., Hudson, J., Hornung, T. & Frasch, W. D. Fo -driven Rotation in the ATP Synthase Direction against the Force of F 1 ATPase in the Fo F1 ATP Synthase. *The Jou. of Bio. Chem.* (2015).

144. Martin, W. F., Garg, S. & Zimorski, V. Endosymbiotic theories for eukaryote origin. *Philos. Trans. R. Soc. B Biol. Sci.* (2015).

145. Martín-Maestro, P., Gargini, R., Perry, G., Avila, J. & García-Escudero, V. PARK2 enhancement is able to compensate mitophagy alterations found in sporadic Alzheimer's disease. *Hum. Mol. Genet.* (2016).

146. Masters, C. L. *et al.* Amyloid plaque core protein in Alzheimer disease and Down syndrome. *Med. Sci.* (1985).

147. Masuda, A. *et al.* Cognitive deficits in single App knock-in mouse models. *Neurobiol. Learn. Mem.* (2016).

148. Mattiazzi, M. *et al.* Mutated human SOD1 causes dysfunction of oxidative phosphorylation in mitochondria of transgenic mice. *J. Biol. Chem.* (2002).

149. McCarthy, J. V., Twomey, C. & Wujek, P. Presenilin-dependent regulated intramembrane proteolysis and γ-secretase activity. *Cellular and Molecular Life Sciences* (2009).

150. McKee, A. C., Stein, T. D., Kiernan, P. T. & Alvarez, V. E. The neuropathology of chronic traumatic encephalopathy. in *Brain Pathology* (2015).

151. Meraz-Ríos, M. A., Franco-Bocanegra, D., Toral Rios, D. & Campos-Peña, V. Early onset Alzheimer's disease and oxidative stress. *Oxidative Medicine and Cellular Longevity* (2014).

152. Milward, E. A. *et al.* The amyloid protein precursor of Alzheimer's disease is a mediator of the effects of nerve growth factor on neurite outgrowth. *Neuron* (1992).

153. Minta, A., Kao, J. P. Y. & Tsien, R. Y. Fluorescent indicators for cytosolic calcium based on rhodamine and fluorescein chromophores. *J. Biol. Chem.* (1989).

154. Morrison, B. M., Lee, Y. & Rothstein, J. D. Oligodendroglia: metabolic supporters of axons. *Trends Cell Biol.* (2013).

155. Mucke, L. *et al.* High-Level Neuronal Expression of Aβ 1–42 in Wild-Type Human Amyloid Protein Precursor Transgenic Mice: Synaptotoxicity without Plaque Formation. *J Neurosci*. (2000)

156. Mudher, A. & Lovestone, S. Alzheimer's disease - Do tauists and baptists finally shake hands? *Trends in Neurosciences* (2002).

157. Nakamura, K. *et al.* Direct membrane association drives mitochondrial fission by the Parkinson disease-associated protein α-synuclein. *J. Biol. Chem.* (2011).

158. Needham, B. E. *et al.* Identification of the Alzheimer's disease amyloid precursor protein (APP) and its homologue APLP2 as essential modulators of glucose and insulin homeostasis and growth. *J. Pathol.* (2008).

159. Nelson, P. T. *et al.* Correlation of Alzheimer Disease Neuropathologic Changes With Cognitive Status: A Review of the Literature. *J Neuropathol Exp Neurol* (2012).

160. Ng, C.-H. *et al.* AMP Kinase Activation Mitigates Dopaminergic Dysfunction and Mitochondrial Abnormalities in Drosophila Models of Parkinson's Disease. *J. Neurosci.* (2012).

161. Ninomiya, H., Roch, J. -M, Jin, L. -W & Saitoh, T. Secreted Form of Amyloid β/A4 Protein Precursor (APP) Binds to Two Distinct APP Binding Sites on Rat B103 Neuron-Like Cells Through Two Different Domains, but Only One Site Is Involved in Neuritotropic Activity. *J. Neurochem.* (1994).

162. Nithianantharajah, J. & Grant, S. G. N. Cognitive components in mice and humans: Combining genetics and touchscreens for medical translation. *Neurobiol. Learn. Mem.* (2013).

163. Nunan, J. & Small, D. H. Regulation of APP cleavage by K-, L-and Q-secretases. *FEBS Lett.* (2000).

164. Nunomura, A. *et al.* Oxidative damage is the earliest event in Alzheimer disease. *J. Neuropathol. Exp. Neurol.* (2001).

165. Ohno, M. Alzheimer's therapy targeting the β-secretase enzyme BACE1: Benefits and potential limitations from the perspective of animal model studies. *Brain Research Bulletin* (2016).

166. Okano, H. *et al.* Brain/MINDS: A Japanese National Brain Project for Marmoset Neuroscience. *Neuron* (2016).

167. Ong, W. Y., Tanaka, K., Dawe, G. S., Ittner, L. M. & Farooqui, A. A. Slow excitotoxicity in alzheimer's disease. *Journal of Alzheimer's Disease* (2013).

168. Ortega-Arellano, H. F., Jimenez-Del-Rio, M. & Velez-Pardo, C. Life span and locomotor activity modification by glucose and polyphenols in Drosophila melanogaster chronically exposed to oxidative stress-stimuli: Implications in Parkinson's disease. *Neurochem. Res.* (2011).

169. Ossenkoppele, R. *et al.* Tau PET patterns mirror clinical and neuroanatomical variability in Alzheimer's disease. *Brain* (2016).

170. Ozmen, L., Albientz, A., Czech, C. & Jacobsen, H. Expression of transgenic APP mRNA is the key determinant for beta-amyloid deposition in PS2APP transgenic mice. *Neurodegener. Dis.* (2008).

171. Palmer, A. E. *et al.* Ca^{2+} Indicators Based on Computationally Redesigned Calmodulin-Peptide Pairs. *Chem. Biol.* (2006).

172. Palop, J. J. *et al.* Aberrant Excitatory Neuronal Activity and Compensatory Remodeling of Inhibitory Hippocampal Circuits in Mouse Models of Alzheimer's Disease. *Neuron* (2007).

173. Pchitskaya, E., Popugaeva, E. & Bezprozvanny, I. G Model Calcium signaling and molecular mechanisms underlying neurodegenerative diseases. *Cell Calcium* (2017).

174. Pendin, D., Greotti, E., Lefkimmiatis, K. & Pozzan, T. Exploring cells with targeted biosensors. *J. Exp. Physiol.* (2017).

175. Penna, E., Espino, J., De Stefani, D. & Rizzuto, R. The MCU complex in cell death. *Cell Calcium* (2017).

176. Perl, D. P. Neuropathology of Alzheimer's Disease. *Mt Sinai J Med* (2010)

177. Petronilli, V., Szabò, I. & Zoratti, M. The inner mitochondrial membrane contains ion-conducting channels similar to those found in bacteria. *FEBS Lett.* (1989).

178. Pfeiffer, B. D. *et al.* Tools for neuroanatomy and neurogenetics in Drosophila. *Proc. Natl. Acad. Sci.* (2008).

179. Phillips, N. R., Simpkins, J. W. & Roby, R. K. Mitochondrial DNA deletions in Alzheimer's brains: A review. *Alzheimer's Dement.* (2014).

180. Pini, L. *et al.* Brain atrophy in Alzheimer's Disease and aging. *Ageing Research Reviews* (2016).

181. Poole, A. C. *et al.* The PINK1/Parkin pathway regulates mitochondrial morphology. PNAS (2008)

182. Pothuizen, H. H. J., Zhang, W. N., Jongen-Rêlo, A. L., Feldon, J. & Yee, B. K. Dissociation of function between the dorsal and the ventral hippocampus in spatial learning abilities of the rat: A within-subject, within-task comparison of reference and working spatial memory. *Eur. J. Neurosci.* (2004).

183. Praticò, D., Uryu, K., Leight, S., Trojanoswki, J. Q. & Lee, V. M.-Y. Increased Lipid Peroxidation Precedes Amyloid Plaque Formation in an Animal Model of Alzheimer Amyloidosis. *The Journal of Neuroscience* (2001).

184. Price, J. L. & Morris, J. C. Tangles and Plaques in Nondemented Aging and ' Preclinical ' Alzheimer's Disease. *American Neurological Association* (1999).

185. Reddy, P. H., Mao, P. & Manczak, M. Mitochondrial structural and functional dynamics in Huntington's disease. *Brain Research Reviews* (2009).

186. Rhein, V. *et al.* Amyloid-β and tau synergistically impair the oxidative phosphorylation system in triple transgenic Alzheimer's disease mice. PNAS (2009).

187. Richards, J. G. *et al.* Behavioral/Systems/Cognitive PS2APP Transgenic Mice, Coexpressing hPS2mut and hAPPswe, Show Age-Related Cognitive Deficits Associated with Discrete Brain Amyloid Deposition and Inflammation. *The Journal of Neuroscience* (2003).

188. Richter, C., Park, J.-W. & Amest, B. N. Normal oxidative damage to mitochondrial and nuclear DNA is extensive. *Genetics* (1988).

189. Rodolfo, C., Campello, S. & Cecconi, F. Mitophagy in neurodegenerative diseases. *Neurochemistry International Journal* (2017).

190. Rojas-Charry, L., Cookson, M. R., Niño, A., Arboleda, H. & Arboleda, G. Downregulation of Pink1 influences mitochondrial fusion-fission machinery and sensitizes to neurotoxins in dopaminergic cells. *Neurotoxicology* (2014).

191. Saito, T. *et al.* Single App knock-in mouse models of Alzheimer's disease. *Nat. Neurosci.* (2014).

192. Saitoh, T. *et al.* Secreted form of amyloid β protein precursor is involved in the growth regulation of fibroblasts. *Cell* (1989).

193. Sanabria-Castro, A., Alvarado-Echeverría, I. & Monge-Bonilla, C. Molecular Pathogenesis of

Alzheimer's Disease: An Update Search Strategy and Selection Criteria. *Ann Neurosci* (2017).

194. Sanderson, T. H., Raghunayakula, S. & Kumar, R. Release of mitochondrial Opa1 following oxidative stress in HT22 cells. *Mol. Cell. Neurosci.* (2015).

195. Sasaguri, H. *et al.* APP mouse models for Alzheimer's disease preclinical studies. *EMBO J.* (2017).

196. Saxena, S. & Caroni, P. Selective Neuronal Vulnerability in Neurodegenerative Diseases: From Stressor Thresholds to Degeneration. *Neuron* (2011).

197. Scaduto, R. C. & Grotyohann, L. W. Measurement of Mitochondrial Membrane Potential Using Fluorescent Rhodamine Derivatives. *Biophys. J.* (1999).

198. Selkoe, D. J. Alzheimer's disease: a central role for amyloid. *J. Neuropathol. Exp. Neurol.* (1994).

199. Selkoe, D. J. Translating cell biology into therapeutic advances in Alzheimer's disease. *Nature* (1999).

200. Selkoe, D. J. & Hardy, J. The amyloid hypothesis of Alzheimer's disease at 25 years. *EMBO Mol Med* (2016).

201. Serban, G. *et al.* Cadherins mediate both the association between PS1 and β-catenin and the effects of PS1 on β-catenin stability. *J. Biol. Chem.* (2005).

202. Shen, J. *et al.* Skeletal and CNS defects in Presenilin-1-Deficient Mice. *Cell* (1997).

203. Shirotani, K. *et al.* γ-Secretase activity is associated with a conformational change of Nicastrin. *J. Biol. Chem.* (2003).

204. Shirotani, K., Edbauer, D., Prokop, S., Haass, C. & Steiner, H. Identification of distinct γ-secretase complexes with different APH-1 variants. *J. Biol. Chem.* (2004).

205. Small, D. H. *et al.* A Heparin-binding Domain in the Amyloid Protein Precursor of Alzheimer's Disease Is Involved in the Regulation of Neurite Outgrowth. *J. Neurosci.* (1994).

206. Smith, I. F., Hitt, B., Green, K. N., Oddo, S. & LaFerla, F. M. Enhanced caffeine-induced Ca^{2+} release in the 3xTg-AD mouse model of Alzheimer's disease. *J. Neurochem.* (2005).

207. Soba, P. *et al.* Homo- and hetero-dimerization of APP family members promotes intercellular adhesion. *EMBO J.* (2006).

208. Swerdlow, R. H., Burns, J. M. & Khan, S. M. The Alzheimer's disease mitochondrial cascade hypothesis: Progress and perspectives. *Biochimica et Biophysica Acta - Molecular Basis of Disease* (2014).

209. Swerdlow, R. H. & Khan, S. M. A 'mitochondrial cascade hypothesis' for sporadic Alzheimer's disease. *Medical Hypotheses* (2004).

210. Szabo, I. & Zoratti, M. The giant channel of the inner mitochondrial membrane is inhibited by cyclosporin A. *J. Biol. Chem.* (1991).

211. Szabo, I., Bernardi, P. & Zorattis, M. Modulation of the Mitochondrial Megachannel by Divalent Cations and Protons. *The Journal of Biological Chemistry* (1992).

212. Takeuchi, H., Kobayashi, Y., Ishigaki, S., Doyu, M. & Sobue, G. Mitochondrial localization of mutant superoxide dismutase 1 triggers caspase-dependent cell death in a cellular model of familial amyotrophic lateral sclerosis. *J. Biol. Chem.* (2002).

213. Terry, R. D. The cytoskeleton in Alzheimer disease. *J Neural Transm Suppl* (1998).

214. Teslaa, T. & Teitell, M. A. Techniques to monitor glycolysis. *Methods Enzymol.* (2014).

215. Tolia, A. & De Strooper, B. Structure and function of γ-secretase. *Seminars in Cell and Developmental Biology* (2009).

216. Ulrich Pietrzik, C. *et al.* From differentiation to proliferation: The secretory amyloid precursor protein as a local mediator of growth in thyroid epithelial cells. *Med. Sci.* (1998).

217. van Strien, N. M., Cappaert, N. L. M. & Witter, M. P. The anatomy of memory: an interactive overview of the parahippocampal–hippocampal network. *Nat. Rev. Neurosci.* (2009).

218. Vassar, R. & Citron, M. Aβ-Generating Enzymes: Recent Advances in β- and γ-Secretase Research. *Neuron* (2000).

219. Vetrivel, K. S. *et al.* Association of γ-secretase with lipid rafts in post-golgi and endosome membranes. *J. Biol. Chem.* (2004).

220. Wakabayashi, T. & De Strooper, B. Presenilins: Members of the gamma -secretase quartets, but part-time soloists too. *Physiology* (2008).

221. Walker, J. E. ATP synthesis by rotary catalysis. *Angewandte Chemie - International Edition* (1998).

222. Walker, J. E. The ATP synthase: the understood, the uncertain and the unknown. *Biochem. Soc. Trans.* (2013).

223. Walter, J., Kaether, C., Steiner, H. & Haass, C. The cell biology of Alzheimer's disease: Uncovering the secrets of secretases. *Current Opinion in Neurobiology* (2001).

224. Wang, J. M. & Sun, C. Calcium and neurogenesis in Alzheimer's disease. *Front. Neurosci.* (2010).

225. Wang, X. *et al.* Oxidative stress and mitochondrial dysfunction in Alzheimer's disease. *Biochimica et Biophysica Acta - Molecular Basis of Disease* (2014).

226. Weydt, P. *et al.* Thermoregulatory and metabolic defects in Huntington's disease transgenic mice implicate PGC-1α in Huntington's disease neurodegeneration. *Cell Metab.* (2006).

227. Winblad, B. *et al.* Defeating Alzheimer's disease and other dementias: A priority for European science and society. *The Lancet Neurology* (2016).

228. Wittig, I., Braun, H.-P. & Schägger, H. Blue native PAGE. *Nat. Protoc.* (2006).

229. Wolfe, M. S. *et al.* Two transmembrane aspartates in presenilin-1 required for presenilin endoproteolysis and gamma-secretase activity. *Nature* (1999).

230. Wong, G. T. *et al.* Chronic Treatment with the γ-Secretase Inhibitor LY-411,575 Inhibits γ-Amyloid Peptide Production and Alters Lymphopoiesis and Intestinal Cell Differentiation. *J. Biol. Chem.* (2004).

231. Wu, J. W. *et al.* Small misfolded tau species are internalized via bulk endocytosis and anterogradely and retrogradely transported in neurons. *J. Biol. Chem.* (2013).

232. Wu, M. *et al.* Multiparameter metabolic analysis reveals a close link between attenuated mitochondrial bioenergetic function and enhanced glycolysis dependency in human tumor cells. *AJP Cell Physiol.* (2006).

233. Yakes, F. M. & Houten, B. Mitochondrial DNA damage is more extensive and persists longer than nuclear DNA damage in human cells following oxidative stress. *Cell Biol.* (1997).

234. Ye, L. *et al.* Persistence of Aβ seeds in APP null mouse brain. *Nat. Neurosci.* (2015).

235. Ye, X., Sun, X., Starovoytov, V. & Cai, Q. Parkin-mediated mitophagy in mutant hAPP neurons and Alzheimer's disease patient brains. *Hum. Mol. Genet.* (2015).

236. Yoo, A. S. *et al.* Presenilin-Mediated Modulation of Capacitative Calcium Entry. *Neuron* (2000).

237. Young-Pearse, T. L., Chen, A. C., Chang, R., Marquez, C. & Selkoe, D. J. Secreted APP regulates the function of full-length APP in neurite outgrowth through interaction with integrin beta1. *Neural Dev.* (2008).

238. Zahs, K. R. & Ashe, K. H. β-Amyloid oligomers in aging and alzheimer's disease. *Front. Aging Neurosci.* (2013).

239. Zampese, E. *et al.* Presenilin 2 modulates endoplasmic reticulum (ER)-mitochondria interactions and Ca^{2+} cross-talk. *Proc. Natl. Acad. Sci.* (2011).

240. Zatti, G. *et al.* Presenilin mutations linked to familial Alzheimer's disease reduce endoplasmic reticulum and Golgi apparatus calcium levels. *Cell Calcium* (2006).

241. Zeviani, M. & Di Donato, S. Mitochondrial disorders. *Brain* (2004).

AKNOWLEDGEMENTS

I am grateful to Prof. Tullio Pozzan for the opportunity to work in his lab and to Dr. Emy Basso for leading my project and for all her advices.

Special thanks to my colleagues and of course to my family, Luca and friends.